Heteromeric composition of the Kv 1.3 channelosome

Composició heteromèrica del canalosoma Kv1.3

Antonio Serrano Albarrás

Universitat de Barcelona
Facultat de Biologia
Departament de Bioquímica i Biomedicina Molecular
Programa de Doctorat en Biomedicina

Heteromeric composition of the Kv1.3 channelosome

Composició heteromèrica del canalosoma Kv1.3

Tesi Doctoral
Memòria presentada per Antonio Serrano Albarrás
per optar al grau de Doctor per la Universitat de Barcelona

Barcelona, Setembre 2018

L'interessat,

Antonio Serrano Albarrás
Estudiant del Programa de Doctorat
en Biomedicina
Universitat de Barcelona

Vist i plau del director i tutor de la Tesi,

Antonio Felipe Campo
Professor Titular del Departament de
Bioquímica i Biomedicina Molecular
Universitat de Barcelona

ACKNOWLEDGEMENTS

ACKNOWLEDGEMENTS!

Pfff… Llevo más de 3 años pensando que poner aquí y aún no sé cómo de largo o corto va a salir. Bueno, tengo tiempo para meditarlo, estoy empezando a escribirlo en 3 de enero de 2018. Siempre lo dice mi madre: no dejes para mañana lo que puedas hacer hoy… siendo mañana un día que bien podría ser de aquí a 10 meses, claro. Je, je, je. Lo siento para mis fans, pero creo que no haré metáforas con patatas y comida… o bueno, ¡ya veremos! *(Nota del autor, 02JAN2018)*

Como hay que encontrar un orden en las cosas, empezaré por lo que me queda más cerca: ***MP***, e iré divergiendo a partir de ahí. MP es una familia muy grande y extensa, y seguro que no puedo dedicaros a todos ni la mitad del espacio que desearía, el cual es ya de por sí menos de la mitad del que en realidad merecéis. En todo caso, vamos allá:

Muchas gracias en primer lugar a **Antonio** (Felipe, senior, gros, el jefe). Gracias por darme la oportunidad de formar parte de este magnífico grupo donde he aprendido y disfrutado tanto y, seamos sinceros, padecido (un poco). Espero que tu vista para encontrar buena gente entre esa inmensidad de entrevistas no falle nunca y que, cuando llegue ese día en que decides colgar los hábitos, nos llames a todos, estemos donde estemos, para hacerle homenaje de la mejor manera posible (una barbacoa, por ejemplo).

Muchas gracias a los que, en este punto en el tiempo sois ex-MP.

Gràcies **Núria**, per ensenyar-me la gran majoria del que se d'electrofisiologia. El teu bon rotllo i les teves ganes de parlar de la vida sempre aconsegueixen que vegi la ciència amb uns altres ulls. Gràcies **Laura** (Solé) (i **Xevi**, òbviament); l'altre dia vaig trobar-me el menú de la boda i vaig pensar: coi, encara continua sent la millor boda a la que he assistit. Espero que tot us vaig molt bé per Fort Collins i que sigueu molt feliços allà on decidiu estar. Moltes gràcies **Mireia**; tant per ser un referent en quant a moralitat com per aportar riure i bon humor a la vida; per mi sempre has tingut i per ara conserves el millor riure del laboratori (i segur que a Pittsburgh també el tindràs). Moltes gràcies **Anna** (Oliveras) per estar sempre a tope i donar-ho tot, tant a la ciència com a fora d'ella. Encara miro rient-me les fotos d'aquella gran barbacoa amb corre-cases inclosa i la festa post-tesis de la Mireia; vam gaudir tant! Espero que puguem repetir-ho tots algun dia (i espero que no calgui esperar a que l'Antonio Felipe es jubili!). Estic segur que a Berlín ho estaràs petant màxim, com ho feies aquí. Moltes gràcies **Albert** (Vallejo) i **Sara** (Roig); perquè tot i que em rigui de la xorrada de 2006, formeu un bon pack. Perquè vau ser les primeres persones que vaig conèixer i em van ensenyar a MP i perquè sempre us he admirat. Potser ara esteu molt allunyats (uns 8700 km separen San Francisco de Holanda) però no deixeu que aquesta nimietat us separi! Thank you very much **Kasia**, for your sense of humor and your will of making the world easier. Wherever you go, remember, the bureaucracy is the enemy! Moltes gràcies a la **Clara** i la **Jesusa**; per donar-me tants bons moments, encara que hagi d'aguantar "Me rehúsos" i reggaeton vari i perquè la línia recta entre dos punts en un mapa sempre creua Hawaii. Moltes gràcies al **Dani** per ser el meu referent per parlar de política (¡Oceanía siempre ha estado en guerra con Eurasia!) i

patch-clamp al laboratori; i a la **Irene** per ser la meva referent en quant a Marvel i videojocs al laboratori. He gaudit molt ensenyant-vos el (poc) que se de la ciència. Se molt bé que al principi la tesis sembla una muntanya inexpugnable, però no deixeu que el repte us faci fer un pas enrere. Tots dos valeu moltíssim, com a persones i com a investigadors, i sou capaços d'aconseguir el que voleu. Grazie mille, Silvia! Porque tu buen humor, tu motivación por la ciencia y tu cariño siempre me han inspirado desde que llegaste. No permitas que la tesis te cambie. Moltes gràcies al **Sergi** i la **Maria**, perquè sou la futura generació de doctorands: us podeu menjar el món i ho fareu, que ningú us digui el contrari. També vull agrair als ex-MP que, tot i que no hi hagi coincidit gaire, si que hi he interactuat: **Rubén, Ramón** i **Joanna**, sense vosaltres MP no seria el que és avui.

También me gustaría agradecer a Carmen Valenzuela, porque pese a ser una magnífica investigadora, me ha enseñado que lo más importante de la vida suele estar fuera del laboratorio: la gente con la que convives, te relacionas y disfrutas. Mención especial a todo su grupo por hacer muchísimo más amenos todos los congresos en los que coincidimos.

Fora del laboratori, però, hi ha molta altra gent que fa que el ***Departament*** sigui aquell lloc on podries estar-te hores parlant i rient: **Raquel**, **Toni** i **Anna** (Orozco), gràcies al vostre esforç dia rere dia, així com el vostre bon humor i bromes feu que el Departament sigui una mica més càlid. També vull agrair a la gent d'altres grups els bons moments: gent de TAM (**Laura**, **Cèlia**, **Samantha**), RST (**Albert** Viel, **Liska**, **Olga**) i INS (**Xico**, **Helena**). Consti, anava a posar una llista inacabable de noms, però per raons d'espai he posat només uns pocs; que no hi sigueu no significa que no pensi en vosaltres!!!

Vull fer una menció especial, abans de sortir del Departament, a la gent de LPL. Per una banda a la gent amb la que he coincidit més durant la tesis: **Pere** i **Joana**, gràcies pels bons moments. Per altra banda, vull agrair a la **Eva**, el **David** i la **Dolores** (així com al **Vicens**) la excel·lent direcció i gestió del postgrau en gestió de projectes.

En fi... tot el Departament en només una pàgina i pico, eh? Rècord! Jejeje, si, ja ho se, m'enrotllo... En tot cas, no he acabat amb la ***uni***! Ara venen els grups d'amics!

Moltes gràcies al grup de Biologia, tant als AALMAAA inicials que vam anar a Escòcia: **Laura** (Zango), **Albert** (Ros), **Aina**, **Alicia**, **Agnès** i **Miquel**; com als que vaig conèixer a posteriori o a arrel de vosaltres: **Guillem**, **Genís**, **Lara**, **Miguel Ángel**, **Xaviers** (Curto i Simó), **Albert** (Jiménez), **Oriol**, **Ferran**... Amb alguns de vosaltres he viscut Escòcia, Camino de Santiago, Suissa, la Selva Negra, Sallagosa i Benidorm, entre altres aventures. Tot i que en els últims temps no ens puguem veure gaire, ni per un moment m'oblido de vosaltres!

Moltes gràcies al grup de Ciències Biomèdiques: **Laura** (Torrente), **Aleix**, **Jorge**, **Patty**, **Neus** i **Mónica**. Perquè tot i que tinguem una agenda que ens impedeix quedar i només ens veiem 4 cops a l'any (2 presencialment i 2 per Skype) quedar amb vosaltres continua sent igual de divertit que sempre. Res em treu els viatges que hem fet (Holanda, Itàlia, Madrid) i espero amb ànsies veure cap on ens porten els diferents camins de cadascú.

Muchas gracias a toda **La Colla™**. Muchas gracias a **Edu** por haber aguantado mis dibujos de arte esquemático tantos años (muchos) y por tener siempre un comentario ocurrente para cada situación; a **Lucía** por ser tan random como preocupada por sus amigos; a **Eric** por ser capaz de aguantar a Lucía y aun así tener tiempo de cocinarnos un brownie; a **Sara**

(Porcel) por intentar que este mundo sea algo mejor a nivel social; a **Rubén** por ser nuestra foto oficial de grupo; y a **Pol** por las noches de masacre zombi en las que casi siempre acabamos perdiendo. Por último, muchas gracias a ti también, **Irene**, porque pese al tiempo, las evidentes limitaciones para quedar y haberme conocido tanto; aún encontramos tiempo para compartir, hablar de la vida y reír juntos.

Gracias también a los Mancus: **Marina**, **Joan**, **Alberto** i **Xavi** (Rodríguez). Porque esos jajas, esas mancuras y esos "¡¡¡vamos no me jodas!!!" al final me han dado la vida, me han ayudado a afrontar el mundo real y a canalizar la frustración.

Bueno, creo que con esto cierro el episodio de los grupos de amigos. Obviamente siempre hay alguien que por mi traicionera memoria o por temas de espacio no aparece mencionado, pero sí que está en mi corazón. Ahora queda la ***familia***.

Muchas gracias a mis padres. Estoy seguro de que sin ellos no habría podido llegar hasta aquí. Me han dado una infancia y juventud tranquila y los medios para poder ir a la universidad, pese a nuestros humildes orígenes. Pero obviamente, no sólo me han dado cosas materiales.

Gracias, **mama**, tú me has enseñado a tener pensamiento crítico, a dudar de todo, incluso de mis propios pensamientos (especialmente de mis propios prejuicios) y de que no hay una verdad indiscutible, solo puntos de vista. También he aprendido de ti que el hablar sin conocer todas las caras de la moneda no es muy diferente a mentir y a contrastar mis opiniones antes de darlas por ciertas (si, los que me llamáis friky de la Wikipedia podéis culparla de ello).

Gracias, **papa**, tú me has enseñado que para ser feliz no es necesario ser el mejor, sino estar orgulloso de tu propio trabajo y de tus propias decisiones. De ti he aprendido que ser una buena persona significa ser honesto, íntegro y consecuente conmigo mismo y para con los demás.

Gracias, **Carlos**, porque pese a que somos muy diferentes, siempre nos hemos llevado muy bien. Y sí, es un poco rollo todo esto de que nos comparen entre nosotros y nos diferencien (uuuuh, son el día y la noche), pero bueno, estas son las cosas malas; la buena es que siempre me tendrás para lo que sea.

Ahora llega el momento en que empiezo a sacar familia del cajón y me enrollo 2 páginas más, por eso lo abreviaré un poco.

Muchas gracias a mis abuelas **Francisca** y **Dolores** por cuidarme cuando era necesario, por preocuparse por mí y por quererme tanto. También gracias a mis abuelos **José** y **José**, que ya no están aquí y que estoy seguro se sentirían muy orgullosos de mí.

Muchas gracias a la parte de familia que tengo en Calella: **Paco**, **Pepe**, **Maribel** por esas reuniones familiares en las que todo el mundo ~~grita~~ habla fuerte y todos acabamos a reventar de comida. Gracias también a la otra parte de familia, la que tengo en Sabadell: **Imma**, **Pepe**, **David**, **Delia**, **Carla**, **Cristian**, **Francisco**, **Merche**, **Jonathan** y **Sergio**; porqué aunque nos veamos pocas veces al año, todas son entrañables.

ACKNOWLEDGMENTS

También muchas gracias a **Francina**, **Javier**, **David** y **Andrea** por todo lo que me habéis dado en los últimos años y tratarme como uno más. Para mí, vosotros ya formáis parte de la familia desde hace mucho tiempo.

Y bueno... ya solo queda una persona que mencionar. Muchas gracias, **Judith**. Durante todos estos años hemos vivido mucho: desde viajes, algunos más apasionantes que otros (Madrid, Marruecos, Laponia, Londres); a las noches de vicio desenfrenado; pasando por la gran cantidad de gatitos (**Luce**, **Nala**, **Wendy**, **Samsi**, **Kali**, **Tell**, **Xena**, **Ares**, **Honey**, **Quinoa**, **Trepa**…). Gracias por aguantar tanto mis manías como mis frikadas, ya que eso me permite mostrarme tal y como soy (#NoFilters). Gracias por los buenos momentos y por los no tan buenos. Gracias por estar a mi lado pese a todo y darme cada día una razón para quedarme un ratito más en la cama. Porque sin ti este libro y yo mismo no seríamos lo mismo, muchas gracias, cariño. Te quiero.

La vida es demasiado corta para derrocharla con miedo - Illaoi

TABLE OF CONTENTS

ABBREVIATIONS

ANOVA: Analysis of Variances

APC: Antigen presenting cells

CaNx: Calnexin

Ct: Carboxy-terminus (Cter)

CFP: Cyan Fluorescent Protein

EC_{50}: Half maximal effective concentration. Concentration of a compound which inhibits half of the current of a given cell

ER: Endoplasmic reticulum

Fiji: Fiji is just imagej

g: Gravitational constant ($6.674 \cdot 10^{-11}$ N $\cdot$ $kg^{-2} \cdot m^{-2}$). Used for centrifugation

G: Conductance

GFP: Green Fluorescent Protein

HEK 293 cells: Human Embryonic Kidney 293 cells

I: Intensity (Current)

I/V: Intensity / Voltage

IB: Immunoblot

IP / coIP: ImmunoPrecipitation / co-ImmunoPrecipitation

JACoP: Just Another Co-localisation Plug-in

Kb: Kilobases

KDa: Kilodaltons

Kv: Voltage-gated potassium channels (VGKC)

K_{Ca}: Calcium-dependent potassium channels

MgTx: Margatoxin

ms: milliseconds

mut: mutated

mm / nm: millimetre / nanometre

mM / nM: millimolar / nanomolar

µL: microliter

ng: nanogram

O.D. / I.D.: Outer Diameter / Inner Diameter

pA: picoampere

pA/pF: picoampere/picofarad

ABBREVIATIONS

PD: Pull-down

pF: picofarad

R: Resistance

S1-6: Transmembrane domains in Kv channels

SDS-PAGE: Sodium dodecyl sulfate polyacrylamide gel electrophoresis

sec: second

SM: Starting Material

SN: Supernatant

SNP: Single Nucleotide Polymorphism

SS6: Region between the selectivity filter and the S6 domain in *Shaker* channels

T1: Tetramerization domain in *Shaker*

T cells: T lymphocytes

TCR: T Cell Receptor

YFP: Yellow Fluorescent Protein

V / mV: Volt / milliVolt

WGA: Wheat Germ Agglutinin

INTRODUCTION

1. INTRODUCTION

1.1. PLASMA MEMBRANE AND PORES

From the advent of life in earth, primitive life forms became partially isolated from the external environment by a lipid layer. Lipid membranes retained the cell components, but also prevented the exchange of ions, either necessary or harmful elements, from the external media. Thus, novel mechanisms had to evolve in parallel to membranes to maintain the passage of ions through it. From the small **pores** of Gram-negative bacteria and, subsequently mitochondria, to the more complex and selective elements in contemporary eukaryotic membranes, channels have a long and diverse evolutionary path [1].

These Membrane Transport devices have been classically (until 1980s) divided between two types by their kinetic behaviour: carriers and pores. On one side, carriers, also known as **transporters**, function by exposing the transport binding site to the intracellular and extracellular media alternatively (e.g.: Na^+/K^+ pump, glucose transporter). On the other side, pores, called **channels**, contain a narrow water-filled tunnel connecting the intracellular and extracellular environments while also functioning as a selectivity filter (e.g.: aquaporins, voltage-dependent ion channels). Thus currently, the main difference between these two transport entities resides in the presence of a continuous path for the substances to cross, which enables open channels to have a much faster rate of passage than transporters. This last feature also explains their importance in many fast-response functions [1].

Channels are divided in 2 main categories depending on the nature of the molecules conducted: (i) **aquaporins**, also called water pores, mainly drive water molecules in and out of the cell while preventing the passage of solutes. However, some members of this category are also selective for some small uncharged solutes like glycerol and urea [2]; (ii) **ion channels,** proteins that conduct ions and that the present work deals with.

1.2. ION CHANNELS

Ion channels are macromolecular protein complexes that, once open drive the passage of ions through the membrane in favour of electrochemical gradient. Ion channels, being fundamental pieces in the membrane of excitable cells, have been gradually acknowledged as the techniques to study them were being developed [1].

Ions play a paramount role in the excitability of muscle and nerves but only the combined works of several notable physicists, chemists, pharmacologists and physiologists have been able to elucidate the internal functioning of these important entities. Thus, while Sydney **Ringer** published a series of works (1881-1888) demonstrating that by perfusing a frog heart with a saline solution (Ringer solution), the organ kept beating for long. Walther **Nernst**, working with the electrical potentials that arise from the diffusion of electrolytes in solution (1887), created the Nernst equation. These advances, among others, triggered new theories

regarding the nature of the intracellular environment and the ionic origin of electric potentials in live cells [1].

Later, Julius **Bernstein** (1902, 1912) suggested that the membrane of excitable cells have a variable permeability to K^+ ions depending on the state of excitation. This *membrane theory* explained the resting potential of nerve and muscle as a diffusion potential, while during excitation other ions are allowed to diffuse across the membrane. This theory supposed the first physicochemist explanation of the bioelectric events [1].

As research concerning cell physiology has progressed, it has become apparent that all the ions present in the Ringer's solution, as well as other inorganic ions of body fluids, have a major cellular role. Consequently; transporters, channels and enzymes have been related to all these ions or molecules and help us to understand the blueprints and the workflow of life itself [1]. The combined advances of such a long display of scientists would be too long to be written in this work, but their contribution remains in the annals of biology for changing our vision of nature and cement the field of **electrophysiology**.

Thus, ion channels are known to be implicated in electrical signalling in nerve, muscle and synapse. Nevertheless, ion channels are not only implicated in electrical excitation, but also to the activation of a wide array of physiological processes. This feature is a result of the high speed achieved by channels, in contrast to other molecular processes like active transport or enzyme catalysis [1] (Fig.I1).

1.2.1. Classification

Ion channels may be classified by gating - what causes the opening and close.

- **Voltage-gated channels:** channels which open and close in response to the membrane potential.
- **Ligand-gated channels:** also known as ionotropic receptors, these channels open in response to the extracellular domain of the protein binding to specific ligand molecules (e.g.: $GABA_A$ receptor).
- **Other gating mechanisms:** channels gated by the presence – or absence – of certain second messengers like Ca^{2+} (e.g.: $K_{Ca}3.1$), or other physic phenomena like light (e.g.: channelrhodopsin) or temperature (e.g.: TRPV1).

We will focus on voltage-gated channels, as the present work aims the ones selective for the potassium ions, which are also the largest and most diverse group of ion channels [3].

1.3. VOLTAGE-GATED POTASSIUM CHANNELS

Voltage-gated potassium channels (VGKCs or **Kvs**) are channels with their gating linked to changes on membrane potential being selective for K^+. Kv are the largest and most diverse subfamily of channels. They differentiate from other ion channels by the **selective filter**, which ensures that K^+ ions pass with much more frequency than any other ion. We will discuss about the selectivity filter in future chapters of the introduction.

Amongst their functions we can highlight their implication on the **action potential**, where they are in charge of returning the cell to the resting state. Nevertheless, their presence in

other systems must not be underestimated, as they play important roles in rapid reaction events like immune response [4] or insulin secretion [5].

Kv typically refers to both the alpha and beta subunits. While alpha subunits form the conducting pore by which ions pass [3], beta subunits are auxiliary proteins which associate with alpha subunits but provoke no currents [6]. The pore is formed by the **tetramerization** of 4 alpha subunits [7]. The ratio between alpha and beta subunits can scale up to 4:4.

1.3.1. Elemental basis of Kv channels

Open K^+ channels maintain the membrane potential closer to the **potassium equilibrium potential**, keeping it away from the firing threshold. Thus, in excitable cells, K^+ channels set the resting potential, short the action potential, end high activity periods, regulate the intervals during repetitive firing and reduce the effectiveness of excitatory inputs when they are open [1].

As mentioned, Kv architecture is typically formed by the tetramerization of 4 copies of alpha subunits arranged as a ring [7]. In contrast, Na^+ and Ca^{2+} channels are formed by a unique protein that is, in fact, four repeats of the same pattern [8, 9]. Nav, Cav and Kv units share the topology of six transmembrane domains. Thus, four copies of Kv tetramerize to form a structure closely similar to Na^+ and Ca^{2+} channels.

1.3.2. Classification of alpha subunits

According to the International Union of Pharmacology (IUPHAR), Kv are divided into 12 families (Kv1-12), each including several isoforms. Even though alpha subunits of Kv can be grouped by different criteria, they are normally grouped according to the **function** by which they were firstly identified [1, 3]:

- **Delayed rectifier (I_{DR}):** channels that cause an outward current of K^+ following a depolarization of the membrane. The opening is caused by the influx of Na^+ ions to the cell, which increases the membrane potential. These channels repolarize the membrane. This repolarization restricts the duration of the nerve impulse and participates in the regulation of repetitive firing of the neuron. Also, these channels slowly inactivate or do not inactivate at all. This group includes members of Kv1 (KCNA, *Shakers*), Kv2 (KCNB, *Shabs*), Kv3 (KCNC, *Shaws*), Kv7 (KCNQ) and Kv10.1 (KCNH1, eag1) families.
- **A-type (I_A):** channels that also cause an outward current of K^+ with little delay after depolarization. Unlike delayed rectifiers, A-type channels open by depolarization following hyperpolarization. As this hyperpolarization increases the interval between action potentials, it helps neurons to fire repetitively at low frequencies. This group also includes members of Kv1 (Kv1.4), Kv3 (Kv3.3 and Kv3.4) and all the members of Kv4 (KCND, *Shals*).
- **Modifier/silencer:** proteins that, despite having similar sequences and structures to other categories, do not generate ion currents by themselves. In contrast, they heterotetramerize with members of Kv2 family, modifying or suppressing their activity. This category includes members of Kv5 (KCNF), Kv6 (KCNG), Kv8 (KCNV) and Kv9 (KCNS).

- **Other:** Some other channels do not fall into either category or up until now has not been extensively studied to be classified. This is the case of Kv10.2, classified sometimes as outward-rectifying; Kv11.2 and Kv11.3, relative of inwardly-rectifying Kv11.1; and Kv12, considered separately as slowly activating.

The different families (*Shaker*, *Shab*, etc) are named according to the homologous gene family found in *Drosophila melanogaster*. In the present work we will cover **Kv1.3** and **Kv1.5**, members of the *Shaker* family (Kv1), whose genes are also known as KCNA3 and KCNA5.

1.4. K_V1

Kv1 channels are also named ***Shaker*** because the homologous protein of *Drosophila melanogaster*. The *Shaker* gene was the first K^+ channel to be cloned and instead of being identified by a purified protein or a partial amino acid sequence, it took place by the characterization of a mutation of the flies which resulted in the shaking of the legs when they were under anaesthesia, suggesting a function in the termination of nerve impulse. By characterization of the mutant locus, it became apparent that the gene codified a **K^+ channel** by its similarities to the Na^+ channels already known [10].

The technological advances enabled to clone and identify genes. These new approaches resulted in the characterization of several mammalian orthologous to the fruit fly's *Shaker* from different physiological mammal species [11, 12].

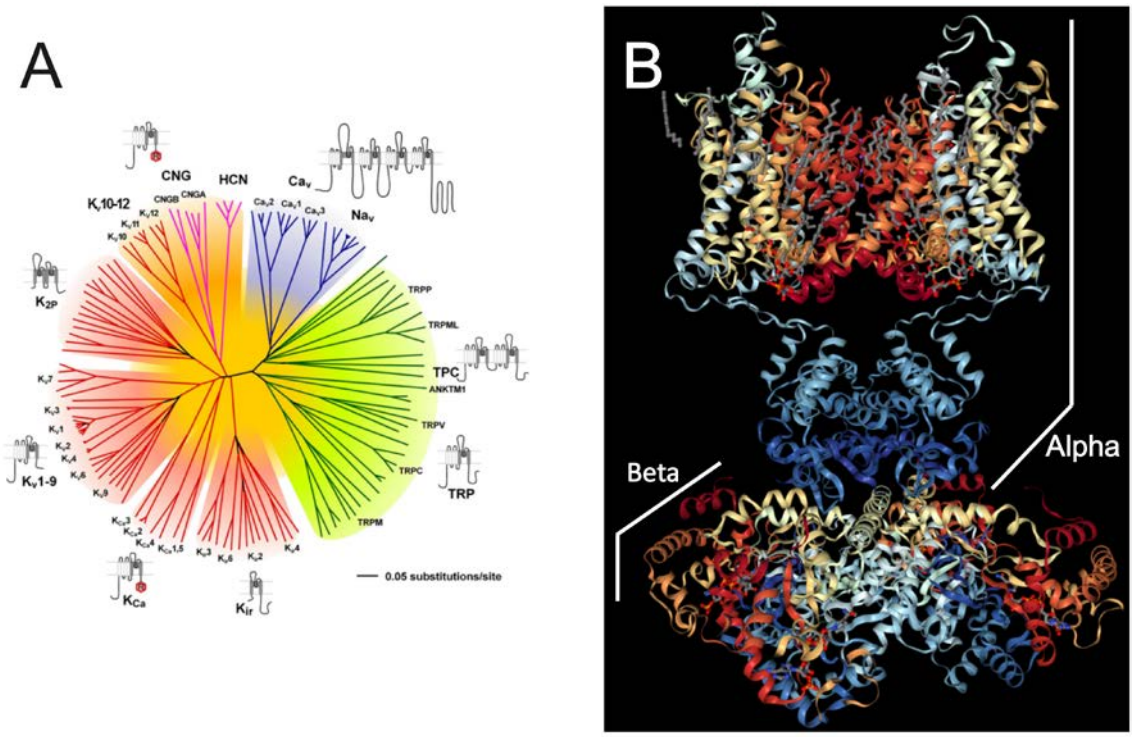

Fig. I1: *Diversity of ion channels.* ***A:*** *Phylogenetic tree of ion channels (IUPHAR/BPS Guide to Pharmacology).* ***B:*** *Structural model of Kv1.2/Kv2.1 paddle chimaera channel in association with a beta subunit (PDB 2R9R).*

1.4.1. Structure of Kv1

Kv1 are formed by the tetramerization of 4 copies of α subunits which form a central transmembrane pore in the structure. Additionally, each α subunit presents six membrane-spanning hydrophobic α-helical sequences (named S1 through S6) that are linked together

with intracellular and extracellular loops (called linkers), as well as cytoplasmic amino- and carboxyterminal sequences. These transmembrane domains contain both the pore, formed by the collaboration of S5 and S6 of the different subunits, while the rest of transmembrane domains (S1-S4) serve as voltage sensors, which regulate the opening of the channel [13].

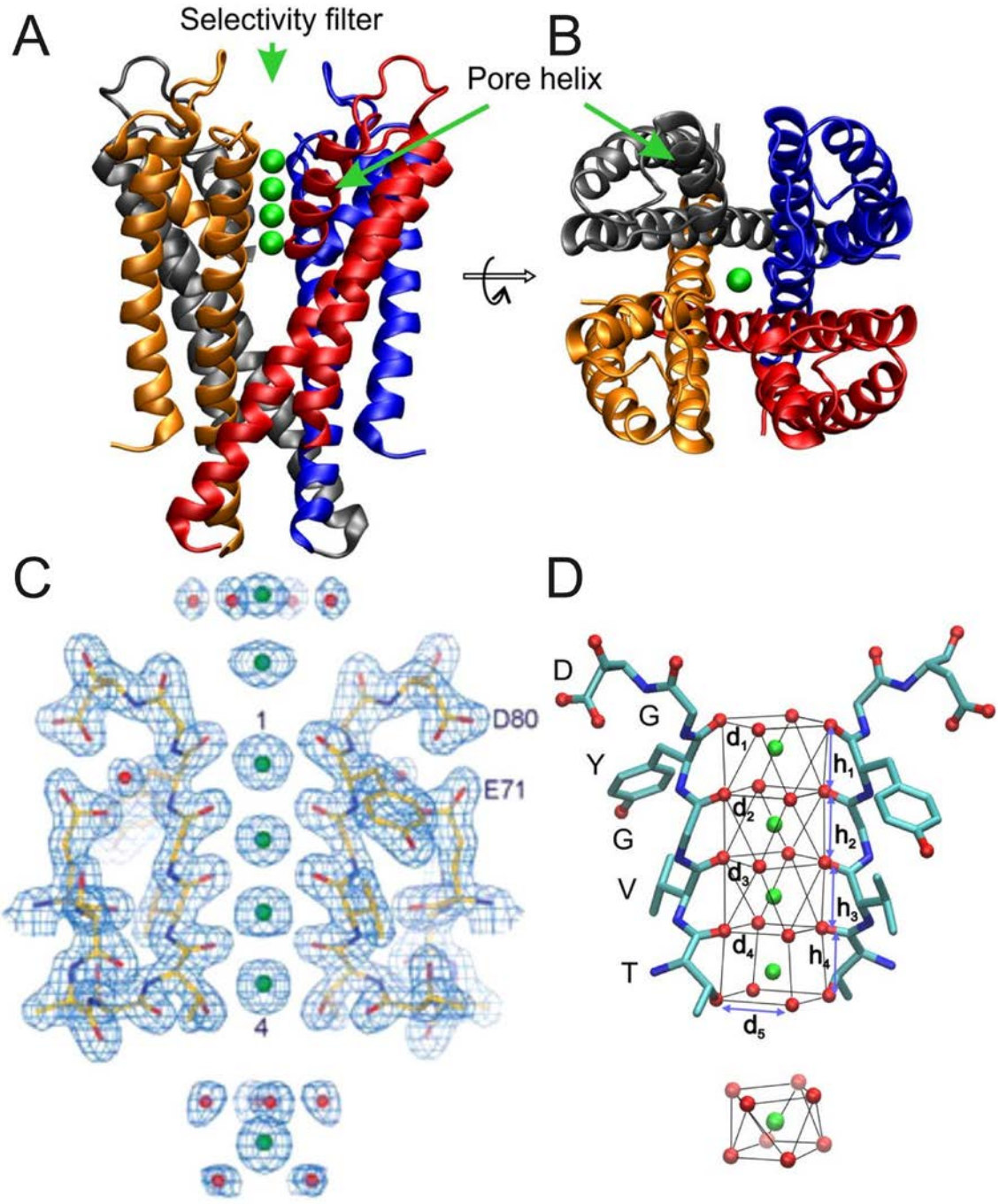

Fig. I2: *Structural features of the KcsA channels and K^+ coordination structure in the pore [14].* ***(A-B):*** *Membrane-omitted side and top views of the KcsA K^+ channel (PDB 1K4C).* ***C:*** *High-resolution electronic density map showing the two diagonal subunits and the orientation of the carbonyl oxygen atoms to coordinate K^+ ions. The numbers correspond to the four binding sites determined by the sequence TVGYG.* ***D:*** *Antiprism and cubic cages forming the selectivity filter binding sites.*

1.4.1.1. The pore

Even though Kv channels' α subunits are considered to have 6 membrane-spanning sequences (mirroring the 24 transmembrane domains of Na^+ and Ca^{2+} channels), early studies already predicted the presence of 7 potential membrane-spanning regions [10]. This seventh

transmembrane domain, which is situated between the S5 and S6, came to be known as **P-loop**, as it didn't really cross the membrane, but looped in and outside of the bilayer [15].

As early as 1986 [16], it was hypothesized that what we call nowadays the S5-S6 linker and the P-loop enters the membrane as a hairpin and forms the pore of the Na^+ channel when emerging to the extracellular side. The resolving of the structure of bacterial K^+ channel KcsA confirmed twelve years later this structure for K^+ channels [17]. Additional evidence in the following years resulted in the assumption that both K^+, Na^+, Ca^{2+} and CNG channels **conserve** this structure, and that mutation of this region caused changes in conductance or ion selectivity, amongst other features.

Studies with *Shaker* blockers, which physically plug the pore, and mutations within the pore region gave further insight into which residues and regions were directly involved in the ionic conduction [14, 18] (Fig.I2). By this way, different regions of the pore were identified [1]:

- **Turret** (*Shaker* G420-P430): connects the S5 with the P-loop and serves as docking for toxins that block the pore.
- **Pore helix** (*Shaker* D431-M440): Forms the floor of the central cavity, which represents the last wide spot in the inner vestibule before the narrow selectivity filter.
- **Selectivity filter** (*Shaker* **T^{442}VGYGD^{447}**): represents the most conserved region of all K^+ channels – their signature sequence. The carbonyl oxygens from the residues VGYG of the four subunits reach out to passing K^+ to catalyse their passage across the pore. Passage of smaller ions (e.g.: Na^+) is not favoured, as their smaller atomic diameter doesn't enable the ion to pass stably; while bigger ions (e.g.: Rb^+) can't cross as their diameter inhibit it. Mutations of this sequence either destroy the K^+ selectivity of the pore or abolish its capacity to conduct ions.
- **Post-selectivity filter region** (*Shaker* M448-W454): contains the mouth of the pore, formed by the T449 from *Shaker* and its homologous residues in other channels. In its last section connects with the S6.

Access to the pore is regulated by the C-terminal end of S6, as it forms a **blocking bundle** when the channel is closed. Changes in membrane voltage modify this conformation and enables the passage of K^+ ions [19, 20]. This phenomenon is possible thanks to a highly conserved sequence inside the S6 helix: PxP, a flexible sequence which acts as a hinge [21, 22].

1.4.1.2. The voltage-sensor

The pore (S5-S6, but specially the **P-loop**) sets the criterion to discern the channel selectivity. However, the voltage-sensor (S1-S4, but specially S4) sets aside the voltage-gated channels from the other types of regulations.

Before the molecular cloning of any channel, the gating charge was hypothesised as a collection of charged residues buried in the membrane [1]. Early assumptions postulated about pairs of positive and negative gating charges on different components of the channel [23]. The change in membrane potential would result in the sequential move of the different charged residues, leaving the positive charge outward and the negative charge inward.

The cloning of channels in later years suggested the **S4 transmembrane domain** as a key region of the voltage sensor as it contained several cationic residues. This sequence was composed by mostly nonpolar or hydrophobic residues while every third position there was a positively charged residue (R or K), a pattern strictly conserved in all known voltage-gated channels.

Early mutagenesis studies with cloned channels were focused on the domain I of rat Na^+ channels (homologous to one of the four subunits of K^+ channels). The mutation of one basic residue in S4 to neutral or acidic residues resulted in effects over the steepness of the voltage dependence and the voltage of activation amongst other gating characteristics [24].

The replica of this approach on K^+ reported similar results. Neutralizing any of the first five basic residues in S4 shifted the midpoint and at least two positions reduced the steepness of gating [25]. Besides, conservative changes of neutral residues also shifted the voltage dependence of the channel.

These residues are in an α-helix crossing the membrane but not all are buried inside. On the contrary, studies confirmed that the S4 segment lies at the interface of invaginations from the outside and the inside media. Thus, the helical segment can slide with respect to this interface or twist to transfer charged groups from one invagination to the other [26]. These movements can be studied optically by using a FRET approach, which relates them with an optical signal (fluorescence).

In summary, the voltage sensor is a highly specialized structure which includes S4, but also S1-S3 transmembrane domains forming the invaginated surfaces that surround S4, shaping the voltage-sensing module. The membrane potential-dependent movements of this sensor result in a series of sequential changes of conformation that causes the opening, or closure, of the channel.

1.4.2. Regulation of the channel

While the pore and the voltage sensor explain the gating and conduction of ions, they do not explain the additional events that the channel suffers.

1.4.2.1. Electromechanical coupling

Even though the voltage sensor causes a conformational change, this event would be useless if the movement did not result in changes in the pore region.

The S4-S5 linker, the intracellular loop between S4 and S5, is the responsible of this transmission of movement. Several studies postulate that some residues in the S4-S5 linker interact with other residues in the proximal C-terminus, near the PXP region. Thus, changes in membrane potential provoke a sequential movement that forces the conformation of the gate of the channel [27, 28].

1.4.2.2. Tetramerization

A crucial phenomenon is the formation of the **tetramer**. Contrary to the Na^+ and Ca^{2+} channels, formed by a unique peptide containing 4 repeated domains, K^+ channels are formed by 4 independent subunits that must interact to form the channel. During the 90s, experiments aimed to discover the minimum part of the protein able to form a tetramer. By

following this approach, *Drosophila* Shaker B potassium channel was steadily truncated and the polypeptide containing as little as 114 amino acids of the N-terminal sequence could form a homomultimer [29]. Additional experiments also demonstrated that this domain was well-conserved in *Shaker* channels and could be replicated in Kv1.1 [30]. This domain was named T1 domain and is the key to the phenotype variability of Kv1 channels, as it enables the formation of heterotetramers between members of the same family (e.g., Kv1.3 and Kv1.1). All Kv channels contain these domains but they are family-specific. Thus, a Kv2 subunit with the T1 domain grafted from Kv1 will only tetramerize with Kv1 subunits [29]. In fact, even though this domain is located in the N-terminus in Kv1 subunits, other families, like Kv7, have their T1 domain in the C-terminus.

1.4.2.3. Channel inactivation

The cytosolic sequences of the channels are sometimes implicated in the regulation of the **gating** [31] (Fig. I3):

- **N-type inactivation**, also known as hinged-lid or *ball-and-chain* inactivation is a model which explains the fast inactivation mechanism in Kv channels and other families. By following this model, the channel can be either open, closed or inactivated. This inactivated state takes place in a fast fashion by the physical blockage of the pore. A "ball"-like structure is responsible for blocking the channel [32-34]. This ball is typically part of the N-terminal (hence its name) cytoplasmic domain of the same protein, but the interaction with some beta subunits can also confer this ability to channels lacking it [35, 36].
- **C-type inactivation**, on the other side, is a slower type of inactivation. It takes place when prolonged activation provokes a movement in the residues near the selective filter of the channel [27, 28]. Thus, in this model, the selectivity filter acts as a second gate.

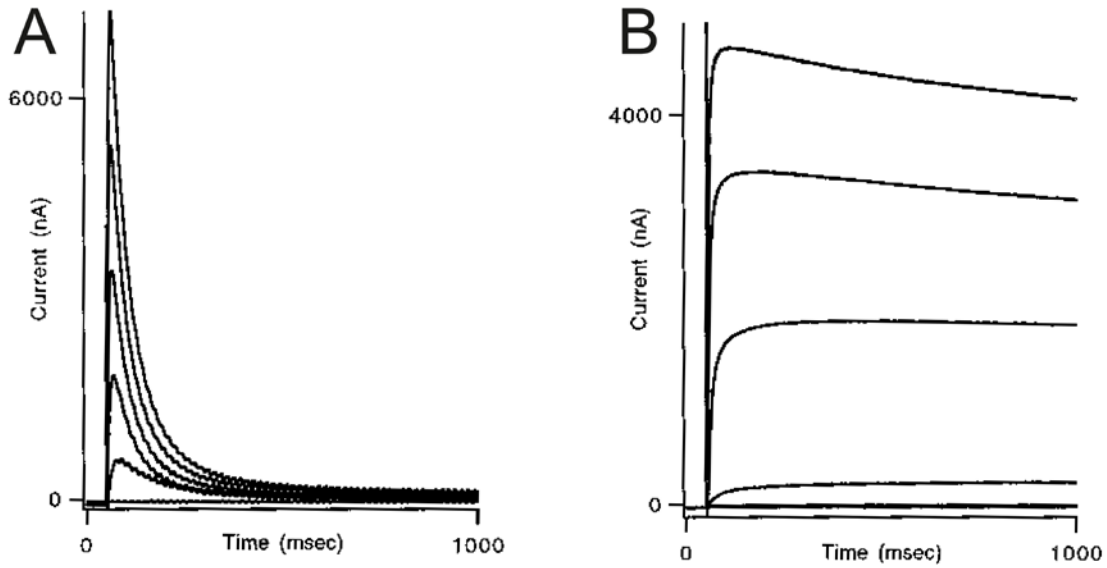

Fig. I3: *Types of inactivation in ion channels [31].* ***A:*** *N-type inactivation.* ***B:*** *C-type inactivation.*

1.4.2.4. Biogenesis and traffic

Kv channels are synthesized in the rough endoplasmic reticulum (ER) [37] but contrary to other membrane proteins, they have no canonical ER target signals. Instead, the S2 domain is the main target signal [38]. While still being synthetized, T1 domains of Kv channels interact and promote the full tetramerization once the subunits are in the ER [39, 40]. Next, Kv tetramers exit the ER following a quality control checkpoint [41].

Several signal sequences, such as RXR, KKXX or KDEL, promote the intracellular retention of Kv [42-44]. Proper folding, tetramerization or additional interactions may mask these signals and facilitate anterograde transport. Signals that promote the anterograde transport are VXXSL or the recently described non-canonical YMVIEE [45-47].

The forward trafficking of the tetramer will depend on the balance of those signals on the channel. That is, heterotetramers containing subunits with strong retention signals (e.g., Kv1.5), will probably be more intracellularly located than channels (e.g., Kv1.3) showing plasma membrane facilitating motifs [48, 49].

Like other membrane proteins, most Kv channels follow the typical pathway from ER, through Golgi compartments, accumulating post-translational modifications such as glycosylations or phosphorylations [50-52]. Another type of post translational modifications which Kv suffers is ubiquitination [53-56].

1.5. *SHAKER* MEMBERS

The ***Shaker*** family contains up to 8 homologous subunits in vertebrates, distributed among all the genome. Following some studies, these 8 copies are postulated to be the result of successive gene duplications and neofunctionalization during the emergence of *teleostei* (ray-finned fishes) [57, 58], along the duplication of other ion channel families and the Hox genes early in vertebrate evolution. These studies also suggest that this gene duplication phenomenon justify that some of the *Shaker* genes tend to appear in cluster containing several of them (KCNA3-2-10, KCNA6-1-5) [58].

The members of the *Shaker* family are as follows:

- **Kv1.1 (*KCNA1*):** located in human chromosome 12, in a cluster with Kv1.5 and Kv1.6. It is synthesized prominently in dendrites associated with translational “hotspots”, which are spots of translation of proteins important for the synaptic sites [59]. Regardless, detection of surface-expressed channels has revealed that they are only expressed in the axonal membrane [60], suggesting a role in repolarization of these membranes. Accordingly, it has been linked to neurologic pathologies including epilepsy and ataxia in mammals [61].
- **Kv1.2 (*KCNA2*):** located in human chromosome 1, in a cluster with Kv1.3 and Kv1.8. It is typically concentrated along axons and axon terminals of neurons, as well as presynaptic sites [61], following a similar distribution pattern to Kv1.1. Some studies have linked this channel to several processes linked to pain like neuropathic pain [62] or diabetic hyperalgesia [63]. Similar to Kv1.1, mutations have been linked with epileptic encephalopathies [64].

- **Kv1.3 (*KCNA3*):** located in human chromosome 1, in a cluster with Kv1.2 and Kv1.8. Regarding the nervous system, Kv1.3 can be found mainly in mitral cells of the olfactory bulb mediating glucose-sensitivity [65]. Contrary to the previous channels, Kv1.3 also has significant roles in immune system, where it can be detected in both antigen presenting cells [66] and lymphocytes [67]. Mutation of this channel results in no effect over nervous or immune system, but a deep and still-in-study alteration on metabolic regulation which will be further discussed in following chapters. Dysregulation of Kv1.3 has been also linked to neoplastic processes in a wide array of tissues [68, 69].
- **Kv1.4 (*KCNA4*):** located in human chromosome 11. Like Kv1.1 and Kv1.2, it is mainly located in the nervous system, highly concentrated along axons and in the axonal membrane [70]. Here, Kv1.4 can regulate the extent of nerve terminal depolarization. Some studies suggest that the phosphorylation of this channel could be implicated in the regulation of neuronal excitability, synaptic plasticity and neuronal survival [71].
- **Kv1.5 (*KCNA5*):** located in human chromosome 12, in a cluster with Kv1.1 and Kv1.6. Kv1.5 is expressed in many tissues, including but not limited to nervous system, circulatory system (cardiac and vascular), immune system (antigen presenting cells) and smooth muscle in general [72-75]. Accordingly, dysregulations or mutations of said channel may result in arrhythmias, pulmonary hypertension or increased proliferation of diverse cancer types.
- **Kv1.6 (*KCNA6*):** located in human chromosome 12, in a cluster with Kv1.1 and Kv1.5. Contrary to Kv1.1 and Kv1.2, which are located in the axonal membrane, Kv1.6 tends to be located in the soma of neurons. On a macroscopic level, Kv1.6 appears uniformly distributed around the bovine brain, as well as in cardiac tissue and smooth muscle [76-79]. Functionally, some studies have suggested the implication of Kv1.6 in the excitability of sensory neurons, but it has also been postulated to have a role in amyotrophic lateral sclerosis (ALS) [80, 81].
- **Kv1.7 (*KCNA7*):** located in human chromosome 19. Kv1.7 has been described to be expressed in heart and skeletal muscle, as well as the kidney and pancreas beta cells [82-84]. Functionally, it offers a potential strategy for enhancing GSIS with minimal risk of hypoglycaemia in the treatment of Type 2 diabetes [84].
- **Kv1.8 (*KCNA10*):** located in human chromosome 1, in a cluster with Kv1.2 and Kv1.3. Unlike the rest of the family, Kv1.8 is not only activated by voltage, but its gating is regulated by cyclic nucleotide [85]. Furthermore, its expression in brain is minimal, while being present in the hair cells of the inner ear, kidney and vascular tissues [86-88]. Studies have suggested its association with auditory dysfunction and LQTS (Long QT Syndrome) [85, 86].

These 8 *Shaker* isoforms represent 8 different phenotypes of the same family. However, the possibility of heterotetramerization opens up a large supply of different electrophysiologic, pharmacologic and distribution profiles. For example, Kv1.1 can tetramerize with Kv1.2, Kv1.3, Kv1.4 and Kv1.6 subunits [77], and Kv1.3 is able to interact with Kv1.1, Kv1.2, Kv1.5 and Kv1.6 [89, 90]. This already gives us up to 8 different combinations, not even counting the phenotype differences between **ratios** (1:3, 2:2, 3:1)

neither the formation of heteromers from 3 or 4 different isoforms, which is also possible [77]. The possibilities are endless. This promiscuity between subunits of the same family (a constant inside each family) and the presence of multiple ancillary proteins, which will be further discussed, are two potential mechanisms for generating the enormous diversity of K^+ currents observed electrophysiologically.

Even though in native cells, as explained, the limit between different isoforms is rather blurry, in the current work we will focus upon Kv1.3 and Kv1.5, which are the more prominent Kv1 channels in the immune system.

1.6. K_V1.3

Also known as *KCNA3*, MK3, HGK5, HLK3, PCN3, PCN3 and HUKIII; Kv1.3 is a member of the *Shaker* family of voltage-gated potassium channels. In summary, it contains six membrane-spanning domains with several positive charges in the fourth segment. It is part of the delayed rectifier class, directly implicated in the repolarization after an action potential. The *KCNA3* gene is intronless and located in chromosome 1, specifically 1p13.3, clustered together with *KCNA2* (Kv1.2) and *KCNA10* (Kv1.8).

1.6.1. Distribution

The gene was cloned simultaneously in 1990s from human **T lymphocytes**, resulting in a 575 amino acid-long protein [91] and from rat brain, resulting in a 525 amino acid-long protein [92].

In the **central nervous system** (CNS), Kv1.3 is located in hippocampal, olfactory bulb and cortex neurons (being the main potassium channel), dentate gyrus, striatum and piriform cortex and medial nucleus of the trapezoid body [90, 93-95]. Regarding **immune** system, Kv1.3 stands up as one of the most important channels in all the cells. As such, it is easily found in both types of lymphocytes (T and B); and macrophages and some of their specialized forms like microglia, dendritic cells and osteoclasts [96-99].

Aside from nervous and immune systems, Kv1.3 has been identified in a high amount of non-excitable cells regulating several cell physiology processes. Theses tissues include, but no limited, to platelets, epithelia of kidney and colon, actively participating in ion absorption/excretion; adipose tissue and skeletal muscle cells, associated with peripheral insulin response; smooth muscle; and testes [100].

1.6.2. Functional relevance

As expected from this wide distribution, Kv1.3 has an important role in several physiological processes. As other ion channels, Kv1.3 is implicated in regulating resting membrane potential and cell volume, but its role transcend these functions [101-103] (Fig. I4).

1.6.2.1. Immune function

Kv1.3 is present in all **immune** system cells – both antigen-presenting cells (APC), cytotoxic and regulatory cells – where it controls the leukocyte physiology.

When APCs (such as macrophages) contacts an antigen, CRAC channels open and leak Ca^{2+} from the ER to the cytosol. The high Ca^{2+} activates the K^+ channel $K_{Ca}3.1$ and, consequently, the change in membrane potential opens Kv1.3. This event marks the onset of APC activation and increases Kv1.3 (facilitating successive activations) and cell proliferation [99]. Similarly, other immune cells activated by antigen **presentation** of APC (T lymphocytes) express Kv1.3 clustered together with the TCR in lipid rafts. Lymphocytes, despite being of a different cell lineage that APCs (macrophage lineage), work in a very similar way. Thus, the antigen presentation triggers a rise in intracellular Ca^{2+}, which activates $K_{Ca}3.1$ and Kv1.3 [4, 96-98, 104].

An elevated Kv1.3 in the immune physiology generates more activated and aggressive cell phenotypes. As mentioned, and especially relevant for T helper lymphocytes, sequential activations alter the expression of ion channels. Thus, while naïve T lymphocytes express a modest amount of both Kv1.3 and $K_{Ca}3.1$, the more aggressive T helper effector memory cells (**T_{EM}**) express a huge amount of Kv1.3 [105]. Coincidentally, these T_{EM} mediate immune response in autoimmune diseases such as Multiple Sclerosis or Psoriasis [106].

It has been demonstrated that Kv1.3 is crucial in both normal and pathological immune cell physiology. On one side, both in vitro and in vivo studies indicate that pharmacological Kv1.3 **blockade** attenuates immune response and reduces thymic development of T cell subsets [107, 108]. On the other side, the interaction of Kv1.3 with modulatory proteins restricting its activity also compromises the activity of immune cells [109, 110].

As such, study of Kv1.3 and all its regulation pathways and potential pharmacological agents are potential **therapeutic** targets for the treatment of autoimmune diseases. This fact justifies the engineering of plenty new pharmacological entities for Kv1.3 blocking [111, 112].

1.6.2.2. Cancer

Kv1.3 takes part in the regulation of the cell proliferation/apoptosis balance in many cell types. This balance is one of the main factors that result in **neoplastic** growth and, ultimately, cancer.

Kv1.3 participates during the transient hyperpolarizing step during G_1/S progression. This hyperpolarization provides the driving force for Ca^{2+} entry during this phase of cell cycle [113]. Furthermore, evidences have suggested that Kv1.3 could modify cell **proliferation** independently of ion conduction by voltage-dependent conformational changes or by phosphorylation of the channel [114]. Thus, Kv1.3 would promote cell proliferation.

Other studies suggested Kv1.3 implication in cell **survival**. Kv1.3 is since long known to localize in the inner mitochondrial membrane [115]. In the **mitochondria**, Bax can interact with Kv1.3, being this interaction a *condicio si ne qua non* for provoking apoptosis by Kv1.3 inhibition [116]. Thus, absence of Kv1.3 would result in an increased survival of cells.

As seen, the role of Kv1.3 in cancer is very complex, as either an upregulation or downregulation may result in neoplastic formation. Nevertheless, a hypothesis was recently postulated. Such hypothesis suggests that proliferative activity, considered as primary **tumorigenesis**, would involve upregulation of Kvs (including Kv1.3); while invasion, or secondary tumorigenesis, courses with Kv downregulation, promoting the pro-invasive activity of voltage-gated sodium channels [103, 117].

1.6.2.3. Insulin pathways

During early 2000s, a Kv1.3-deleted mouse was genetically engineered in expectations of high affectations in immune system. Contrarily, KO mice had a normal immune phenotype, caused by a remodelling of a plethora of other different Kv channels that could counteract Kv1.3 deficiency [118, 119]. Instead, mice exhibit 1,000-fold higher sensitivity of detection of odours and enhanced ability to discriminate between odorants. Animals were named "the ***super-smeller mice"***. Furthermore, these mice exhibited a resistance to diet-induced obesity.

After more intensive studies, these two unexpected phenotypes raised an interesting hypothesis: the resistance to diet-induced obesity came from an increase in physical activity and basal **metabolic rate**, which depends on the olfactory bulb [120]. This process would include the activation of the insulin receptor in the olfactory bulb, resulting in an inhibitory-phosphorylation of Kv1.3 [121]. Loss of function of Kv1.3, either by genetic ablation or inhibition by antagonists such as kaliotoxin, confers mice with resistance to diet-induced obesity and an improvement in mood and **associative learning**. These studies could support Kv1.3 as a target not just for obesity, but also for psychiatric diseases [122]. In fact, several projects are already in motion for the use of Kv1.3 blockers in palliating the effects of neurodegenerative disorders [122, 123].

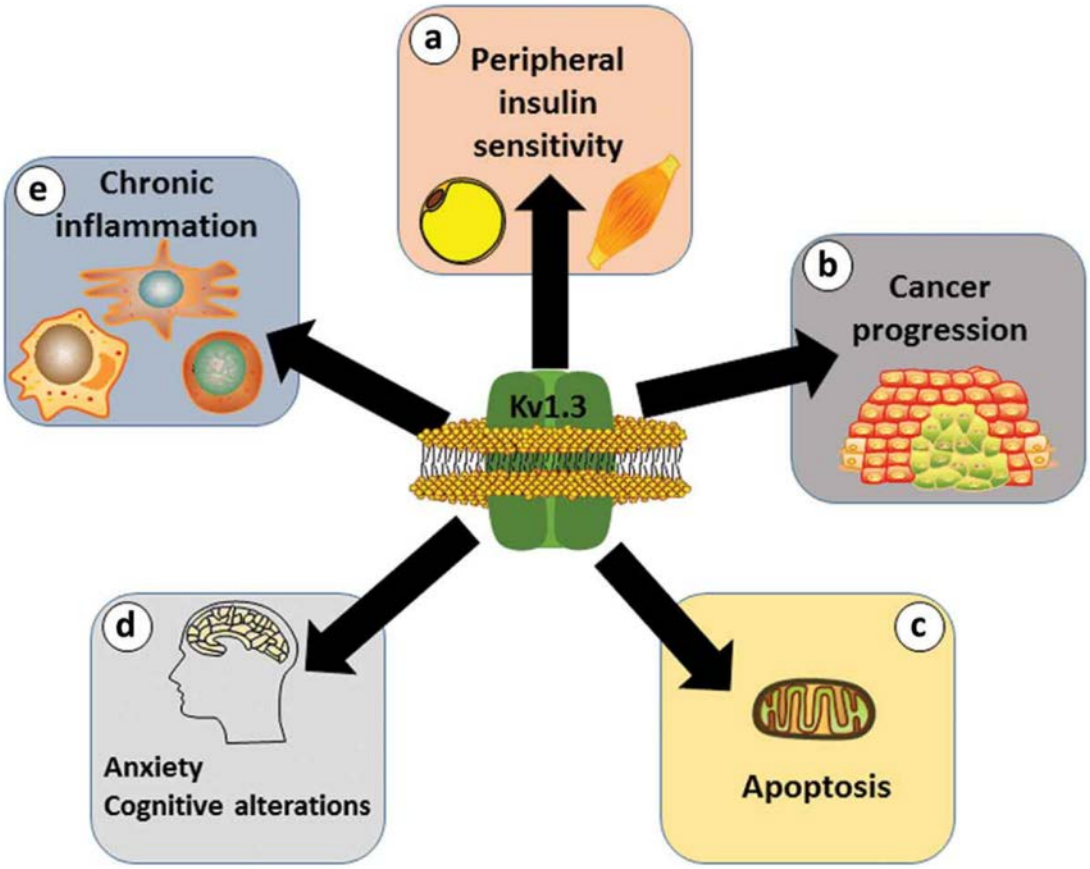

Fig.I4: *Implication of Kv1.3 in various physiological and pathological processes [103].* ***A:*** *Impaired Kv1.3 expression alters adipocyte and skeletal muscle insulin sensitivity.* ***B:*** *Most evidences support that the expression of Kv1.3 correlates with neoplastic behaviour and malignancy.* ***C:*** *Kv1.3 is present in the inner membrane of mitochondria, regulating the sensitivity to apoptosis.* ***D:*** *Abnormal activity of Kv1.3 in the central nervous system during insulin resistance has been associated to the development of cognitive alteration and anxiety.* ***E:*** *An exacerbated expression of Kv1.3 in activated immune cells triggers chronic and degenerative inflammatory diseases.*

Kv1.3 is expressed in other tissues where insulin sensitivity is of paramount importance, such as the adipose tissue [124]. Kv1.3 has been documented in both white and brown adipocytes [125, 126]. Pharmacological inhibition of the channel increases the peripheral sensitivity to insulin by promoting the membrane translocation of GLUT4 [127-129]. Some other reports argue against the presence of Kv1.3 in human adipose tissue [120, 127]. As such, the participation of Kv1.3 in the glucose homeostasis in adipose tissue is an open **debate** nowadays and most probably should be looked at by considering adipose tissue as a true heterogeneous organ [124]

1.6.3. Molecular properties

Kv1.3 has a biogenesis similar to other Kv channels. Thus, it is synthetized by ribosomes that get attached to the ER by a signal peptide on its S2 domain, contrary to usual membrane proteins, which have an N-terminal signal [38]. Kv1.3 anterograde traffic is also similar to other membrane proteins, except for the necessity of having the YMVIEE signal in its C-terminus. **YMVIEE**, as commented in a previous chapter, contains a di-acidic element located in the C-terminus of some Kv1 channels being necessary for the anterograde transport. This sequence interacts with Sec24D, an element of the COPII machinery, which drives Kv1.3 onward from the ER to the Golgi network. If such signal is absent or masked, Kv1.3 impairs the membrane expression and gets retained intracellularly [47].

Like other Kv channels, Kv1.3 is activated by depolarization of the membrane. The half-activation voltage is -35 mV. Kv1.3 shows a maximum peak of conductance about 10 ms after the depolarizing stimulus and exhibits marked **C-type** and **cumulative** inactivations. The cumulative inactivation consists in a progressive decrease in the potassium current after the application of repetitive depolarizing pulses. Kv1.3 channel typically shows a conductance of about 13 pS [130, 131].

Kv1.3 pharmacology is very specific. Typical **blockers** of potassium channels like quinidine, 4-aminopiridine and TEA can inhibit Kv1.3. However, derivatives from benzamide or 5-(4-phenyl-butoxy) psoralen (Psora-4) are more potent blocking Kv1.3 [112, 132]. Regardless, the most powerful blockers for Kv1.3 have been developed from natural venoms. Margatoxin (*Centruroides margaritatus*), charybdotoxin (*Leiurus quinquestriatus*) and Pi2 and Pi3 toxins (*Pandimius imperator*) come from scorpion venom [139]. Additional **venom-derived blockers** include α-dendrotoxin (*Dendroaspis angusticeps*) from snakes or Shk (*Stichodactyla helianthus*) from anemone [133-135]. Kv1.3 already-mentioned implication in several systems has really encouraged research in derivatives of the afore-mentioned blockers hoping for the discovery of a highly selective and safe blocker for the treatment of autoimmune or neurodegenerative disorders or cancer [103].

Kv1.3 may form **heterotetramers** with members of the *Shaker* family like Kv1.1, Kv1.2, Kv1.4, Kv1.5 and Kv1.6 in several tissues [74, 136-138]. As a result of these interactions, the properties of the channel get modified depending on the stoichiometry of the complex [109]. Thus, different ratios of subunits are expressed in different physiological states of the tissues.

Additionally, Kv1.3 is able to interact to plenty of **regulatory** subunits that modulate its traffic and electrophysiological properties. Amongst such subunits, KCNE4 stands out as a

potent negative regulatory peptide. KCNE4 is a member of the KCNE family and will be further discussed.

1.7. K_V1.5

Also known as ***KCNA5***, ATFB7, HCK1, HK2, HPCN1 or PCN1, Kv1.5 is also a member of the *Shaker* family. Kv1.5 is located in the chromosome 12, in 12p13.32, in a cluster with Kv1.1 and Kv1.6.

1.7.1. Distribution

Like Kv1.3, Kv1.5 plays an important role in **immune** system, especially in antigen-presenting cells such as macrophages and B lymphocytes [109]. Although it can be found in other lymphocytic subtypes, its expression is very minor and sometimes almost undetectably.

Kv1.5 has a paramount position in **muscle** tissues. It is expressed in heart, in both atria and ventricles, and in vascular muscle [72, 73, 75]. Additionally, smooth muscle tissues, such as intestine and airways epithelia, also have a remarkable Kv1.5 expression [139, 140].

Regarding other tissues, Kv1.5 can be found in kidney, lung, pituitary and brain. Although it is abundantly expressed in the **brain tissue** and spinal cord, it is not found in peripheral nerves [141-143].

1.7.2. Functional relevance

In immune cells, Kv1.5 typically plays a role of **physiological balance** against Kv1.3 [109]. While Kv1.3 has a prominent membrane trafficking and exhibits a threshold for activation of about -30 mV, Kv1.5 is mostly retained in the ER and has a more positive voltage of half-activation. Although Kv1.5 expression is normally constant under different degrees of immune activation, Kv1.3 expression increases and, as such, the excitability and aggressiveness of immune cells grows. Kv1.5 expression is usually linked to less aggressive phenotypes [109].

Kv1.5 is expressed more abundantly in atrial myocytes, where it is the responsible for the ultrarapid-activating K^+ current in heart (IK_{UR}) [144]. In normal situations, the activity of Kv channels in heart puts an end to action potential by repolarizing the membrane [145]. Thus, it is not surprising that loss-of-function mutations of Kv1.5 have been reported to cause **atrial fibrillation** [146].

Like Kv1.3, Kv1.5 is implicated in cell cycle regulation [113]. Kv1.5 expression changes during the cell cycle progression with a peak of expression during the G_1/S phase [147]. It is also involved in proliferation of oligodendrocytes, astrocytes, hippocampal microglia, macrophages and myoblasts [148-152]. Additionally, Kv1.5 is aberrantly expressed in many human **cancers** [113].

Kv1.5 has also been suggested to be involved in **volume regulation** in spermatozoa [153] and affections in other tissues such as chronic mechanical stress [154], hyperoxia [155] or hypothyroidism [143].

1.7.3. Molecular properties

Kv1.5 biogenesis is similar to other Kv channels [38]. Unlike Kv1.3, however, Kv1.5 does not traffic efficiently to the membrane and presents a notable ER retention. Unlike Kv1.3, the reason for this fact seems to be that Kv1.5 lacks the **YMVIEE** signal or any similar sequence in its C-terminus [47].

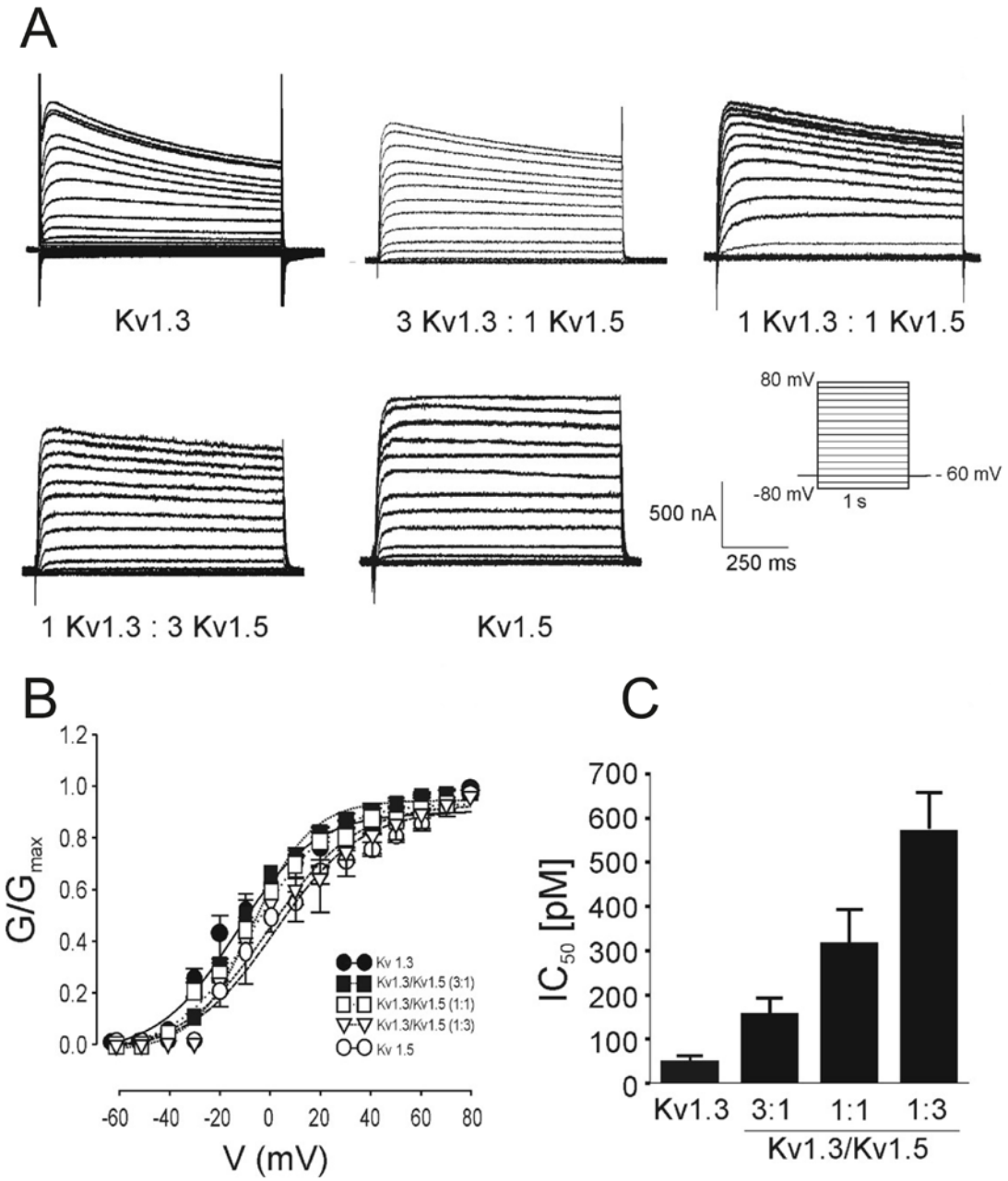

Fig. I5: *Expression of different ratios of Kv1.3 and Kv1.5 in Xenopus oocytes [74].* ***A:*** *Representative traces of K^+ currents evoked in oocytes injected with different ratios of Kv1.3 and Kv1.5.* ***B:*** *Plot of normalized conductance against test potential.* ***C:*** *IC_{50} for margatoxin-sensitive K^+ currents in homo-(Kv1.3) and various heterotetrameric (Kv1.3/Kv1.5) channels.*

Kv1.5 is activated by depolarization of the membrane having a half-activation voltage of **-14 mV** [156]. Unlike Kv1.3, Kv1.5 does not present such marked cumulative and C-type inactivations, but some studies have reported that, at physiological conditions, Kv1.5 presents some C-type inactivation [156]. Kv1.5 channel shows a conductance of 8 pS.

Kv1.5 is inhibited by non-specific typical K^+ channel **blockers** such as 4-aminopiridine, TEA or quinidine. Regarding specific inhibitors, unlike Kv1.3, Kv1.5 does not have efficient and

selective blockers. For instance, Psora-4 inhibits Kv1.5 (EC_{50}= 7.7 nM), but also Kv1.3 with a higher efficiency (EC_{50}= 3 nM) [112]. Being implicated in the correct function of the heart, there are currently plenty of research trying to develop selective blockers against Kv1.5 [157].

Kv1.5 can form **heteromeric** structures with other *Shaker* subunits such as Kv1.3 and Kv1.4 [138, 158]. Kv1.5 has been described to be able to interact with β subunits Kvβ1.2, Kvβ1.3 and Kvβ2.1, which shift the steady-state activation and inactivation curves to more negative potentials [173]; and Kvβ3.1, which triggers a very fast inactivation [159].

1.8. K_V1.3/K_V1.5 HETEROTETRAMERS

The **promiscuity** of Kv subunits results in the formation of a wide selection of different channel phenotypes. In recent years, the discovery of the Kv1.3/Kv1.5 heteromeric channel has brought a new perspective to the molecular physiology of immune cells, where both subunits share expression [74, 109].

Early 2000s, some studies on Kv channels expression described that presence of both Kv1.3 and Kv1.5 in macrophages. Thus, it was suggested the possibility of both subunits forming a heteromeric channel [109]. Later on, the association between Kv1.3 and Kv1.5 in macrophages was certified [74]. This interaction modifies the traffic and retains the complex intracellularly [89]. Additionally, the half-activation voltage and pharmacology of the heteromeric channel show an **intermediate phenotype** to those of the homomeric tetramers [74] (Fig. I5).

This interaction has physiological relevance because, as previously mentioned, both isoforms are present in immune cells (notably in mononuclear phagocytic cells). When leukocytes get activated, they increase the expression of Kv1.3 keeping Kv1.5 stable. A higher amount of Kv1.3 displaces Kv1.5 in the tetramer and, thus, the complex has more Kv1.3 in their compositions. More units of one isoform shift the properties of the channel to those of the dominant isoform. Therefore, Kv1.3, with a lower threshold of activation, generates more easily activated cells. This fact is also supported by the correlation between Kv1.3 expression and aggressiveness in the different degrees of activation of immune cells. In contrast, it is also interesting to consider that dexamethasone, a typical **immunomodulatory** agent, reduces Kv1.3 expression, shifting the tetramer ratios to Kv1.5-dominant [151]. Finally, this interaction can also have additional relevance in the case of cancer, as several neoplastic tissues show altered expression of one or both isoforms.

The study of the heterotetramer in its different ratios and its potential interactions is thus of paramount importance in the study of the molecular physiology of both **autoimmune diseases** and **cancer** and a potential source of future treatments.

1.9. KCNE FAMILY

There are several ancillary proteins that interact with Kv1.3. Among them the most relevant are the **KCNE** and KCNAB families.

The KCNE family (Potassium voltage-gated channel subfamily E), which is subject of the study in the present memory, is a group of single-transmembrane-domain proteins which cannot form pores. Regardless, the KCNE family proteins can interact with alpha subunits and

modify several properties of the channel, such as electrophysiological characteristics or traffic.

The KCNE family contains 5 isoforms. In this work we will focus on **KCNE4** and **KCNE1**.

1.9.1. KCNE1

Also known as ISK, JLNS, JLNS2, LQT2/5, LQT5 or MinK; KCNE1 is the first member of the KCNE family. *KCNE1* is located in the chromosome 21 at 21q22.12 [160]. KCNE1 is mainly expressed in both atria and ventricles of **heart**, but it can also be found in the inner ear and kidneys.

KCNE1 was firstly identified as a component of the cardiac $\mathbf{I_{KS}}$ current [161, 162]. This I_{KS} current was later characterized as being KCNE1 regulating **Kv7.1** when expressed in *Xenopus* oocytes, which express Kv7 subunits endogenously. This regulatory subunit enhances the current density of Kv7.1 by potentiating single channel conductance. Additionally, KCNE1 shifts Kv7.1 voltage-dependence of activation to more depolarized potentials, slows the channel kinetics and removes the inactivation. Furthermore, KCNE1 confers the cAMP pathway-dependent modulation characteristic of I_{KS} [161, 163, 164].

Even though the most important partner of KCNE1 is Kv7.1, KCNE1 share the characteristic promiscuity of β subunits. As such, KCNE1 is able to interact with Kv11.1 [165], generating the I_{KR} current. Preliminary evidence suggests that KCNE1 also interacts with **Kv1.5** (Fig. I6). The nature of this interaction has not been unveiled yet [166].

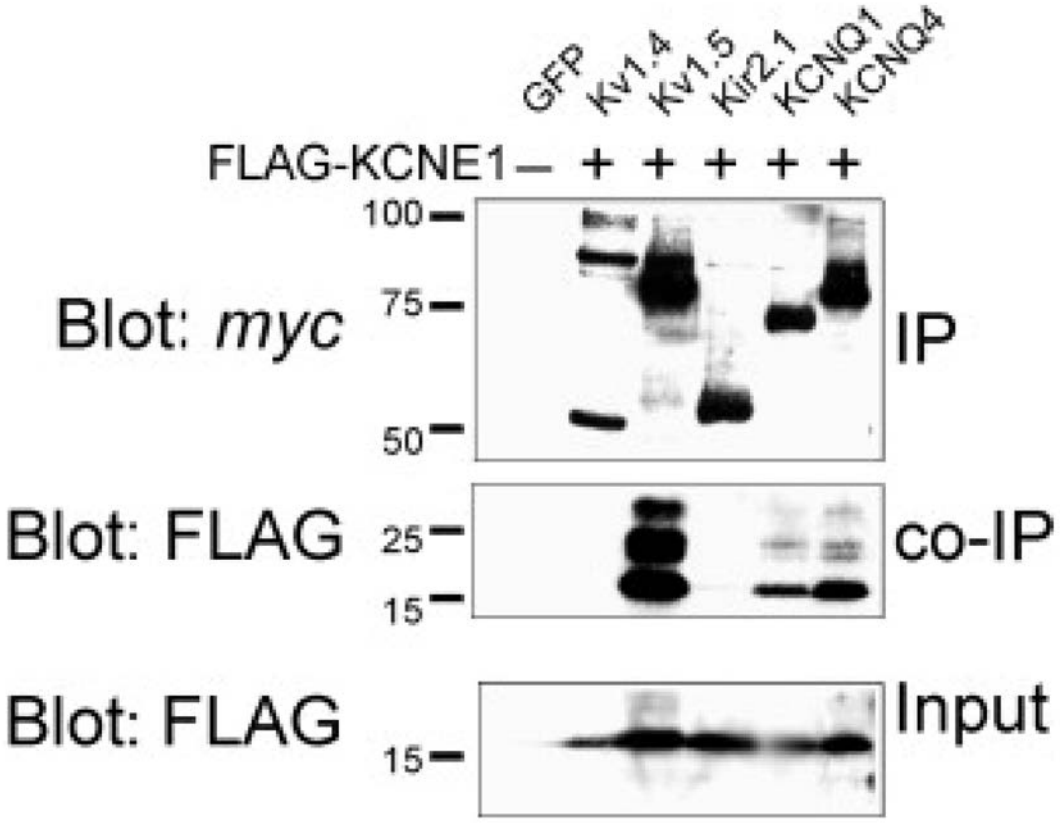

Fig. I6: *Co-immunoprecipitation of KCNE1 to several K^+ channels [166].*

1.9.2. KCNE4

Also known as MIRP3 (MinK-related peptide 3), KCNE4 is the largest member of the KCNE family, having a long C-terminus domain divergent from the family. *KCNE4* is located in chromosome 2 at 2q36.1. KCNE4 is notably expressed in cardiac and skeletal muscle, uterus and kidney. KCNE4 is also expressed, albeit in minor concentrations, in placenta, lung, liver, brain and blood cells. Notably, KCNE4 is present at diverse concentrations in **leukocytes**, such as macrophage and lymphocyte cells [167-170].

KCNE4 was firstly described as a modulatory subunit to Kv7.1, acting as a **dominant-negative** partner. This result was observed in both *Xenopus* oocytes and HEK-293 cells. Additionally, KCNE4 also inhibits Kv1.1, Kv1.3, K_{Ca}1.1 and Kv4.2 channels [167-169, 171-173].

KCNE4 modulates Kv1.3 **traffic**, **membrane surface** and **electrophysiological kinetics**. Extensive research has deciphered the molecular determinants implicated in this interaction. The folded structure of KCNE4 C-terminal domain identifies the region of the Kv1.3 interaction. Coincidentally, this KCNE4 C-terminus interacts with the C-terminus of Kv1.3, which concentrates several forward trafficking motifs: HRETE and YMVIEE. Thus, the interaction could hinder the capacity of Kv1.3 trafficking forward [110, 160].

It has been above mentioned the implication of the proximal **C-terminus** in the gating of the channels. Logically, it does not come as a surprise that the compromise of this region by the interaction with a regulatory subunit would modulate the electrophysiological properties of the channel. Evidence demonstrates that KCNE4 is not able of interacting with Kv1.5 [110, 168]. However, a specific study supports this interaction [174]. Thus, this interaction remains open to **debate** and will be examined during the discussion.

OBJECTIVES

2. OBJECTIVES

The voltage-dependent potassium channel Kv1.3 plays an important role in the physiology of the immune system, as well as with other important cellular processes. In addition, Kv1.3 may form heteromeric channels with Kv1.5, which modulates the function of the complex. Kv1.5 alters the traffic, activity and pharmacological profile of Kv1.3. These changes depend on the subunit stoichiometry of the functional complex. The composition of heterotetramers is difficult to control both in native cells or heterologous models because subunits, which are under differential regulation, freely interact while being synthesised.

Kv1.3 and Kv1.5 interact to each other mostly via the tetramerization domain. However, the complexity of the channel structure suggests that other interactions can occur that have not been discovered yet. *In silico* research have gained great relevance in drug discovery because of its reduced costs. Therefore, deciphering putative interactions which govern the function of the channel is crucial.

Pore forming subunits are also able to interact with regulatory subunits. Kv1.3 may interact with KCNE4, which impairs many features of the channel. In these context, Kv1.3/Kv1.5 heterotetramers share tissue expression with KCNE4. However, KCNE4 does not associate with Kv1.5. Therefore, we wonder whether KCNE4 could modulate hybrid Kv1.3/Kv1.5 channels. On the other hand, KCNE1, a regulatory subunit of paramount importance in the generation of cardiac I_{KS} currents, was discovered in T-lymphocytes. KCNE1 interacts with Kv1.5 with unknown effects.

Because all these interactions may affect the functionality of the complex, potentially modifying the development or treatment of autoimmune diseases, in the present dissertation we aimed to study:

- Intramolecular interactions of the Kv1.3-Kv1.5 heterotetramer.
- Effects of regulatory subunits on the Kv1.3 and Kv1.5 channels.
- Genetic study of these channels subunits in human samples from multiple sclerosis patients.

METHODOLOGY

3. METHODOLOGY

3.1. CELL CULTURE

3.1.1. Cell lines

- HEK 293: Human embryonic kidney cells 293 are a cell line originally generated by transformation of normal human embryonic kidney cells with adenovirus 5 DNA by Alex van der Eb's laboratory in Leiden [175]. This transformation came to be by inserting around 4.5 Kb from the left arm of the viral genome, which incorporated into human chromosome 19 [176]. Even though they have been considered for some years to be a product of transformed fibroblastic or epithelial cells, they are also speculated to be from neuronal lineage because of many of their properties [177]. It is the main cell line used in heterologous expression in the present work due to its scarce expression of ion channels and its simplicity of culture and transfection.
- Jurkat: Immortalized strain of human T lymphocyte cells initially generated from the peripheral blood of a 14-year old boy with T cell leukaemia [178]. It is generally used as a model to study both T cell leukaemia and T cell gene expression and signalling. In the present work, it is used as a native model with expression of both Kv1.3 and KCNE4.
- CY15: Immortalized cell line of murine histiocytic tumour isolated from an IFNγ$^{-/-}$ mouse. The morphology and surface marker phenotype resemble thus of immature dendritic cells. Said cell line is able to take up antigens and stimulate T lymphocytes, although with less effectivity than its normal counterparts [179]. In the present work, it is used as a native model with expression of heterotetramer-forming Kv1.3 and Kv1.5; as well as regulatory subunit KCNE4.
    - CY15 LvE4: CY15 cell strain with genetically reduced expression of gene KCNE4 by lentiviral infection previously developed at our research group [180].

3.1.2. Cell lines culture

- HEK 293: HEK 293 were cultured in DMEM (Dulbecco's Modified Eagle Medium, Lonza) supplemented with 4 mM of L-glutamine, 10% FBS (Foetal Bovine Serum, Nibco®) and 1% Pen Strep (Penicillin & Streptomycin, Gibco). When passing the cells, they were washed with PBS and then incubated with 1 mL of Trypsin (Gibco) for 5 minutes to detach them. Trypsin was inactivated with culture media and suspended cells were precipitated by centrifugation at 400 g for 4 minutes. Precipitated cells were resuspended in culture media and seeded in new flasks or dishes.
- Jurkat: Jurkat cells were cultured in RPMI (Roswell Park Memorial Institute, Lonza) supplemented with 10% heat-inactivated (56ºC for 30 minutes) FBS and 1% Pen Strep. When passing the cells, they were collected from the original flask and seeded in new flasks.

- CY15: CY15 cells were cultured in RPMI supplemented with 10% heat-inactivated FBS and 1% Pen Strep. When passing the cells, they were washed with PBS and then scraped from the dish. Cells were then collected from the original dish and seeded in new ones.

Cells were used for up to 20 passes. All cell lines were grown at 37ºC and 5% CO_2.

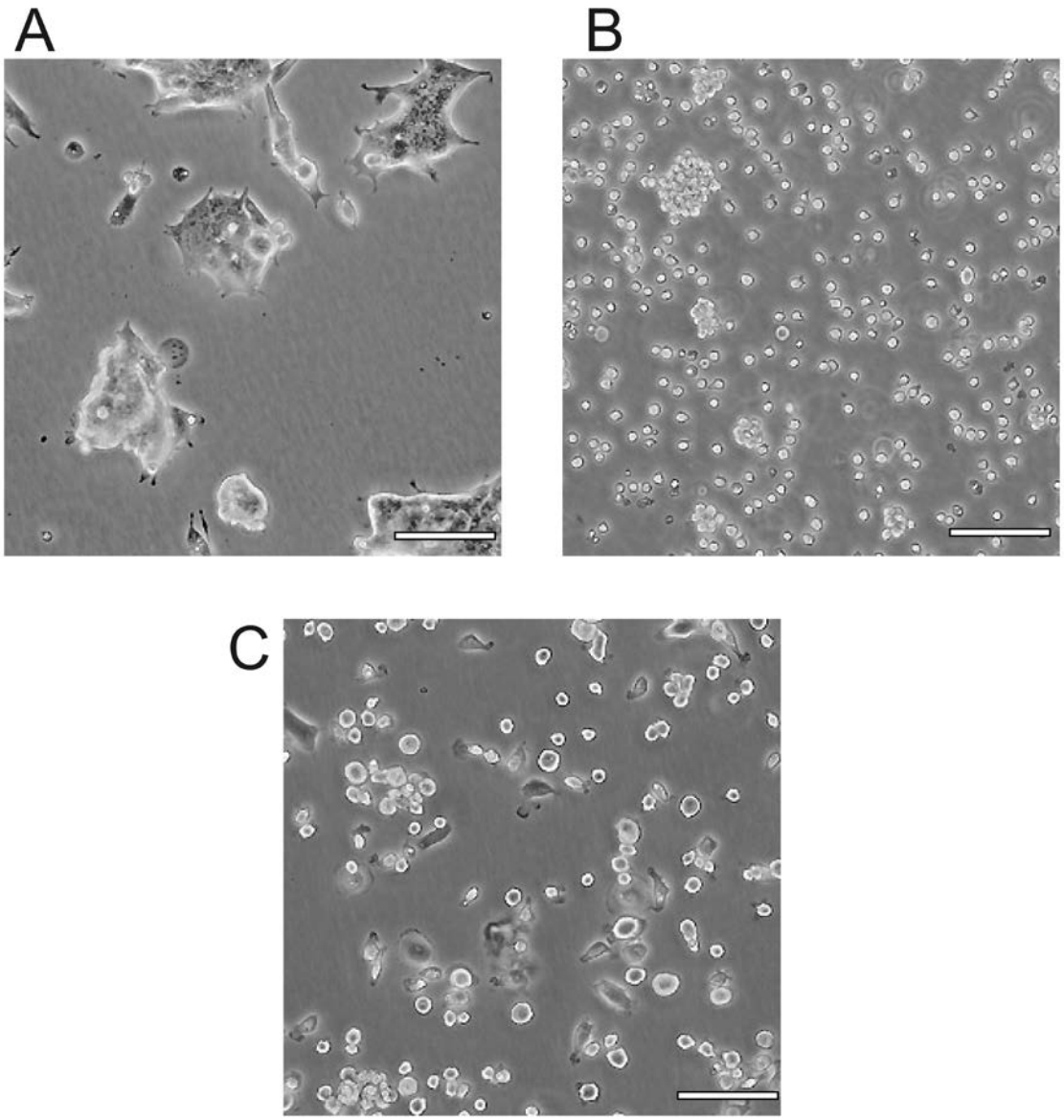

Fig. M1: *White field Images of the cell lines used in the present thesis (ATCC: https://www.lgcstandards-atcc.org/).* ***A:*** *HEK 293 cells.* ***B:*** *Jurkat T lymphocytes.* ***C:*** *CY15 dendritic cells.*

3.1.3. Cell line freezing and thawing

Freezing

Protocol for freezing the different cell lines begins similar to how they are passed until the cells are detached

- HEK 293: As HEK 293 cells are detached with trypsin, 5 mL of culture media were added to inactivate it and cells were precipitated by centrifugation at 400 g for 4 minutes. Precipitated cells were resuspended in freezing media.

- Jurkat: As Jurkat cells don't attach themselves to the flasks, they were directly collected from it and precipitated by centrifugation at 400 g for 4 minutes. Precipitated cells were resuspended in freezing media.
- CY15DC: After being scraped from the dish, CY15 cells were precipitated by centrifugation at 400 g for 4 minutes. Precipitated cells were resuspended in freezing media.

All cell lines were collected in cryogenic vials and placed in a room temperature pre-chilled cooler. Cells were kept for 2-3 days at -80ºC and finally stored with liquid N_2.

Thawing

To thaw the cells, 1 mL of complete media was added to the cryogenic vial where they were stored. The cellular suspension was mixed with additional 8 mL of complete media and precipitated by centrifugation at 400 g for 4 minutes. Precipitated cells were resuspended with culture media and seeded in a 10 cm diameter dish. Culture media was replaced the following day.

3.1.4. Cell transient transfection

Depending on the subsequent protocol, HEK 293 cells were transfected with either linear PEI (Polyethyleneimine, TCI chemicals), Lipotransfectin ® (Niborlab), or FuGENE® 6 (Promega).

PEI

PEI was used when transfecting cells for confocal microscopy. PEI is a stable cation polymer with repeating unit composed of the amine group and two-carbon aliphatic CH_2CH_2 spacer. PEI condenses DNA into positively charged particles, which easily binds to the anionic residues in the cell surface and promotes their endocytosis. Once inside the cell, protonation of the amines provokes an influx or counter-ions, lowering the osmotic potential. This event results in the burst of the vesicle, liberating the polymer-DNA complex, which eventually separates and enables the free diffusion of the DNA to the nucleus. Although is a highly economic reagent, it is also important to note that has a narrow window between its transfecting concentration and its toxic concentration.

To execute the protocol, 500 ng of DNA (otherwise stated) and 2.4 µL of 2 mg/mL PEI were mixed in parallel with 150 mM NaCl to a final volume of 50 µL. After an incubation of 15 minutes, the PEI mix was added dropwise to the DNA mix and further incubated for 30 minutes. After this incubation, the mix was added to the 35 mm dish or 6-well multiwell for 4-6 hours, after which the culture media was replaced. 24-30 hours after the transfection, cells were used to mount the microscopy samples.

Lipotransfectin®

Lipotransfectin® was used when transfecting cells for Western Blotting and other biochemistry assays (immunoprecipitation, lipid rafts or surface protein biotinylation). Lipotransfectin® is a transfection reagent based in cationic lipids with colipids in suspension. It works in a similar fashion to PEI but combined with technology that regulates the separation between the polymer and the DNA, optimizing its toxicity profile.

The protocol started by mixing 4 µg of DNA (otherwise stated) and 12 µL of Lipotransfectin® in parallel not-supplemented DMEM up to a final volume of 700 µL. After incubating for 5 minutes, the DNA mix was added to the Lipotransfectin mix, pipetted up and down 10 times and further incubated 20 minutes. After this incubation, the mix was added dropwise to the dish for 4-6, after which the culture media was replaced. 24 hours after the transfection, cells were used for biochemistry assays.

FuGENE®

FuGENE® 6 was used when transfecting cells for electrophysiology experiments. FuGENE® 6 is a non-liposomal formulation designed to transfect DNA into a wide variety of cell lines with high efficiency and low toxicity.

The protocol started by mixing 1.5 µL of FuGENE® 6 were mixed with not-supplemented DMEM up to a final volume of 100 µL minus the volume of DNA and incubated for 5 minutes. On an additional microcentrifuge tube, 300 ng of DNA was added and the FuGENE mix was later combined. After an additional incubation of 20 minutes, the mix was added to the 35 mm dish or 6-well multiwell. In this protocol, it is not advisable the replacement of the media.

3.2. MOLECULAR BIOLOGY

3.2.1. Relevant kits

DNA Extraction kit

During the course of this work, a diverse amount of kits was used to extract DNA from bacteria, eukaryotic samples or gels:

- Bacteria: Kits used for plasmid extraction from bacteria were the GenElute™ Plasmid Miniprep kit (Sigma-Aldrich, PLN350) and GenElute™ Plasmid Midiprep kit (Sigma-Aldrich, PLD35-1KT) (Annex A).
- Eukaryotic samples: PureLink™ Genomic DNA Mini kit (Invitrogen, K182001) was used for the extraction of genomic DNA from the brain samples of multiple sclerosis patients (Annex B).
- Gel: ATP™ Gel/PCR Extraction kit (ATP Biotech, ADF100) was used for the extraction of DNA from agarose gels or PCR mixes (Annex C).

Mutagenesis

All mutagenesis reactions were performed using the QuikChange Lightning Site-Directed Mutagenesis kit (Agilent Technologies, #210519) (Annex D).

Isolation of surface proteins

For the isolation of surface proteins, we used the Pierce™ Cell Surface Protein Isolation kit (Thermo Scientific™, 89881). This kit's approach consists in the biochemical binding of biotin to the surface proteins of living cells. After the lysis of the cells, proteins are incubated with agarose beads-bound NeutrAvidin (a deglycosylated form of native avidin with high affinity to biotin, Thermo Scientific™) (Annex E).

3.3. BIOCHEMISTRY

3.3.1. Total protein extraction

Total protein extraction was performed to analyse protein expression in different samples. The experiment starts with cells plated in 10 cm diameter dishes and is developed in all its stages in cold by incubation of all dishes and tubes in ice.

Plated cells were washed twice with PBS and scrapped in 0.5 mL of Protein Lysis Buffer with protease inhibitors added. Lysates were homogenated 10 times with a 25 G needle. Lysates were incubated at 4ºC for 10 minutes and centrifuged at 16,000 g for 10 minutes. Supernatant was collected, while the pellet was discarded as it contained cell debris and non-lysed cells.

3.3.2. Bradford assay

Bradford assay was used to determine protein concentration (Protein Assay Dye Reagent Concentrate, Bio-Rad) in samples.

1 mL of the Bradford reagent was mixed with 1-2 µL of sample or 2-20 µL of 0.1% BSA as a standard in semi micro cuvettes. After mixing and incubating for 10 minutes, absorbance was measured at 595 nm.

Samples were processed by SDS-PAGE or stored at -20ºC.

3.3.3. Western blotting

Samples were prepared by mixing 50 µg of total protein with protein loading buffer to a final volume of 50 µL and boiled for 5 minutes. Denaturalized proteins were separated by SDS-PAGE in a polyacrylamide gel which was polymerized by preparing both running and stacking fractions of the gel.

After the electrophoresis (120 V), gel content was transferred to PVDF membranes for 2 hours at 360 mA in cold temperature. Said membranes were incubated in blocking solution for 1 hour at room temperature.

Then, blocked membranes were incubated overnight at 4ºC with a primary antibody and washed four times for 5 minutes with PBS Tween. They were incubated for 1 hour with a secondary antibody specific for the species and conjugated to HRP (Horseradish peroxidase) of the primary antibody and washed again.

Finally, membranes were incubated with ECL (enhanced chemiluminescence), a peroxidase substrate containing luminol, and exposed to a LAS 3000 machine (Fuji) to detect the signal. Images of different time exposures were taken to ensure that intense not-saturated images were gotten. In case any experiment was to be quantified, it was performed using Fiji (Fiji is just ImageJ).

3.3.4. Immunoprecipitation

Immunoprecipitation assays were performed to evaluate protein interactions. Target proteins were either pulled down or retained with their partners using specific antibodies. Said antibodies were bound using sepharose beads coated with protein G or A (GE

Healthcare). Protein G and G have different affinities to the constant fraction of immunoglobulins, so they were used following manufacturer's instruction. All the procedure was performed in cold.

As Protein A/G are preserved in 20% ethanol, 400 µL of PBS buffer were added to clean the ethanol. The suspension was centrifuged at 5,000 rpm for 30 seconds and the supernatant, discarded. This step was repeated twice.

Column protocol

1. Column preparation:
    a. 50 µL of Protein A/G were added to a Micro BioSpin™ Column (Bio-Rad) with 500 µL of PBS and the antibody (4 ng antibody/mg of protein to load to the column). Mix was incubated for 1 hour at room temperature.
    b. Column was eluted by centrifugation at 1,000 g for 30 seconds and washed twice with 500 µL of borate buffer.
    c. 2.6 mg of DMP dissolved in 500 µL of borate buffer was added to each column to crosslink the antibody to the protein A/G. Mix was incubated for 30 minutes at room temperature.
    d. Column was washed 4 times with 500 µL of TBS to remove the DMP excess.
    e. Column was washed 4 times with 500 µL of glycine 0.2 M pH 2.5 to stop the DMP reaction.
    f. Column was washed 3 times to TBS. Finally, the column can be stored with 500 µL of TBS and 1.25 µL of sodium azide at 4ºC or it can be already used.
    g. Additional mock columns (with no antibody) were prepared to act as negative controls for each condition.
2. Protein extraction was performed as previously described, albeit with some modifications. A different lysis buffer was used (IP Lysis Buffer), but protease inhibitors were added regardless; and the samples were not homogenated.
3. After the Bradford assay, a minimum of 1 mg per condition was pre-cleaned with protein A/G. Pre-clean consists in an incubation of 90 minutes at 4ºC to reduce the unspecific binding of proteins to both the protein A/G and the sepharose beads. After the incubation, beads were precipitated by centrifugation at 1,000 g for 30 seconds and supernatant was transferred to the prepared column. In parallel, the starting material (SM) was prepared with protein loading buffer as already described.
4. The column with the sample was incubated for 2 hours at room temperature and finally centrifuged. The flow-through, which is considered the non-bound fraction (supernatant or SN), was stored at -20ºC and it would be loaded to the gel for later analysis. The supernatant (SN) was prepared by mixing 80 µL of non-bound fraction with 20 µL of protein loading buffer. The column is then washed 5 times with IP wash buffer column.
5. The column was finally eluted by the addition of 100 µL of 0.2 M Glycine pH 2.5, which released the target protein from the antibody. The flow-through would be the bound fraction (immunoprecipitation or IP), which is prepared by mixing it with 20 µL of protein loading buffer.

6. Prepared samples of SM, SN and IP were then loaded in a polyacrylamide gel for its analysis by western blotting.

Microtube protocol

In some experiment conditions, notably in native cells (Jurkat and CY15DC), performing the immunoprecipitation not in the columns, but in microcentrifuge tubes seemed to work better. The basis of the technique is the same, but some buffers and procedures are slightly different.

1. Protein A/G preparation:
    a. 50 µL of Protein A/G in a microcentrifuge tube were incubated at 4ºC for 3-4 hours in the presence or absence of the specific antibody (4 ng per mg or protein) in a volume of 300 µL of IP wash buffer old.
    b. After the incubation, beads were centrifuged at 5,000 rpm for 30 seconds. Supernatant was discarded, and beads washed with 400 µL of IP wash buffer old. After this step, the beads are prepared.
2. Protein extraction was performed as already described for the column protocol.
3. After the Bradford assay, a minimum of 1 mg per condition was pre-cleaned with protein A/G. Instead of 90 minutes, pre-clean lasted for 3-4 hours at 4ºC.
4. After the pre-clean, sample was centrifuged, and supernatant was transferred to the prepared protein A/G microtube. Incubation in this case was performed overnight at 4ºC.
5. Samples were centrifuged, and supernatant was saved for the SN fraction. Beads were washed 4 times with 400 µL of IP wash buffer old. Finally, 100 µL of protein loading buffer (in water) were added to the beads and they were boiled for 5 minutes. After centrifugation, beads were discarded; and the supernatant, containing the target protein, co-immunoprecipitated proteins and Immunoglobulins, were analysed by western blotting.

3.3.5. Lipid raft isolation

Lipid rafts are microdomains within plasma membrane that are enriched in cholesterol and tightly packed sphingolipids. Thus, lipid rafts are resistant to non-ionic detergent solubilisation, contrary to the rest of the plasma membrane. Starting from that principle, rafts can be biochemically isolated from the rest of the cell as a non-dissolved membrane in non-ionic detergent (detergent resistant membranes, DRM). Protocol was adapted from [181] and entirely performed in cold temperatures by leaving tubes and dishes over ice and with cold buffers.

1. 4 dishes per condition were washed twice with 5 mL of PBS and scraped in 2 mL of PBS twice to recover the maximum number of cells.
2. Suspension was precipitated by centrifugation at 600 g for 25 minutes at 4ºC. Supernatant was discarded.
3. The pellet, which contains cells and membrane fragments, was resuspended in 1 mL of non-ionic lysis buffer.

4. Resuspension was then physically homogenized with a Dounce all-glass tissue grinder (Kimble®) and homogenate was transferred to an ultracentrifuge tube.
5. In the ultracentrifuge tube, a sucrose gradient was formed by using 3 different sucrose solutions. Tube was ultracentrifuged in a *SW41 Ti* Swinging-Bucket Rotor at 39,000 rpm for 24 hours at 4ºC. This centrifugation speed would equal to around 250,000 g force at maximum radius (r_{max}) and 110,000 g force at minimum radius (r_{min}).
6. After centrifugation, tube content was gently extracted millilitre per millilitre, stored separately. Samples were prepared by combining 80% of fraction and 20% of protein loading buffer 5x and were analysed by western blotting. Clathrin was used as non-lipid raft marker, while flotillin and caveolin served as lipid raft markers.

3.4. MICROSCOPY

Imaging experiments were mainly performed by SP2 Leika confocal microscope. The set-up used for the images taken in the confocal microscope is as follows:

- **Line average:** 4. How many times the laser scans the sample before creating the resulting image. This image will appear as the average intensity of all scans.
- **Resolution:** 1024x1024. Number of pixels building up the images.
- **Objective:** HCX PL APO CSS 63x 1.32 OIL.
- **Zoom:** 4. Digital image magnification.

3.4.1. Fluorophores

During the present work, a number of different fluorophores were used. In the following list it can be found the fluorophores used in the present work, their excitation peak and their emission peak (Fig. M2).

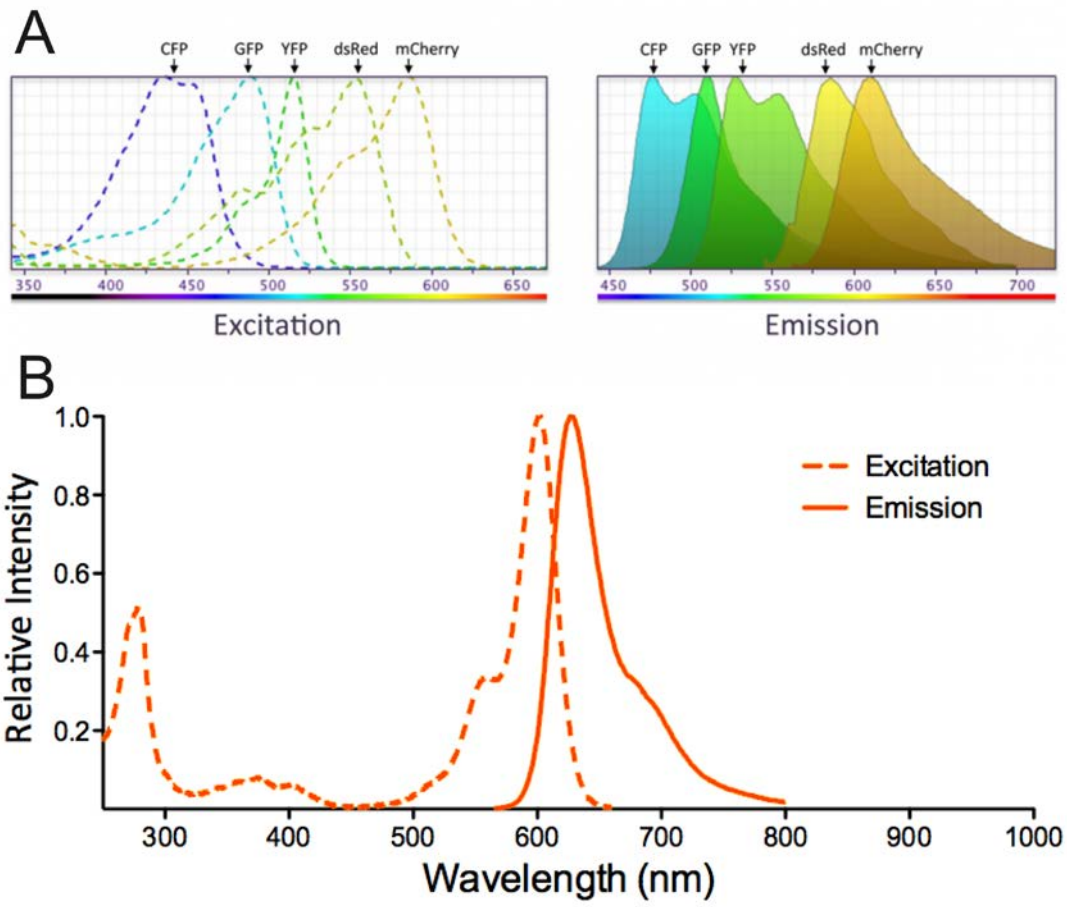

Fig. M2: *Fluorophores used in the present thesis.* ***A:*** *Excitation and emission spectra of CFP, GFP and YFP, among other fluorophores. Image from the webpage of the School of Life Sciences of the University of Dundee (https://www.lifesci.dundee.ac.uk/).* ***B:*** *Excitation and emission spectra of Alexa Fluor 555. Image from the webpage of StressMarq Biosciencies (https://www.stressmarq.com/).*

- Alexa Fluor 555: 555 (green, absorption), 580 (yellow, emission).
- CFP (Cyan Fluorescent Protein): 435 (violet, absorption), 485 (blue, emission).
- GFP: 488 (blue, absorption), 510 (green, emission).
- YFP (Yellow Fluorescent Protein): 514 (green, absorption), 527 (green, emission).

3.4.2. Microscopy sample preparation

Cells were seeded over a poly-D Lysine (Sigma-Aldrich)-treated coverslip inside a 6-well multiwell plate. Cells were transfected by PEI (previously described) 24-30 hours before the preparation of the samples. Protocol was conducted at room temperature unless stated otherwise and the multiwell plates were covered by tinfoil to prevent the fluorophores to fade.

For the preparation of samples, coverslips were washed thrice with 1 mL of K^+-less PBS for 3 minutes. Then, coverslips were treated for 10 minutes with 1 mL of PFA solution (paraformaldehyde) to fixate the cells and washed thrice with K^+-less PBS to clean them of the PFA.

In case no immunocytochemistry is needed (as in the case of the fluorophores being of transfectable nature), coverslips were mounted over slides with Mowiol mounting solution.

3.4.3. WGA staining

WGA (wheat germ agglutinin) is a lectin that binds with great specificity to sialic acid and N-acetil glucosamine, marking the membrane of the cells. Thus, when correctly treated with the reagent, cell membranes get marked with the fluorophore conjugated to WGA, which in this case was Alexa Fluor 555. Unlike the microscopy sample preparation previously described, all this protocol must be performed in in a cold room to prevent WGA internalization.

Coverslips were washed thrice with K^+-less PBS and incubated with WGA binding solution for 5 minutes. Then, they were washed thrice again with K^+-less PBS to minimize additional WGA binding. After this step, cells were fixated with PFA solution and washed thrice with K^+-less PBS. From this point beyond, coverslips can be treated with the immunocytochemistry protocol or directly mounted.

3.4.4. Immunocytochemistry

In some cases, transfectable fluorophores are not available or are not the preferable approach. In these cases, immunocytochemistry was performed after the post-fixation washes. Immunocytochemistry is performed at room temperature conditions and trying for the samples to receive the minimum light possible. Depending on the antibody and the nature of the target protein, the immunocytochemistry was performed with permeabilizing or not-permeabilizing buffers.

1. As an optional step depending on the approach, cells were treated for 10 minutes with permeabilization solution.
2. After washing the coverslips with K^+-less PBS, they were treated with blocking solution for 1 hour and washed again.
3. Coverslips were treated with primary antibody solution overnight at 4ºC and washed with K^+-less PBS.
4. Coverslips were treated with secondary antibody solution for 2 hours at room temperature and washed again.
5. Coverslips were finally mounted over the slides with Mowiol mounting solution.

3.4.5. Image analysis

All images were analysed using Fiji [182] software, always preserving the original values of the signal of the images. All images used were of the maximum intensity possible without being saturated (intensity of pixel = 255).

Co-localisation analysis

1. Images were opened using Fiji and duplicated.
2. Duplicate images were processed using the *Gaussian blur* filter with σ=1.00 and background was subtracted from a 250x250 pixel rectangular select.
3. Brightness and contrast was adjusted automatically in the duplicates to normalize signal. After, duplicates were threshold-adjusted to create a binary mask (255/0) only with the relevant signal using predefined algorithms.
    a. Membrane mask was adjusted using the *Moments* algorithm and the mask for other proteins or fluorophores was adjusted using the *Isodata* algorithm.
4. Additional background noise was minimized using one iteration of each *Open* and *Close* options.
5. The duplicated processed image and the original one were merged by using the operation *Minimum* in the *Image Calculator* menu. This operation takes the minimum value of signal for each pixel in the two images, what results on taking 0 in non-relevant signal pixels and the raw value in the relevant (255) pixels. This way enables us to have the raw data values but just on the relevant pixels.
6. JACoP plug-in [183] was used on the images to calculate the Manders coefficient.

Western blot analysis

1. Image was opened using Fiji.
2. Bands to be analysed were selected by the *Rectangular selection* option and tagged using the *Analyze/Gels/Select first lane* option.
3. Intensity of different bands was taken by using the *Analyze/Gels/Plot lanes* option, which gives a histogram of the intensity of the selection.
4. The histogram was physically divided by the number of bands in the lane by using the *Straight line* option.
5. Each segment of the histogram was quantified by selecting it with the *Wand (tracing) tool*, which gives a quantification of the segment.
6. Said quantification was the intensity value assigned to the corresponding band and was later normalized or further treated in Excel to complete the analysis.

3.5. ELECTROPHYSIOLOGY

3.5.1. Cell preparation

Cells transfected with FuGENE® 6 were incubated for 24 hours and detached by using Accutase® (Life Technologies). Suspended cells were seeded in different 35 mm treated dishes and incubated for 1 additional hour. After this incubation, cells were already reattached, but were round enough to be patched. Dishes were then washed, and the media was replaced by 1 mL of external patch buffer just before the experiment.

3.5.2. Micropipette preparation

Micropipettes were fabricated from 1.2 mm x 0.94 mm (O.D. x I.D.) borosilicate glass capillaries (Harvard Apparatus) by using a P-97 pipette puller (Sutter Instruments Co.) with the following settings: P=500; Heat=481; Vel.=57; Time=200.

Micropipettes were fire-polished by using a MF-830 microforge (Narishige Japan). A micropipette was then filled with internal patch buffer and placed around the electrode at the head-stage, thus attaining a resistance of 2-4 MΩ.

3.5.3. Seal formation and opening

Using a Model PatchStar 1U RACK micromanipulator (Scientifica), the micropipette was sealed with the chosen cell by applying negative pressure. By applying extra negative pressure, the seal was opened.

3.5.4. Pulse protocols

Cells were clamped at -60 mV and ion currents were capacitance- and series resistance-compensated by 80-90%, sampled at 10 kHz and filtered at 2.9 kHz. Diverse pulse protocols were applied, and the resulting currents were registered in the whole-cell configuration:

- **Activation:** to evoke voltage-gated currents, cells were stimulated with 250 ms pulses ranging from -60 to +80 mV in 10 mV steps. Peak amplitude (pA) was normalized using the capacitance values (pF), thus obtaining current density (pA/pF) (Fig. M3A).
- **Steady-state activation:** cells were stimulated with 250 ms pulses ranging from -60 to +60 mV in 10 mV steps followed by a -30 mV tail of 250 msec. This second pulse provokes a downfall of the voltage to near-activating values, which results in a slow decrease of the currents. The values of current in these tails are proportional to the activation dynamics of the channel in that specific voltage. This protocol was analysed by transforming the current value of the tails into conductance [$G_N = I_N / (V_N – V_{REV})$]. Conductances were relativized by their maximum value and fitted the resulting values to a Boltzmann equation (Fig. M3B).
- **C-type inactivation:** a long pulse of +60 mV during 5 sec which inactivates channels. This protocol was analysed by calculating the percentage of current reduction between the beginning and the end of the pulse (Fig. M3C).
- **Cumulative inactivation:** a series of 30 250-msec pulses of +60 mV separated by only 250 ms, which does not let the channel to recover from the use-dependent activation. This protocol was analysed by calculating the percentage of current

reduction between the peak of different pulses and the first, not-inactivated, one (Fig. M3D).

All pulse protocols were applied, and the resulting currents recorded thanks to an EPC10 USB patch-clamp amplifier and the corresponding PatchMaster software (HEKA Elektronik). The analysis of the currents was performed in FitMaster (HEKA Elektronik).

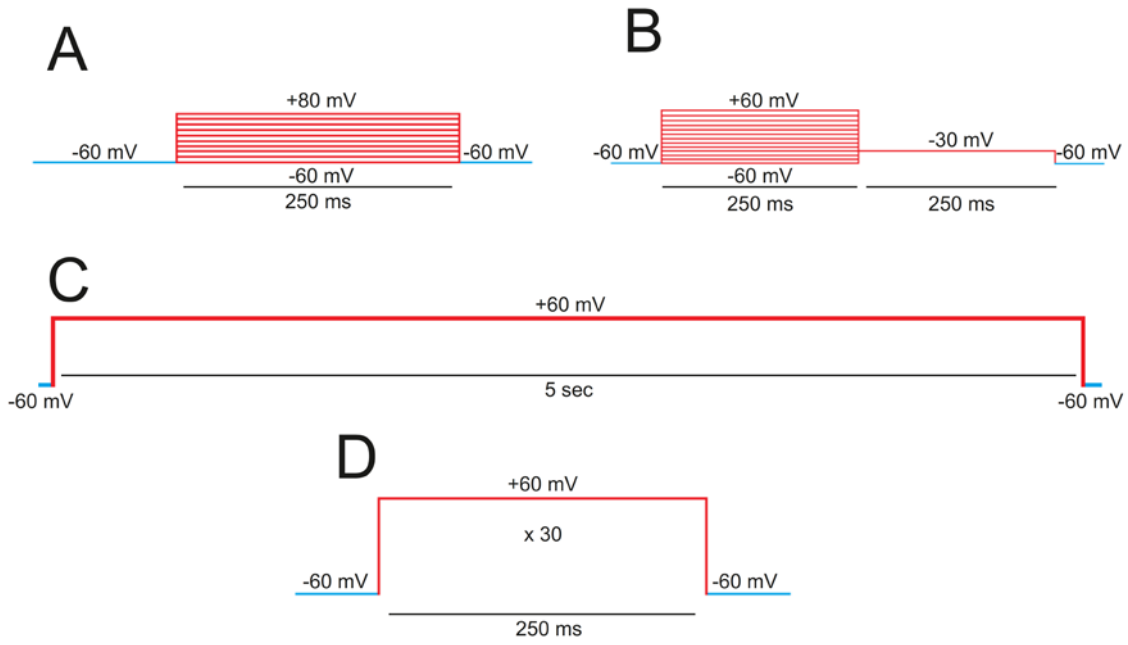

Fig. M3: *Pulse protocols used in the present thesis.* ***A:*** *Activation pulse;* ***B:*** *Steady-state Activation pulse;* ***C:*** *C-type inactivation pulse;* ***D:*** *Cumulative inactivation pulse.*

3.6. MOLECULAR MODELLING

Molecular modelling of Kv1.3-KCNE4 complex was performed by using high-resolution templates of remote or close homologs available from the Protein Data Bank (http://www.rcsb.org/pdb). The transmembrane domain and the N-terminus (except the first 49 amino acids) were modelled with the Kv1.2 potassium channel (PDB code 2R9R). The C-terminus and the remaining 49 amino acids from the N-terminus were modelled with 3HGF (nucleotide binding domain of the reticulocyte binding protein Py235) and 1PXE (zinc-binding domain from neural zinc finger factor-1) codes, respectively [47].

KCNE4 was modelled using high-resolution templates of homologs available from the Protein Data Bank (http://www.rcsb.org/pdb). The N-terminus, transmembrane domain and the proximal C-terminus (residues 1-98) were modelled with the KCNE1 (PDB code 2K21). The distal C-terminus (residues 99-170) was modelled with 3HTC, the best scored model (C-score [-5,2]= -3,96 y 0,29±0,09 (TM-score), 12,2±4,4Å (RMSD)) from i-Tasser modelling server (http://zhanglab.ccmb.med.umich.edu/I-TASSER/). Then, multiple sequence alignment was performed using CLUSTALW [184] from the European Bioinformatics Institute site (http://www.ebi.ac.uk). The homology modelling was performed using the Swiss-Model Protein Modelling Server [185] on the ExPASy Molecular Biology website (http://kr.expasy.org/) under the Project Mode. Structure visualization and modifications were made using Yasara v11.6.16 [186] and DeepView v4 [187]. The orientation and optimization of the side chains were carried out in two steps. First, the residues showing van der Waals clashes were selected and fitted with the “Quick and Dirty” algorithm (DeepView). Second, the models were energy minimized (Yasara). Briefly, this process involved an initial short steepest descent minimization to remove bumps, followed by a simulated annealing minimization. In this procedure, the simulation cell was slowly cooled towards 0K by downscaling the atom velocities. The entire system was subjected to an equilibration process before the molecular dynamics simulation. The equilibration consisted of an initial minimization of the fixed backbone atoms. Next, the restrained carbon alpha atoms were minimized and a short molecular dynamics (10 ps) minimization was performed. The goal of the latter step was to reduce the initial incorrect contacts and to fill the empty cavities. Finally, under periodic boundary conditions in the three coordinate directions, the full system was simulated at 310ºK for 0.5 ns. All dynamic simulations were performed using Yasara [186] with the force field AMBER03 [188]. The cut-off used for long-range interactions was set at 10 Å. In addition, the model was evaluated using PROCHECK to show the residues in the allowed regions of the Ramachandran plots [189, 190]. The final molecular graphic representations were created using PyMOL v1.4.1 (http://pymorl.org/).

The resulting models were used to search for plausible docking interactions between Kv1.3 and Kcne4. The docking process was set in a three-step procedure: (i) Docking the N-terminus and the transmembrane domains of KCNE4. The docking model available for KCNE1-Kv7.1 complex in the open state (Kang et al 2008) was used as template to align the transmembrane regions of Kcne4 (fragment 1-62) on Kv1.3. This docking locates both proteins in the membrane context and restricts the possible conformations of their cytosolic domains. (ii) Docking the interacting regions. To accomplish the docking of the cytosolic

regions between Kv1.3 and Kcne4, we isolated the C-terminus of Kv1.3 (region 439-525) as well as the putative interacting region of Kcne4 (amino acids 63 to 81, containing the leucines 69-72). The fragments were sent to GRAMM server (http://vakser.bioinformatics.ku.edu/resources/gramm/grammx/), for protein-protein docking. The docking solutions were filtered by interaction energy and by complementarity/compatibility with the transmembrane regions. The binding energy of the docked complexes was obtained by calculating the energy between the C-terminus of Kv1.3 and the KCNE4 fragment at infinite distance and then subtracting the energy of the whole complex. The energy in each cluster was stored, analyzed, and applied to select the most likely orientation of the interacting proteins. The energy of the model and the docking complexes were tested using FoldX [191, 192] on the CRG site: http://foldx.crg.es. The force field of FoldX allowed us to evaluate the properties of the structure. Such parameters as the atomic contact map, the accessibility of the atoms and residues, the backbone dihedral angles, the hydrogen bonds and the electrostatic networks of the protein were assessed. (iii) Connection of the KCNE4 domains. The best docking solution of the step (ii) was merged with the complex obtained in step (i). Finally, the distal C-terminus of KCNE4 (fragment 82-170) was joined to obtain the full Kv1.3-KCNE4 complex.

3.7. REACTIVES

3.7.1. Buffers

Buffers were prepared using milli-Q water unless stated otherwise.

- **Antibody solution:**
  - **Primary:** 1/100-1/1000 of primary antibody stock, 10 µL sodium azide, 5% powder milk in 4 mL PBS Tween.
  - **Secondary:** Secondary antibody conjugated to HRP in 4 mL PBS Tween.
    - Mouse: 1/10,000 (Bio-Rad).
    - Rabbit: 1/3,000 (Bio-Rad).
- **Borate buffer:** 0.2M boric acid, pH 9.
- **Blocking solution:** 5% powder milk, 10% goat serum in K^+-less PBS.
  - **Permeabilizing:** 0.05% Triton X-100 in blocking solution.
- **ECL:** 1:1 ECL1:ECL2
  - **ECL1:** 100 mM Tris-HCl pH 8.5, 2.5 mM Luminol, 396 µM p-Coumaric acid.
  - **ECL2:** 100 mM Tris-HCl pH 8.5, 5.632 M H_2O_2.
- **Freezing media:** 90% FBS, 10% DMSO.
- **K^+-less PBS:** 154 mM NaCl, 8.85 mM NaH_2PO_4, pH 7.4.
- **KHMgE buffer:** 70 mM KCl, 30 mM HEPES, 5 mM $MgCl_2$, 3 mM EGTA, pH 7.5.
- **IP Lysis Buffer:** 150 mM NaCl, 5 mM HEPES, 10% Glycerol, 1% Triton X-100, pH 7.4.
- **IP Wash Buffer column:** 150 mM NaCl, 50 mM HEPES, 1% Triton X-100, pH 7.4.
- **IP Wash Buffer old:** 150 mM NaCl, 50 mM HEPES, 10% Glycerol, 0.1% Triton X-100, pH 7.4.
- **MBS:** 150 mM NaCl, 250 µM MES (2-(N-morpholino)ethanesulfonic acid), pH 6.5.
- **Mowiol mounting solution:** 9.6 g of Mowiol in 24 g of Glycerol and 48 mL of Tris HCl 0.2 M pH 8.5.
- **Non-ionic lysis buffer:** 0.01% Triton X-100 in MBS.
- **Sucrose solutions:** 5%, 30%, 53.28% in MBS.
- **Patch-Clamp buffers:**
  - **External:** 5.4 mM KCl, 120 mM NaCl, 2 mM $CaCl_2$, 1 mM $MgCl_2$, 10 mM HEPES, 25 mM D-Glucose. pH = 7.44 with NaOH. Osmolality ≈ 1.1 x Osmolality of internal patch buffer.
  - **Internal:** 120 mM KCl, 1 mM $CaCl_2$, 2 mM $MgCl_2$, 10 mM HEPES, 11 mM EGTA, 20 mM D-Glucose. pH = 7.33 with KOH. Osmolality ≈ 290 mOsm/Kg.
- **PBS:** 140 mM NaCl, 2.7 mM KCl, 1.46 mM KH_2PO_4, 8 mM Na_2HPO_4.
- **PBS Tween:** 0.05% Tween in PBS.
- **Permeabilization solution:** 0.1% Triton X-100 in K^+-less PBS.
- **PFA solution:** 4% paraformaldehyde (Sigma-Aldrich) in K^+-less PBS.
- **Polyacrylamide gel:**
  - **Running:** 6-15% Acrylamide, 375 mM Tris (pH 8.8), 0.1% SDS, 0.1% APS, 0.04-0.08% TEMED.
  - **Stacking:** 5% Acrylamide, 125 mM Tris (pH 6.8), 0.4% SDS, 0.4% APS, 0.1% TEMED.

- **Primary antibody solution:** 10% Goat serum in K^+-less PBS. Varying concentration of antibody.
    - **Permeabilizing:** 0.05% Triton X-100 in primary antibody solution.
- **Protease inhibitors:** 1 mM PMSF, 1 µg/mL Leupeptin, 1 µg/mL Pepstatin, 1 µg/mL Aprotinin.
- **Protein Loading buffer 5x:** 9:1 (Laemmli Buffer:β-Mercaptoethanol).
    - **Laemmli Buffer:** 7 mL H_2O, 1'51 g Tris, 4 g SDS, 23 mL Glycerol, 0.5 mL Bromophenol blue, up to 36 mL with H_2O.
- **Protein Lysis Buffer:** 50 mM Tris, 150 mM NaCl, 1 mM EDTA, 1% Triton X-100.
- **Secondary antibody solution:** 1% BSA in K^+-less PBS. Varying concentration of antibody.
    - **Permeabilizing:** 0.05% Triton X-100 in secondary antibody solution.
- **TBS:** 150 mM NaCl, 25 mM Tris.
- **WGA binding solution:** 1/1500 of WGA-Alexa-555 in K^+-less PBS.

3.7.2. Antibodies

Antibodies used both for immunoblotting (IB), immunoprecipitation (IP) or immunocytochemistry (ICC) are as follow:

- **β-Actin:** Mouse IgG (IB, Sigma-Aldrich, #A5441)
- **Calnexin**: Mouse IgG (IB, BD Transduction Laboratories ™, #610523)
- **Clathrin**: Rat IgG (IB, BD Transduction Laboratories ™, #610500)
- **Flotillin-1 (Flotillin)**: Mouse IgG (BD Transuction Laboratories ™, #610820)
- **GFP (YFP/CFP):** Mouse IgG (IP/IB, Roche, #11 814 460 001)
- **HA:** Rabbit Polyclonal (IB, Sigma-Aldrich, #H 6908)
- **KCNE1:** Rabbit Polyclonal (IB, Alomone labs, #APC-008)
- **KCNE4:** Rabbit IgG (IB, Proteintech ™, #18289-1-AP)
- **Kv1.3:**
    - Mouse IgG (IP/IB/ICC, NeuroMab, #75-009)
    - Rabbit Polyclonal (IP/ICC, Abcam, #ab61200)
- **Kv1.5:** Rabbit Polyclonal (IP/IB/ICC, Alomone labs, #APC-004)

3.8. INSTRUMENTATION AND INFORMATIC SUPPORT

3.7.1. Instrumentation

- **P-97 pipette puller (Sutter Instruments Co.):** Flaming type micropipette puller, ideal for fabricating micropipettes, patch pipettes and microinjection needles. By using a borosilicate capillary, this puller fabricates 2 micropipettes.
- **MF-830 microforge (Narishige Japan):** Fire-polisher which polishes the micropipette tips.
- **Model PatchStar 1U RACK micromanipulator (Scientifica):** Computer-assisted micromanipulator which enables a precise and low-noise movement of the Patch-Clamp electrode.
- **EPC 10 USB Single Patch-Clamp amplifier (HEKA Elektronik):** computer-controlled amplifier that, alongside the PatchMaster software, can clamp voltage or current on cells, as well as access and store variables of recordings.
- **Confocal microscope Leika TCS SP2:** confocal microscope used alongside its corresponding software to record images in the microscopy experiments.
    - **Lasers:** Ar (458, 476, 488, 514 nm), Ar (UV), DPSS (561 nm), He/Ne (633 nm)
- **Fujifilm LAS-3000 imager:** used alongside the Image Reader LAS-3000 software to record both chemiluminescent and traditional images of Western Blot membranes.

3.7.2. Informatic support

- **Clone Manager Suite 7 (Sci Ed Central):** used in the design of primers for their use on DNA. Also used in the analysis of sequences during mutagenesis and digestion-ligation cycles.
- **Fiji (Fiji Is Just ImageJ):** used in the analysis of co-localisation of different proteins in confocal microscopy images and in the analysis of intensity of different bands in western blot membranes.
    - **Plug-in JACoP:** used in co-localisation experiments of confocal microscopy.
- **HEKA Elektronik:**
    - **PatchMaster:** Used in conjunction to EPC 10 USB Single Patch-Clamp amplifier to elicit currents in clamped cells.
    - **FitMaster:** used to analyse patch-clamp recordings.
- **GraphPad Prism 5:** used to both analyse confocal and electrophysiological data, as well as represent said data in graphics.
- **Microsoft Office 2010:** Excel used in analysis of both confocal and electrophysiological data. PowerPoint used for presentations of results in seminars and congresses. Word used for the writing of the present thesis.
- **UCSF Chimera:** Used to visualize and work with 3D structures of proteins.

RESULTS

4. RESULTS

4.1. INTRAMOLECULAR INTERACTIONS OF THE $K_V1.3/K_V1.5$ HETEROMER

4.1.1. Kv1.3 and Kv1.5 have physiological relevance in immune system

4.1.1.1. T cells and dendritic cells possess Kv1.3

Kv1.3 plays an important role in excitable cells, such as sensorial neurons. In addition, Kv1.3 is also expressed in a wide array of non-excitable cells, especially in immune system. Thus, some cell types of paramount importance, like dendritic cells, B or T lymphocytes, express Kv1.3. Therefore, Kv1.3 is present in immortalized cell lines like mouse CY15 dendritic cells and human Jurkat T lymphocytes (Fig. 1). In addition, other proteins, such as Kv1.5 and KCNE4, having a modulatory effect over Kv1.3, are also expressed. A molecular weight shift is consequence of different species origin. Human Kv1.3 has an additional sequence on the N-terminus that represents an increase of 50 amino acids in length. Moreover, this difference affects Kv1.3 in CY15 showing both mature (<75 KDa) and immature (>50 KDa) forms, whereas Kv1.3 in Jurkat only showed the mature form (75 KDa). In addition, both Kv1.5 and KCNE4 are much more abundant in dendritic cells than in T-lymphocytes. This is consistent with previous reports of Kv1.5 and KCNE4 being undetectable or slightly expressed in this type of lymphocytes.

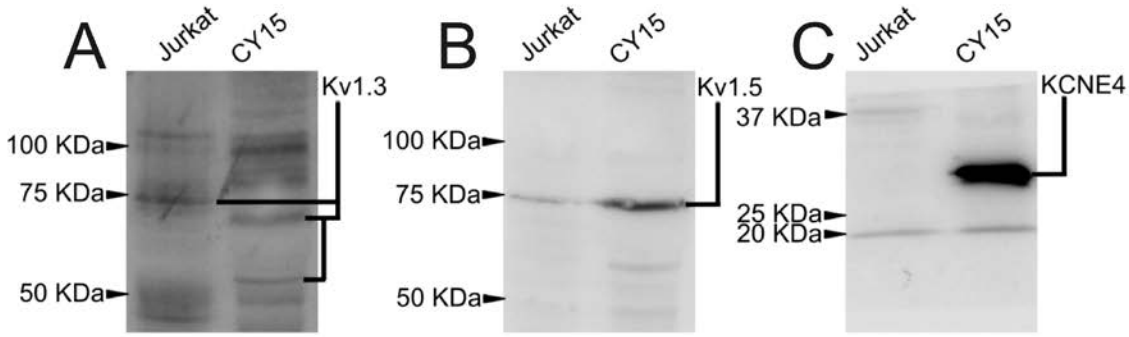

Fig.1: *Expression of Kv1.3, Kv1.5 and KCNE4 in Jurkat and CY15 cells. Samples were immunoblotted against either Kv1.3 (**A**), Kv1.5 (**B**) or KCNE4 (**C**).*

4.1.1.2. Dendritic and T cells exhibit profound electrophysiological differences

Kv1.3 is the predominant Kv channel in Jurkat T-lymphocytes. Therefore, when exposed to depolarizing pulses, Jurkat cells elicit currents similar to Kv1.3. When alone, Kv1.3 exhibits a predominant C-type inactivation, also apparent in Jurkat T-lymphocytes. In comparison, currents of CY15 cells lack this property (Fig. 2A, 2B and 2C). Quantitatively, Jurkat T lymphocytes exhibit much more activity (65 pA/pF at +60 mV) than CY15 (15 pA/pF at +60 mV) (Fig. 2D and 2E).

This difference could be partly due to the large difference in cell size. CY15 dendritic cell membrane has 4 times more capacitance than the Jurkat one (Fig. 2F). Capacitance is directly proportional to the amount of cell membrane being 1 µF/cm^2 of membrane.

The higher presence of inhibitory subunits Kv1.5 and KCNE4, which has been described to greatly impair Kv1.3 current, could also be another reason for this divergence between these two cell types (Fig. 1).

4.1.1.3. Currents in Dendritic and T cells have distinct pharmacology

While Kv1.3 currents are efficiently inhibited by the peptide blocker Margatoxin (MgTx), Kv1.5 shows some resistance. This divergence also echoed on the pharmacologic profiles of Jurkat T-lymphocytes and CY15 dendritic cells. Therefore, having a prominent Kv1.3 expression, currents in Jurkat cells were strongly inhibited by MgTx (Fig. 3A and 3D). Currents in CY15 cells also got a partial inhibition by MgTx, but with a minor efficiency than in Jurkat (Fig. 3B and 3C). Thus, by expressing Kv1.5 in great amount, dendritic cell currents are partially resistant to MgTx, especially at lower concentrations (Fig. 3E).

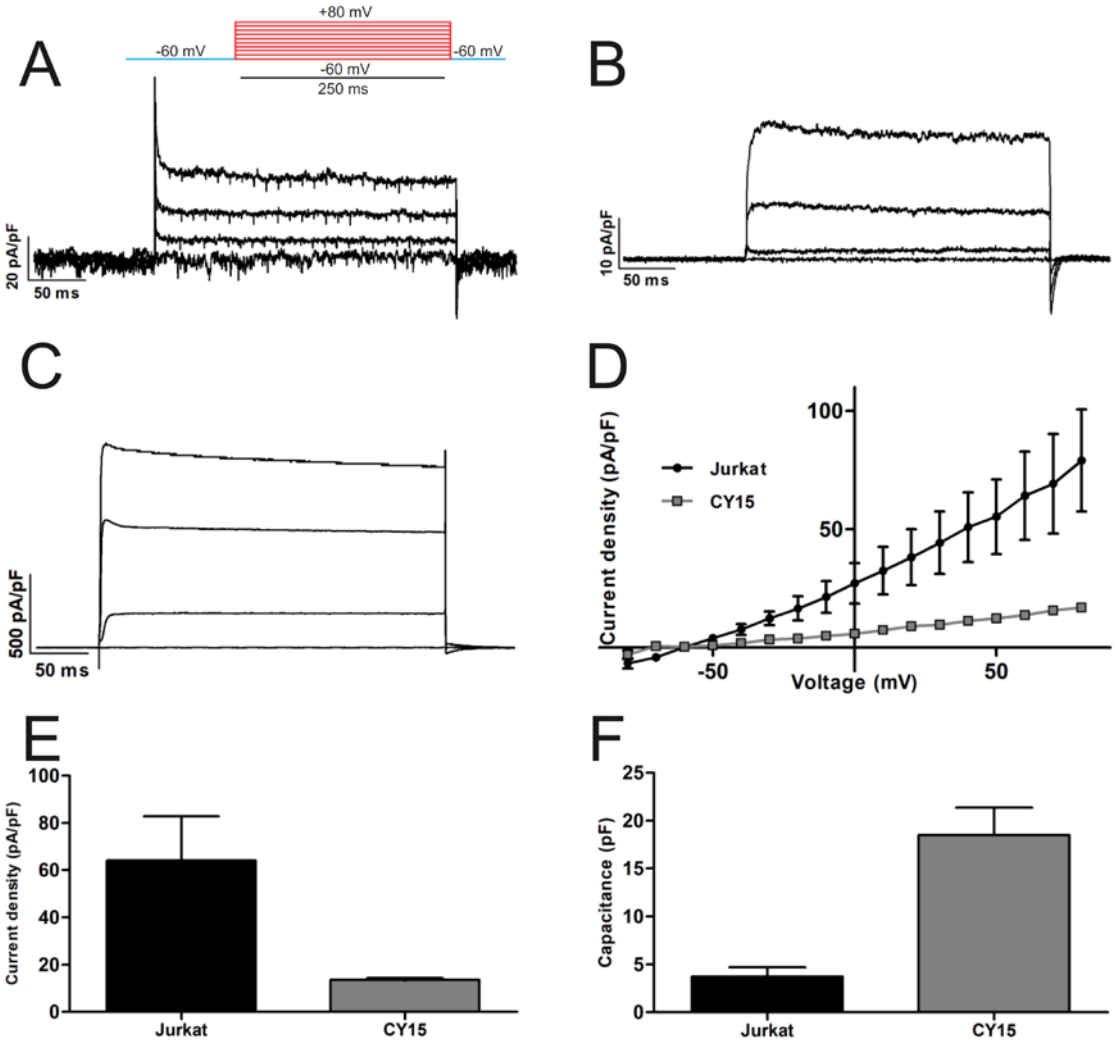

Fig. 2: *Voltage-dependent K^+ currents in Jurkat and CY15 cell lines. Cells were held at -60 mV and 250 ms pulses were applied from -80 mV to +80 mV in increments of 10 mV. Currents were elicited in Jurkat (**A**), CY15 (**B**) and Kv1.3-transfected HEK cells (**C**). **D:** I/V relationship of the currents elicited in Jurkat and CY15 cells. Values used were those of the peak current. **E:** Current density generated by Jurkat and CY15 cells at +60 mV. **F:** Cell capacitance of Jurkat and CY15 cells. Values are mean ± standard error of 3-5 independent cells.*

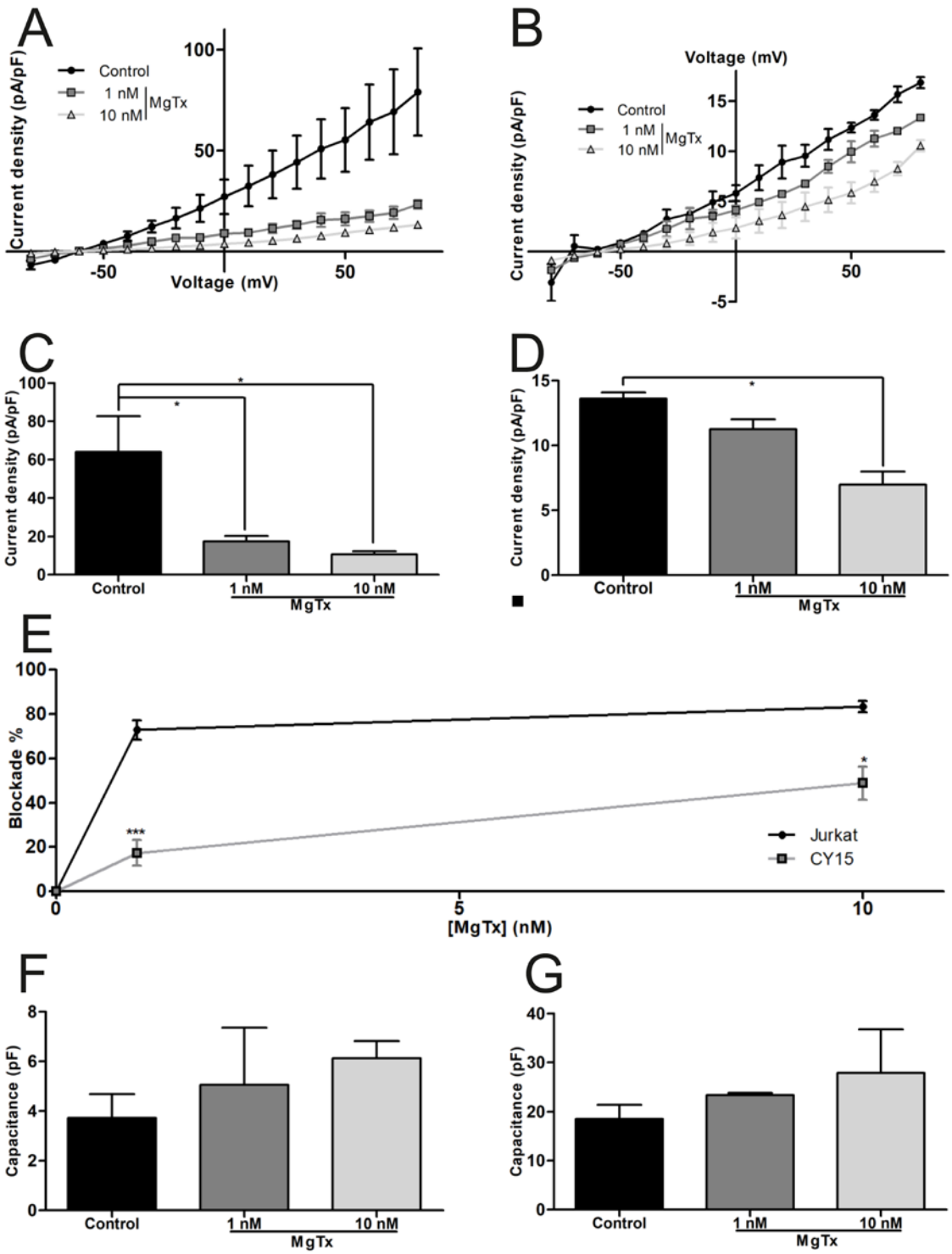

Fig. 3: *Electrophysiological characterization of voltage-dependent K^{+} currents in Jurkat and CY15 cell lines. I/V relationship of the currents elicited in Jurkat (**A**) and CY15 (**B**) cells in different MgTx concentrations. Values used were those of the peak currents. Current density at +60 mV in Jurkat (**C**) and CY15 (**D**) cells in the absence (control) or presence of MgTx. **E:** Percentage of inhibition exhibited in Jurkat and CY15 cells at +60 mV with different MgTx concentrations. Effects of MgTx on Jurkat (**F**) and CY15 (**G**) cell capacitance. Values are mean ± standard error (n=3). *, p<0.05; ***, p<0.005 by One-way ANOVA test.*

Kv1.3 participates in a plethora of diseases, ranging from autoimmune to cancer or metabolic processes. The great versatility of this channel supports why has been postulated as a therapeutic target for many diseases. However, the subunit composition of the functional complex must be taken into consideration in native cells because its ability to form heterotetramers with other Shaker channels exhibiting pharmacological distinct properties.

The presence of MgTx in both cell types generated a variation in cell capacitance (Fig. 3F and 3G). Upon the presence of MgTx both Jurkat T-lymphocytes and CY15 dendritic cells increased cell capacitance, which is directly related to membrane area and consequently, to cell volume. In fact, Kv1.3 background activity, as most voltage-gated channels, is to maintain the cell membrane potential and the cell volume. Therefore, the blockade of K^+ channels provoked by MgTx increases the retention of K^+ into the cell, entering water molecules in, and increasing the cell volume.

4.1.2. Characterization of the Kv1.3-Kv1.5 Tandem

4.1.2.1. Kv1.3-Kv1.5 heterotetramer as a functional entity

Kv1.3 and Kv1.5 form functional heterotetrameric channels in antigen presenting cells (APC) with a ratio that can range from 4:0 to 1:3 (Kv1.3:Kv1.5). Variable stoichiometry depends on the expression levels of both subunits and the activation of the cell directly affecting the antigenic excitability and the gene expression.

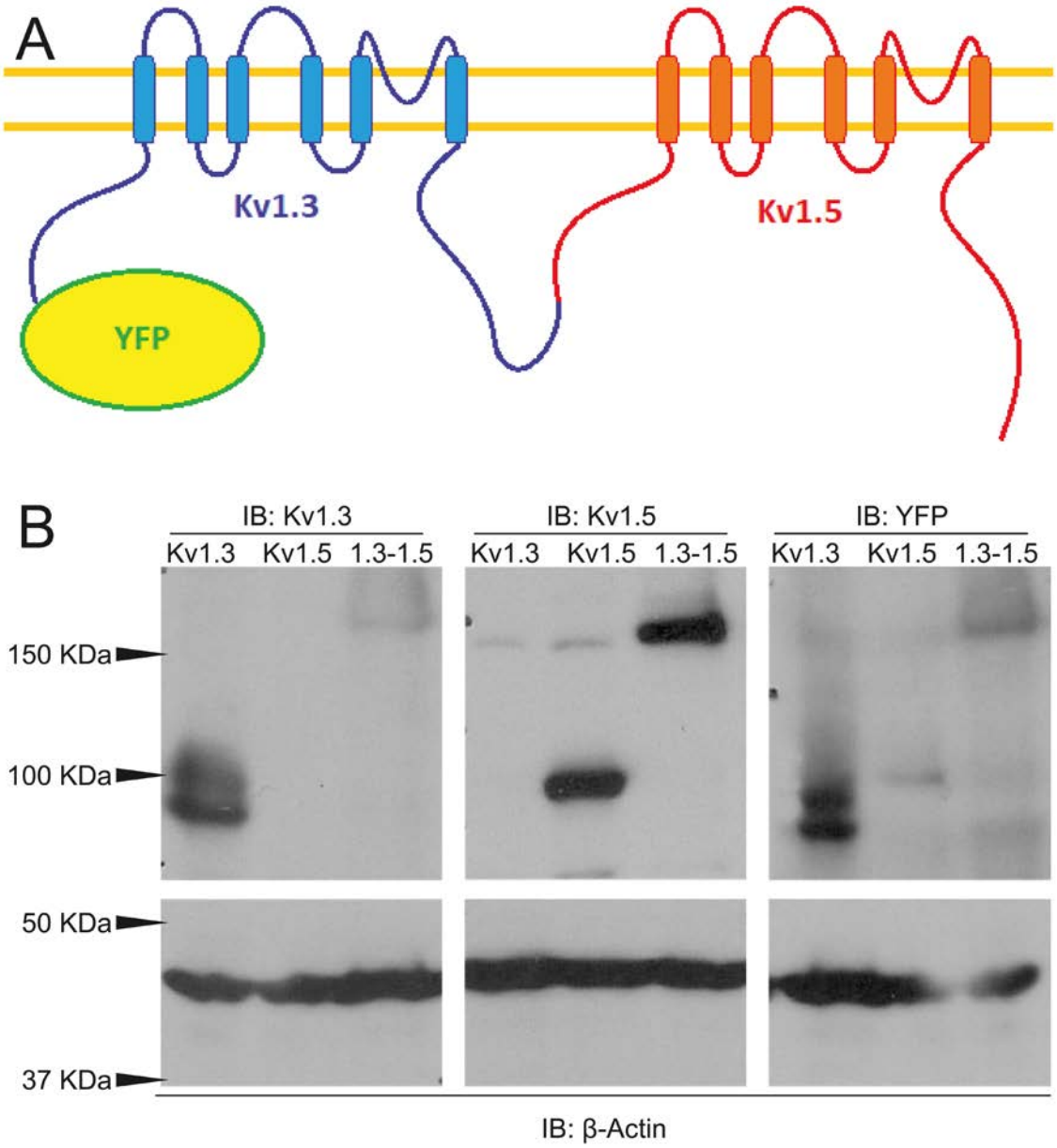

Fig. 4: *Generation of Tandem 1.3-1.5.* ***A:*** *Schematic representation of the protein product of Tandem 1.3-1.5. YFP is linked to the N-terminus of Kv1.3 while Kv1.5 is linked to the C-terminus. Kv1.3 is painted blue; Kv1.5 is painted orange; and YFP is painted yellow.* ***B:*** *Western blot of transfected HEK 293 cells. Cells were transfected either Kv1.3, Kv1.5 or Tandem 1.3-1.5. Cells were lysated and crude protein purified. Samples were loaded in a PAGE-SDS gel and western blotted. Antibodies used for immunoblotting were specific against Kv1.3, Kv1.5 and YFP. IB: Immunoblot.*

In the present work, we aimed to study the interaction between KCNE4 and the heterotetramer formed by Kv1.3 and Kv1.5 as a functional complex. This approach entails a problem: the ratio of the complex is variable and cannot be fixed upon heterologous

expression. Therefore, a fusion protein (aka: tandem, concatemer) was generated by fusing Kv1.3, Kv1.5 and the YFP tag (named Tandem 1.3-1.5 from now on) (Fig. 4A). By this way, the Kv1.3-Kv1.5 ratio remains fixed 1:1 and tetrameric channels are formed 2:2.

The tandem chimera 1.3-1.5 was transfected into HEK 293 cells to characterize the molecular weight of the protein. The tandem exhibited a molecular weight closely similar to the sum of the three proteins (>150 KDa) (Fig. 4B).

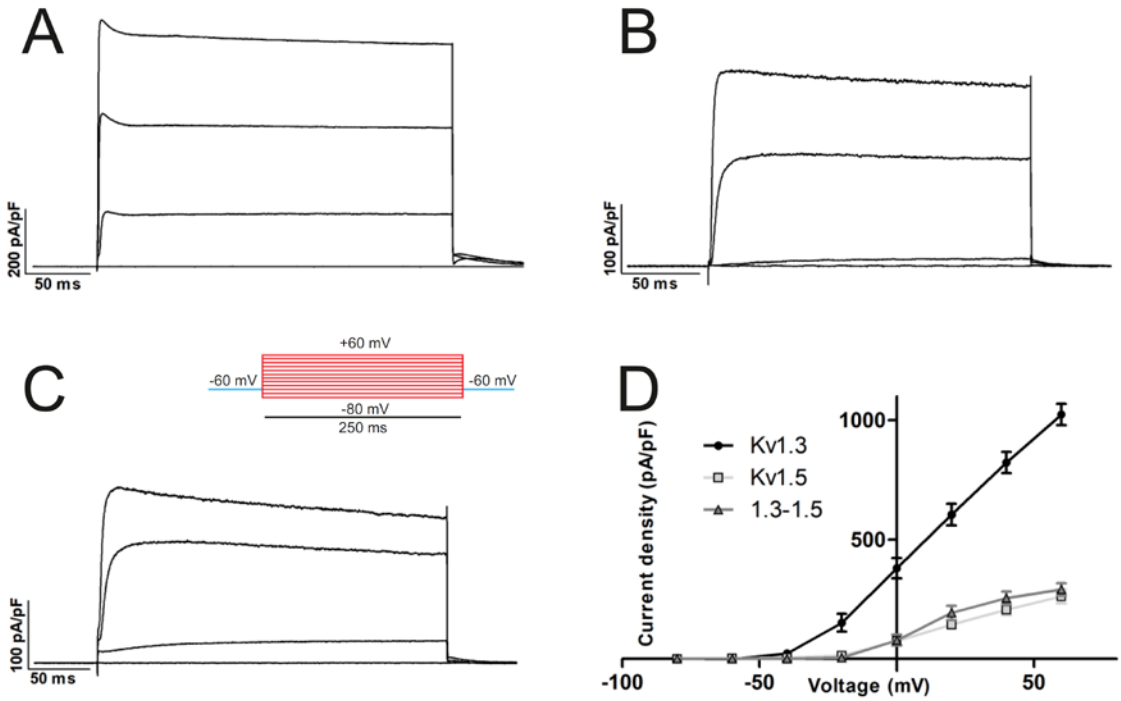

Fig. 5: *Voltage-dependent K^+ currents in transfected HEK 293 cells with Kv1.3, Kv1.5 or Tandem 1.3-1.5. Cells were held at -60 mV and 250 ms pulses were applied from -80 mV to +60 mV in increments of 10 mV.* ***A:*** *Kv1.3;* ***B:*** *Kv1.5;* ***C:*** *Tandem 1.3-1.5.* ***D:*** *I/V relationship of the currents elicited in Kv1.3, Kv1.5 and 1.3-1.5 transfected cells. Values are those at the peak current. Values are mean ± standard error of 3-5 independent cells.*

4.1.2.2. Tandem 1.3-1.5 exhibits the most restrictive functional properties of each subunit

The activity of the Tandem 1.3-1.5 was assessed by patch-clamp experiments in transfected HEK 293 cells. While Kv1.3 exhibited about 1000 pA/pF of current density (Fig. 5A), Kv1.5 showed 300 pA/pF, consistent with the lower conductance of the channel (Fig. 5B). Comparatively, the Tandem 1.3-1.5 showed a current density near 300 pA/pF, similar to Kv1.5 (Fig. 5C). Furthermore, while threshold for activation of Kv1.3 was -40 mV, both Kv1.5 and Tandem 1.3-1.5 activated at -20 mV. These results suggest that Kv1.5 functions as a dominant-negative towards Kv1.3 in the 1:1 ratio (Fig. 5D).

Deciphering further electrophysiological properties of the channel, the Tandem 1.3-1.5 does exhibit some C-type inactivation. The C-type is a type of inactivation closely linked to a conformation change in the pore domain when channels get a prolonged activation. This is very characteristic of Kv1.3 and very limited in Kv1.5 (Fig. 6A and 6B). The Tandem 1.3-1.5 suggests that at least two copies of Kv1.3 are sufficient to present a C-type inactivation comparable to Kv1.3 homotetramers (Fig. 6C and 6D).

Kv1.3 also typically exhibits cumulative inactivation, a kind of inactivation that requires an allosteric cooperation of channel subunits. Unlike the C-type, the cumulative inactivation

onsets with a train of repetitive activations. After 30 fast pulses, Kv1.3 and the Tandem 1.3-1.5 presented a notable inactivation, whereas in the Kv1.5 homotetramer it was absent (Fig. 7A and 7B). Peak currents of the train of 30 pulses were fitted in a non-linear regression using the One Phase Decay equation (Eq. 1 and Fig. 7A).

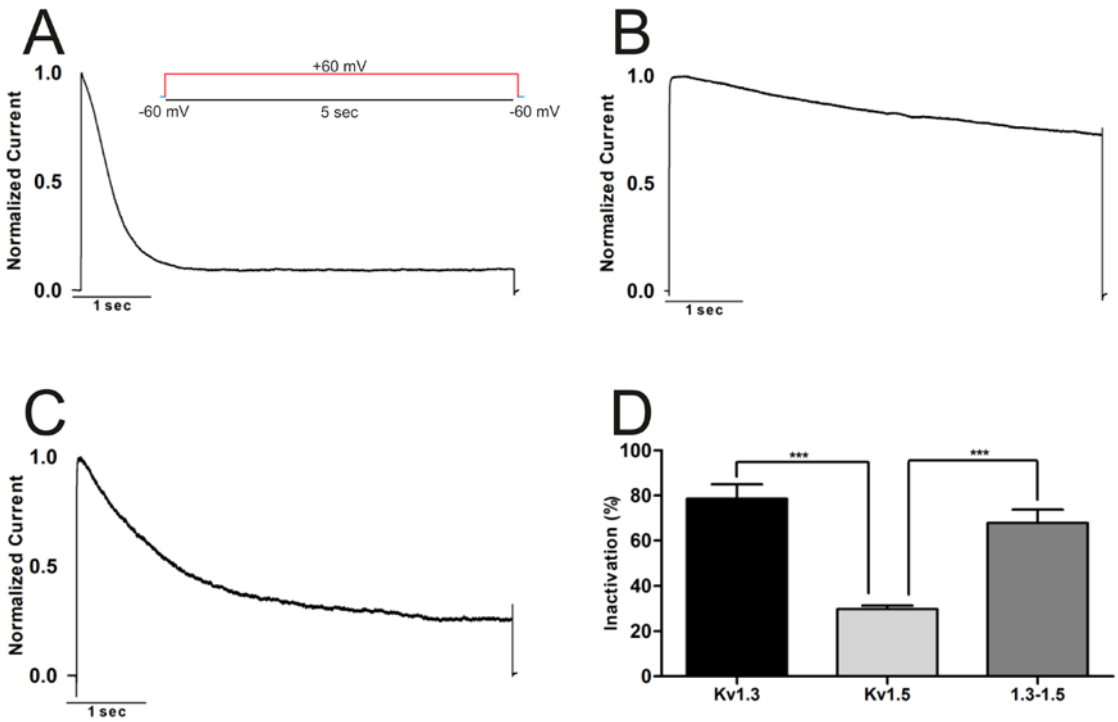

Fig. 6: *C-type inactivation of the K⁺ currents generated by Tandem 1.3-1.5. C-type inactivation is evident when channels are maintained in an open state because of a constant voltage. C-type inactivation leads to a gradual reduction of the current along the time. Cells were held at -60 mV and a 5 seconds depolarizing pulse of +60 mV was applied. Representative traces of the currents elicited were normalized to its maximum value;* ***A:*** *Kv1.3;* ***B:*** *Kv1.5;* ***C:*** *Tandem 1.3-1.5.* ***D:*** *Percentage of inactivation after the 5-second pulse. The inactivation was calculated by comparing the current at the end of the 5-second pulse with the peak current. Values are mean ± standard error of 5-8 independent cells. ***, p<0.005 by One-way ANOVA test.*

$$Eq.1 - One\ phase\ decay: Y = (Y_0 - Plateau) * \exp(-K * X) + Plateau$$

Y_0 represents the maximum current, which tends to 1. The **Plateau** represents the final asymptote, the expected minimum relative current value. **K** is the pendent of the decay curve, which is a reverse logarithm. From this equation, 3 additional parameters can be calculated. The **span** is defined as the difference between Y_0 and the Plateau; thus, it has a similar nature as the percentage of inactivation. The **half-life** is the number of pulses required to inactivate half the maximum value. The **Tau** is the time-constant, the reciprocal of K.

Parameters from this equation were analysed and compared. Kv1.3 and Tandem 1.3-1.5 had a slightly higher, but not significant, Y_0 than Kv1.5 due to the steepness of their curves (Fig. 7C). Differences between Kv1.3 and Kv1.5 were significant on all the parameters referent to dynamics: K, Span, Half Life and Tau (Fig. 7E, 7F, 7G and 7H). The higher K reflects on a steeper curve and the lower plateau ties with the higher span to represent a more profound inactivation of Kv1.3 in comparison to Kv1.5. In parallel, Tandem 1.3-1.5, very likely to Kv1.3, presented no differences with Kv1.3 or Kv1.5 in these parameters.

Kv1.5 homotetramer did not inactivate after 30 pulses, thereby parameters present an abnormally broad confidence interval, overlapping with 1.3-1.5. Finally, all channels showed

differences regarding the Plateau (Fig. 8D). Even though this parameter is redundant with a proper cumulative inactivation, it indicates that, although not significant, Kv1.3 and 1.3-1.5 inactivations are slightly different.

Thus, the Tandem 1.3-1.5 shows the least active properties of either channel. The tandem exhibits the minor current density of Kv1.5, while maintaining both types of inactivation (C-type and cumulative) of Kv1.3. This would be consistent with the delicate balance of residues, domains and forces of ion channels necessary for their activity.

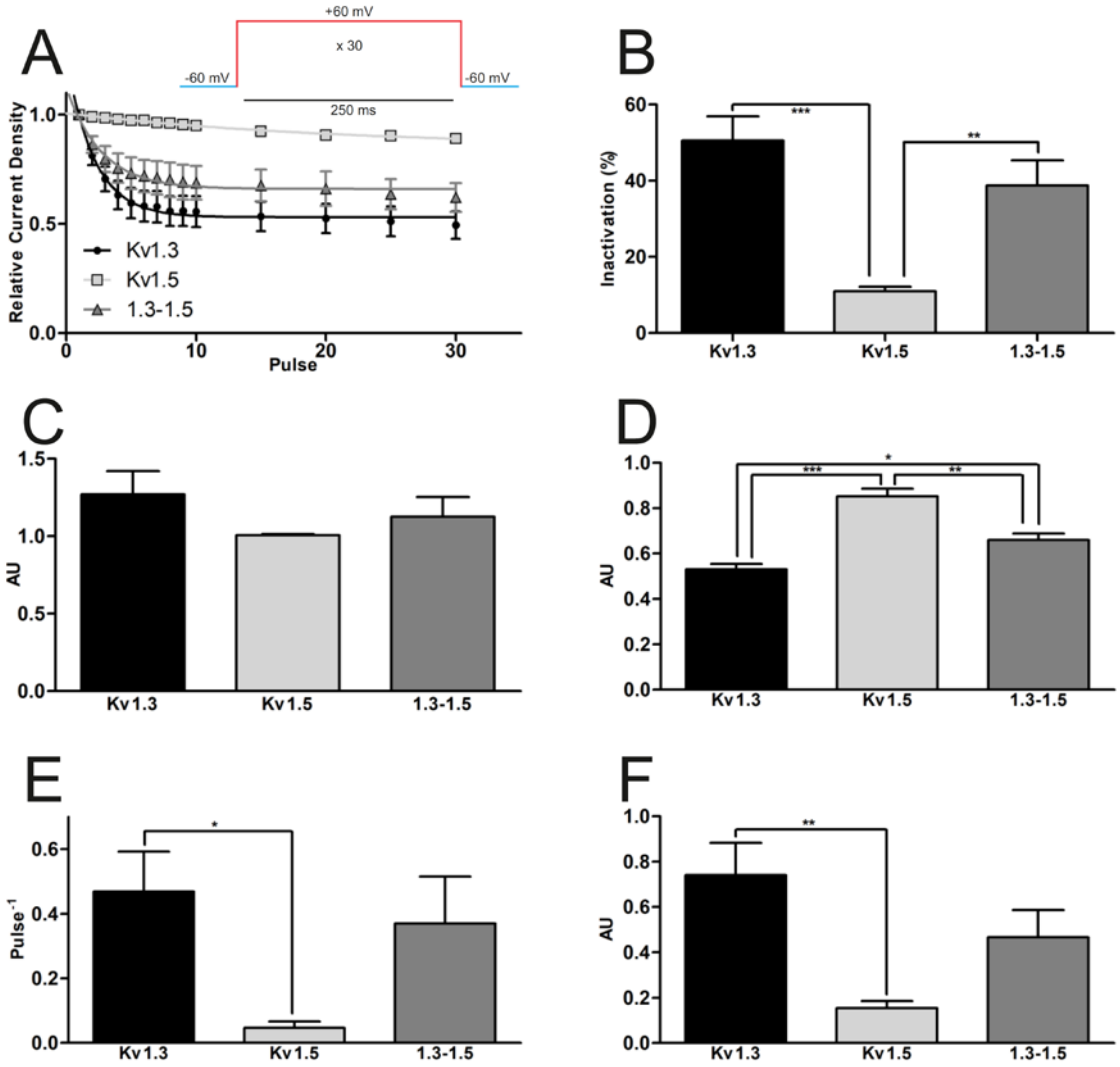

Fig. 7: *Cumulative inactivation of the K^+ currents generated by Tandem 1.3-1.5. Cumulative inactivation is observed when channels are repetitively opened and closed by a train of depolarizing pulses without enough interval to recover from their inactive state. Cumulative inactivation leads to a reduction of macroscopic currents. Cells were held at -60 mV and a 30 pulses train of +60 mV was applied. Pulses were 250 ms long and had an interval of 250 ms in between.* ***A:*** *Peak current from several pulses were relativized by the peak current of the 1st pulse and were fitted to a one-phase decay equation [Kv1.3: Y = (1.27 – 0,53) * exp (-0.4689 * X) + 0.53; Kv1.5: Y = (1.007 – 0.8515) * exp (-0.04662 * X) + 0.8515; 1.3-1.5: Y = (1.126 – 0.6597) * exp (-0.3698 * X) + 0.6597].* ***B:*** *Cumulative inactivation of the currents after 30 pulses. Inactivation was calculated by comparing the peak current of the last pulse with the one of the first pulse. The parameters of the cumulative inactivation dynamics were extracted from the one-phase decay equation.* ***C:*** *Y_0.* ***D:*** *Plateau.* ***E:*** *K.* ***F:*** *Span.* ***G:*** *Half Life.* ***H:*** *Tau. Values are mean ± standard error of 6-8 independent cells. *, p<0.05; **, p<0.01; ***, p<0.005 by One-way ANOVA test.*

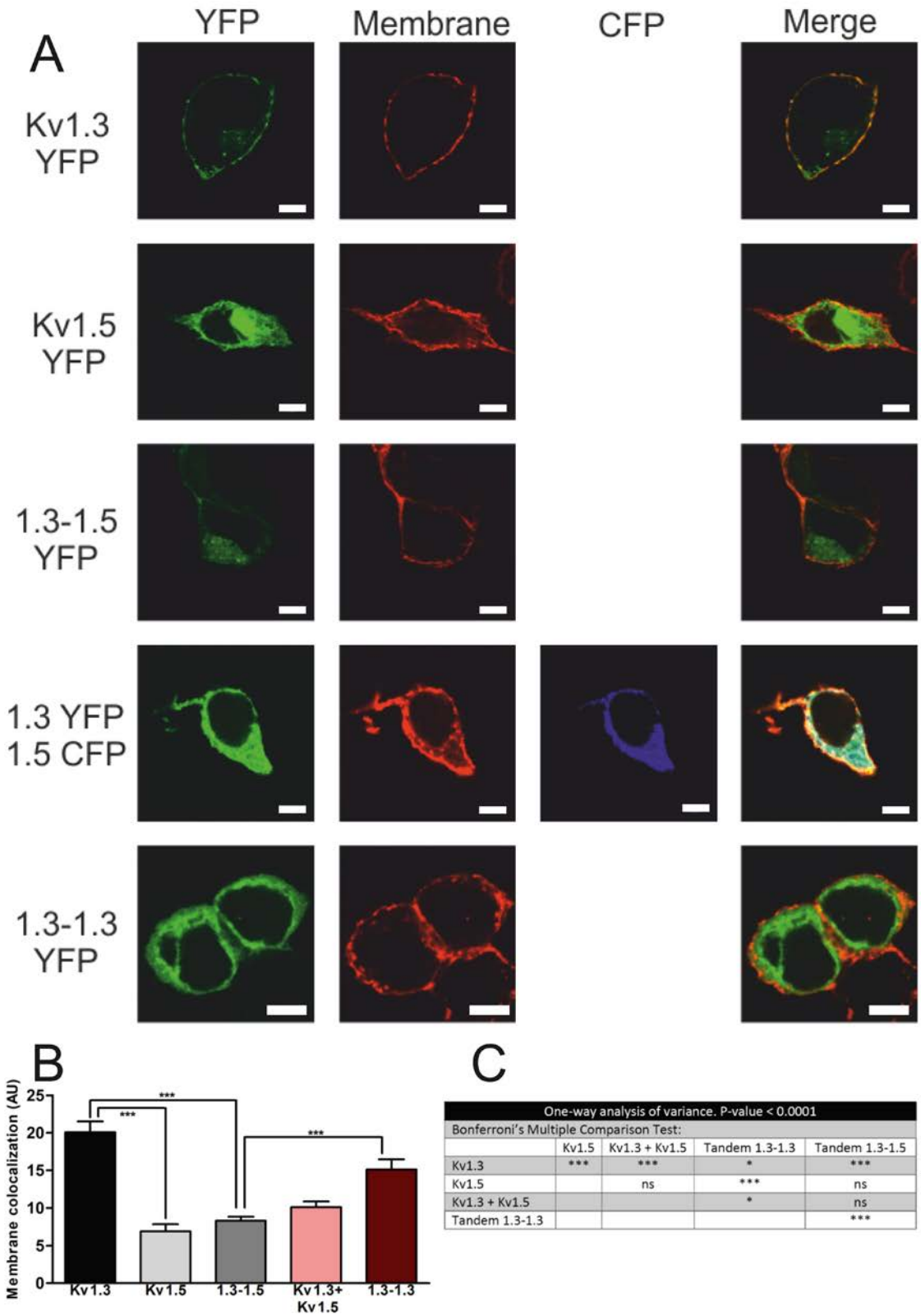

Fig. 8: *Membrane colocalization of Tandem 1.3-1.5. HEK 293 cells were transfected with different constructions: Kv1.3, Kv1.5, Kv1.3 + Kv1.5, Tandem 1.3-1.3 or Tandem 1.3-1.5. Live cells were stained with membrane marker WGA-Alexa555, fixated and mounted for microscopy observation. Preparations were observed in a confocal microscope and images were taken.* ***A:*** *Representatives images of transfected cells. Channel is painted in green, Membrane in red; and Kv1.5 in the co-transfection (Kv1.3 + Kv1.5) in blue. The white bar in the lower right corner represents 5 µm long.* ***B:*** *Membrane colocalization of the different conditions in arbitrary units (AU).* ***C:*** *Statistics. Values are mean ± standard error of 28-37 independent cells. ns, non-significant; *, p<0.05; ***, p<0.005 by One-way ANOVA test.*

4.1.2.3. Kv1.5 acts as a dominant negative for Kv1.3 traffic

Kv1.3 has a very efficient anterograde traffic, decorating the HEK 293 cell membrane. In contrast, Kv1.5 is notably retained at the ER (endoplasmic reticulum). Membrane expression is necessary for Kv channel to function. Therefore, the low current density of Tandem could be linked to a minor membrane targeting.

Thus, several constructs were transfected into HEK cells: Kv1.3, Kv1.5, Kv1.3/Kv1.5 (in a 1:1 stoichiometry), Tandem 1.3-1.5 and Tandem 1.3-1.3. Transfected cells were observed by using confocal microscopy in the presence of WGA, a membrane marker, conjugated to fluorophore Alexa-555. Both Kv1.3 and the Tandem 1.3-1.3 presented a high membrane expression. However, all the conditions with Kv1.5 got an intense intracellular retention. Therefore, regardless whether Kv1.5 was alone, linked to Kv1.3 or merely associated to it, all the complex exhibited a reduction in the membrane targeting (Fig. 8).

Similar results were achieved by membrane protein abundance. HEK 293 cells were transfected with Kv1.3, Kv1.5 and Tandem 1.3-1.5. Cells were processed by using a biotin membrane protein isolation kit and analysed by Western blot. Kv1.3 showed more membrane expression than the rest of conditions containing Kv1.5 (Fig. 9).

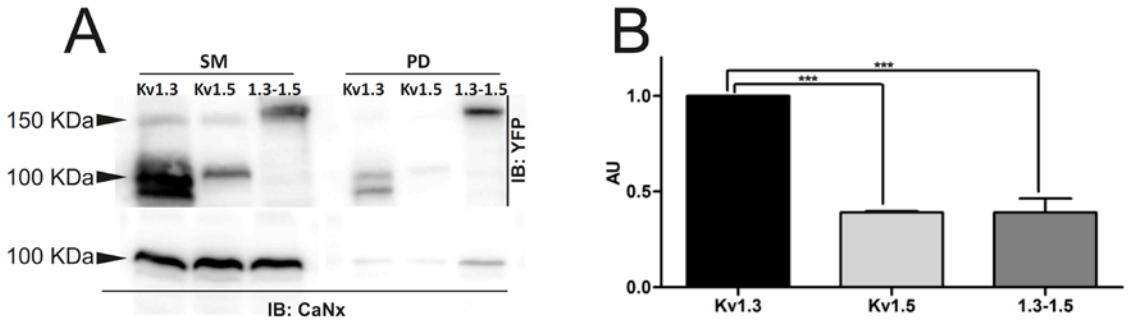

Fig. 9: Membrane protein abundance assay. HEK 293 cells were transfected with Kv1.3, Kv1.5 or Tandem 1.3-1.5 and treated with a biotin reagent which bound to membrane proteins. Cells were lysated (SM: Starting Material) and biotin-bound proteins were separated by binding with streptavidin (PD: Pull-Down). Both SM and PD fractions were loaded in a PAGE-SDS gel and western blotted. ***A:*** *Representative Western Blot of the assay immunoblotted (IB) against YFP and CaNx (Calnexin). CaNx was used both as a housekeeper in the SM fractions and as a negative control in the PD fractions.* ***B:*** *Membrane expression of the proteins. Quantification was performed by relativizing the PD bands with the SM bands and subtracting the CaNx signal. Results were normalized by the maximum value (Kv1.3). Values are mean ± standard error of 3 independent experiments. ***, p<0.005 by One-way ANOVA test.*

4.1.3. Effects of C-terminal domain in the functionality of the channel

4.1.3.1. Kv1.3 and Kv1.5 need to recognize their own C-terminus in the channel to function

Structural determinants within the ion channels have paramount importance on the function of the functional complex. While the amino-terminal domain of Kv1 (Shaker channels) is the responsible for the subunit interaction, the Kv7 (KCNQ family) interacts by using the C-term. In this context, most Kv channels have important molecular at the C-terminus of the channel. In a previous study, we decipher the C-term molecular determinants involved in the anterograde traffic. Surprisingly, in channels that switched the C-terms the function of the channel is greatly impaired. Therefore, to further decipher the molecular relationships that determine the functionality of the heteromeric Kv1.3-Kv1.5 channel, in this work we studied the role of the C-term in depth.

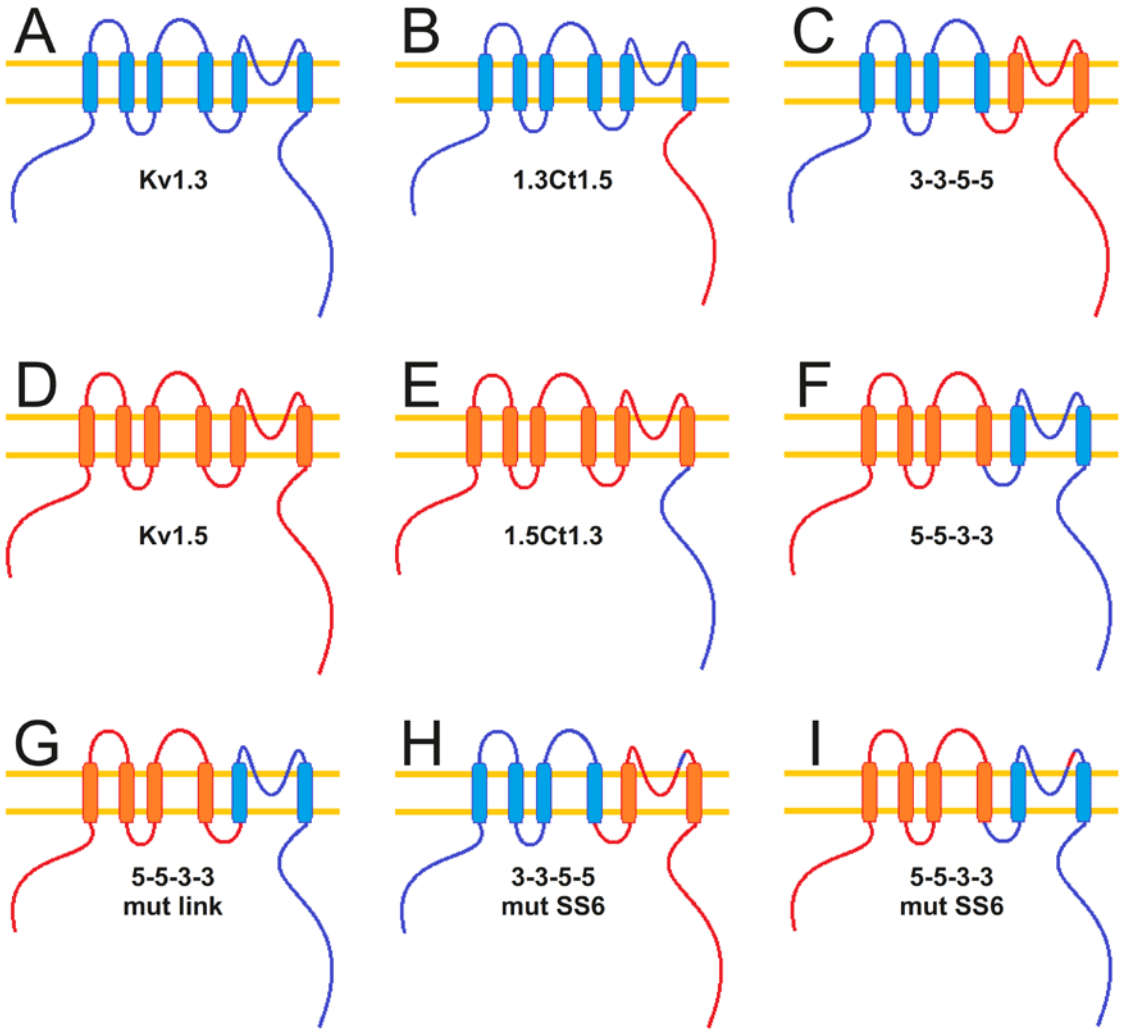

Fig. 10: *Schematic representation of the different mutants and chimaeras. While Kv1.3 domains are coloured in orange, Kv1.5 regions are in blue. Membrane bilayer is shown in yellow.* ***A:*** *Kv1.3.* ***B:*** *1.3Ct1.5 (Kv1.3 channel with Kv1.5 C-terminus).* ***C:*** *3-3-5-5 (Kv1.3 channel with the S4-S5 linker, the pore-forming domain and C-terminus of Kv1.5).* ***D:*** *Kv1.5.* ***E:*** *1.5Ct1.3 (Kv1.5 channel with Kv1.3 C-terminus).* ***F:*** *5-5-3-3 (Kv1.5 channel with the S4-S5 linker, pore-forming domain and C-terminus of Kv1.3).* ***G:*** *5-5-3-3 mut link (Kv1.5 channel with the pore-forming domain and C-terminus of Kv1.3).* ***H:*** *3-3-5-5 mut SS6 (Kv1.3 with the S4-S5 linker, pore-forming domain and C-terminus of Kv1.5; but the SS6 region of Kv1.3).* ***I:*** *5-5-3-3 mut SS6 (Kv1.5 with the S4-S5 linker, pore-forming domain and C-terminus of Kv1.3; but the SS6 region of Kv1.5).*

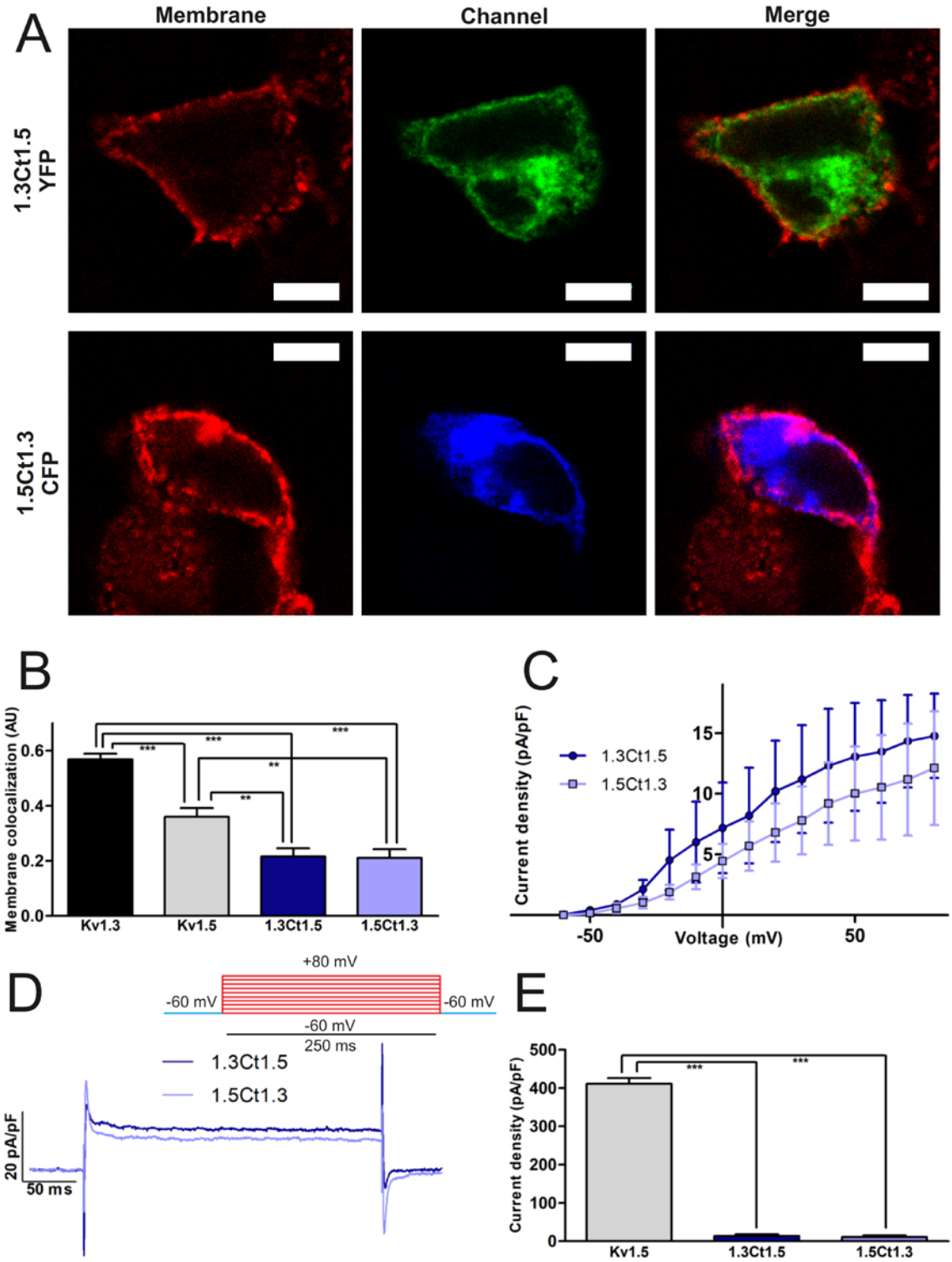

Fig. 11: *Electrophysiological and traffic properties of the C-terminal chimaeras. HEK 293 cells were transfected with Kv1.3, Kv1.5, 1.3Ct1.5 or 1.5Ct1.3. Cells were stained with membrane marker WGA-Alexa555, fixated and mounted for microscopy observation. Preparations were observed in a confocal microscope and images were taken. In addition, transfected cells were held at -60 mV and 250 ms pulses were applied from -60 mv to +80 mV in increments of 10 mV.* ***A:*** *Representative images of transfected cells. Membrane is painted in red; 1.3Ct1.5 in green; and 1.5Ct1.3 in blue. White bars represent 5 µm.* ***B:*** *Membrane colocalization of the different conditions calculated by using the Manders coefficient. Values are mean + standard error of 15-18 independent cells.* ***C:*** *I/V relationship of the currents elicited in transfected HEK cells. Values used are those of the peak current.* ***D:*** *Currents elicited by a +60 mV pulse in 1.3Ct1.5 and 1.5Ct1.3 transfected cells.* ***E:*** *Current density generated by Kv1.5, 1.3Ct1.5 and 1.5Ct1.3 transfected cells at +60 mV. Values are mean ± standard error of 4-7 independent cells. **, p<0.01; ***, p<0.005 by One-way ANOVA test.*

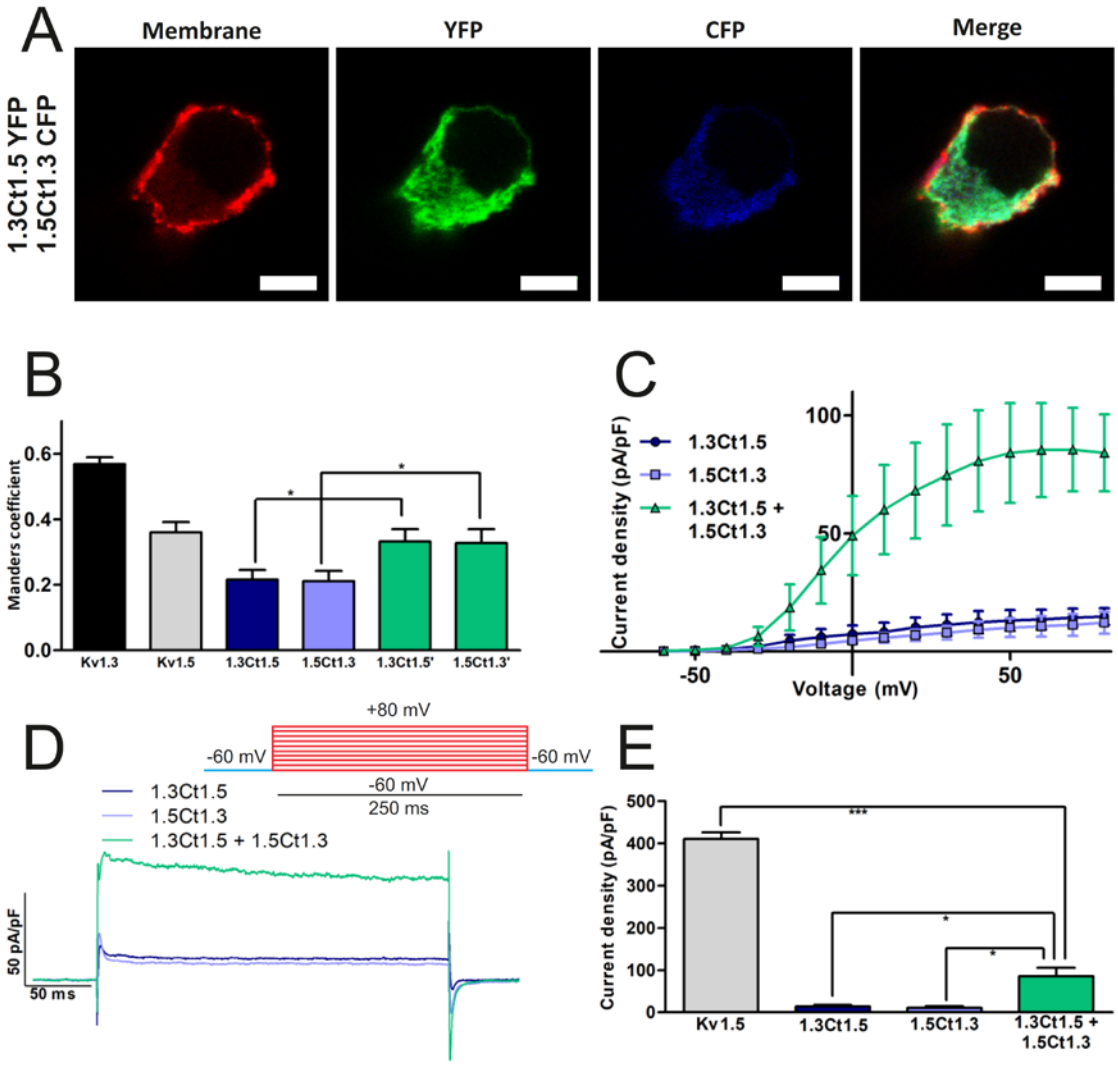

Fig. 12: *Electrophysiological and traffic properties of the co-transfected C-terminal chimaeras. HEK 293 cells were transfected with Kv1.3, Kv1.5, 1.3Ct1.5, 1.5Ct1.3 or 1.3Ct1.5+1.5Ct1.3. Live cells were stained with membrane marker WGA-Alexa555, fixated and mounted for microscopy observation. Preparations were observed in a confocal microscope and images were taken. In addition, cells were held at -60 mV and 250 ms pulses were applied from -60 mv to +80 mV in increments of 10 mV.* ***A:*** *Representative images of transfected cells. Membrane is painted in red; 1.3Ct1.5 in green; and 1.5Ct1.3 in blue. White bars represent 5 µm.* ***B:*** *Membrane colocalization of the different conditions calculated using the Manders coefficient. 1.3Ct1.5' and 1.5Ct1.3' represent the two chimaeras when co-transfected. Values are mean + standard error of 15-18 independent cells.* ***C:*** *I/V relationship of the currents elicited in transfected cells. Values used are those obtained atthe peak current.* ***D:*** *Currents elicited by a +60 mV pulse in 1.3Ct1.5, 1.5Ct1.3 and 1.3Ct1.5+1.5Ct1.3 transfected HEK.* ***E:*** *Current density generated by Kv1.5, 1.3Ct1.5, 1.5Ct1.3 and 1.3Ct1.5+1.5Ct1.3 transfected cells at +60 mV. Values are mean ± standard error of 3-7 independent cells. *, p<0.05; ***, p<0.005 by One-way ANOVA test.*

Kv1.3 and Kv1.5 chimerical constructions were generated. 1.3Ct1.5 is the Kv1.3 channel with its C-terminus swapped by that of Kv1.5 (Fig. 10B). In addition, 1.5Ct1.3 is the Kv1.5 protein with its C-terminus swapped by the one of Kv1.3 (Fig. 10E). Unlike the wild type channels, both chimerical channels exhibited almost no current density (Fig. 11C) (Fig. 11E). The current pulse showed an aberrant shape difficult to differentiate from leak currents (FIG. 11C and 11D).

Membrane expression was also assessed. C-terminal chimaeras exhibited even more deficient traffic to the membrane than Kv1.5. This 1.3Ct1.5 result could be explained by the lack of the Kv1.3 YMVIEE signal, which would hamper the anterograde traffic. On the

contrary, the 1.5Ct1.3 would gain the YMVIEE. However, both are largely retained. Thus, other retention mechanisms could exist in the rest of the channel (Fig. 11A and 11B).

Even though some correlation between the chimaeras' forward trafficking and their activity existed, the almost absent of function it did not seem justified. For instance, Kv1.3 express additional anterograde trafficking HRET(E/D) signals. In addition, the YMVIEE signal transfer to Kv1.5 would target the channel more efficiently to the membrane. Thus, the results from membrane expression do not match the expectations, which could suggest that the channels were just not functionals without their C-terminus.

To further analyse the event, both 1.3Ct1.5 and 1.5Ct1.3 chimaeras were co-transfected into HEK 293 cells. A significant increase of current density was observed (Fig. 12C and 12E). In addition, current traces resembled that of Kv1.3 or the Tandem 1.3-1.5 (Fig. 12D). Although the current density did not reach levels of Kv1.3 or Kv1.5 this event is not just additive (Fig. 12E).

Furthermore, the co-transfection of both chimaeras also had a positive effect over the membrane expression of individual 1.3Ct1.5 and 1.5Ct1.3. Thus, the combination of both reached levels similar to Kv1.5 (Fig. 12A and 12B). In this context, this effect, while being consistent with an improvement in the current density of the chimaeras, also denotes an additional cause impairing the function linked to the C-terminal recognition of the channel. The fact that the complex formed by 1.3Ct1.5 and 1.5Ct1.3 recovered the membrane expression of Kv1.5 (and 1.3-1.5) means that the channels needed their correspondent C-terminal domains to travel effectively to the membrane. Albeit with similar Kv1.5 levels at the membrane, the chimaeras did not elicit currents similar to Kv1.5. These data would suggest that the interaction between the C-terminal domain and the rest of the protein is needed in order to show a normal behaviour.

41.3.2. Pore domain in concordance with the C-terminus rescues the activity of the channel

The C-terminal domains of K^+ channels, and especially Shaker subunits, are known to be intrinsically disordered regions. Thus, when they do not interact with other proteins or regions, they tend to an amorphous structure, often aggregating or hiding certain motives. Our data would indicate that the C-terminal domain of the channel need an interaction with the rest of the channel in order to correctly fold, traffic and function. This impaired behaviour would be partially recovered by the presence of such domain upon co-expression of chimerical constructions.

In order to further decipher which domain interacts with the C-terminal in each subunit, several new chimerical constructions were generated. For that reason, proteins containing half moieties of Kv1.3 and Kv1.5 channels were constructed. Thus, the 3-3-5-5 chimaera expressed the N-terminus and the first four transmembrane domains (voltage sensor domain) of Kv1.3; while the S4-S5 linker, the additional two transmembrane domains (S5-S6, the pore domain) and the C-terminus of Kv1.5 (Fig. 10C). Accordingly, the 5-5-3-3 chimaera has the reciprocal combination (Fig. 10F).

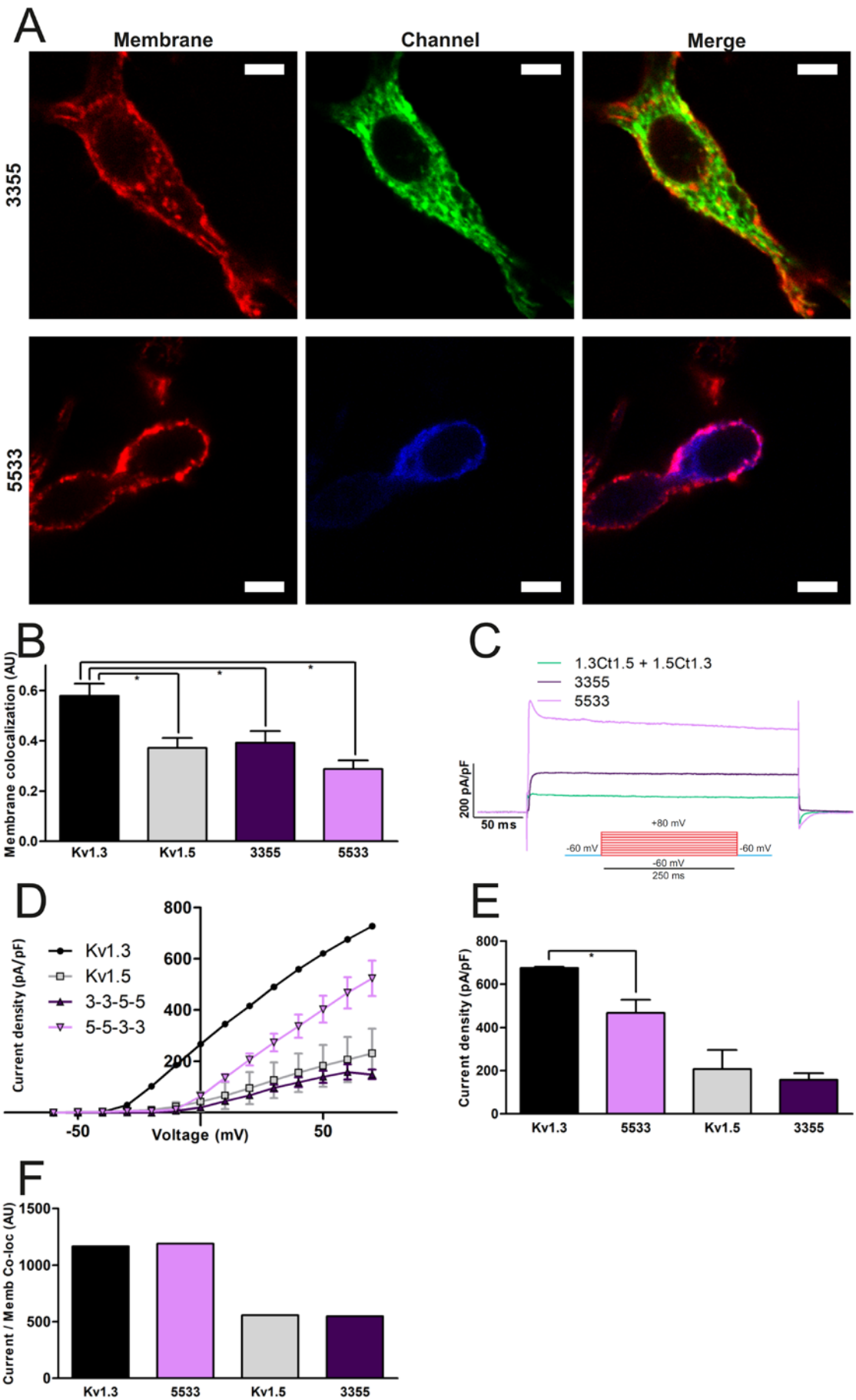
A
Membrane
Channel
Merge
3355
5533
B
Membrane colocalization (AU)
0.0
0.2
0.4
0.6
Kv1.3
Kv1.5
3355
5533
C
1.3Ct1.5 + 1.5Ct1.3
3355
5533
200 pA/pF
50 ms
+80 mV
-60 mV
-60 mV
-60 mV
250 ms
D
Current density (pA/pF)
Kv1.3
Kv1.5
3-3-5-5
5-5-3-3
800
600
400
200
-50
Voltage (mV)
50
E
Current density (pA/pF)
800
600
400
200
0
Kv1.3
5533
Kv1.5
3355
F
Current / Memb Co-loc (AU)
1500
1000
500
0
Kv1.3
5533
Kv1.5
3355

(←) Fig.13: *Electrophysiological and traffic properties of the S4-S5 chimaeras. HEK 293 cells were transfected with Kv1.3, Kv1.5, 3-3-5-5, 5-5-3-3 or 1.3Ct1.5+1.5Ct1.3. Cells were stained with the membrane marker WGA-Alexa555, fixated and mounted for microscopy observation. Preparations were observed in a confocal microscope and images were taken. In addition, transfected cells were held at -60 mV and 250 ms pulses were applied from -60 mv to +80 mV in increments of 10 mV.* ***A:*** *Representative images of transfected cells. Membrane is painted as red; 3-3-5-5 as green; and 5-5-3-3 as blue. White bars represent 5 µm.* ***B:*** *Membrane colocalization of the different conditions calculated by using the Manders coefficient. Values are mean ± standard error of 11-15 independent cells.* ***C:*** *Currents elicited by a +60 mV pulse in 3-3-5-5, 5-5-3-3 and 1.3Ct1.5+1.5Ct1.3 transfected HEK cells.* ***D:*** *I/V relationship of the currents elicited in transfected HEK cells. Values used are those at the peak current.* ***E:*** *Current density generated by Kv1.3, Kv1.5, 3-3-5-5 and 5-5-3-3 at +60 mV. Mean current density generated by HEK cells transfected with Kv1.3, Kv1.5, 3-3-5-5 or 5-5-3-3 chimaeras at +60 mV pulse.* ***F:*** *Current density relativized by the membrane colocalization of the constructs. Values are mean ± standard error of 3-5 independent cells. *, p<0.05 by Student's t test.*

When voltage-dependent K+ currents were elicited by depolarizing pulses in HEK cells expressing these proteins, chimaeras 5-5-3-3 and 3-3-5-5 exhibited an activity similar to that observed in wild type Kv1.3 and Kv1.5 channels, respectively. Thus, 5-5-3-3, having the pore and C-terminus of Kv1.3, expressed a Kv1.3-like activity, and 3-3-5-5, containing the pore and C-terminus of Kv1.5, almost recovered the function of Kv1.5 (Fig. 13C, 13D and 13E).

When comparing their I/V relationships with that of wild type channels, a difference in their voltage-dependence became apparent. Both 3-3-5-5 and 5-5-3-3 exhibit a shift in their voltage-dependence activation, starting to open at more depolarizing values as -10 and 0 mV. This event could be explained by the fact that their S4-S5 linker belonged to the second part of the chimaera (thus, it corresponded with the pore and C-terminus, not the voltage-sensing domain). The S4-S5 linker is an important piece in the transmission of movements from the voltage-sensing domain to the pore.

We also analysed the membrane co-localization. Both 3-3-5-5 and 5-5-3-3 showed membrane expression similar to Kv1.5 (Fig. 13A and 23B). This result brings together the current density values with the structure of the chimaeras. Thus, 3-3-5-5, not expressing the YMVIEE, presented an intracellular retention very similar to Kv1.5. in addition, 5-5-3-3, which has YMVIEE but also the strong retention signals, probably on the N-terminus of Kv1.5, did not traffic efficiently to the membrane. This reduced membrane expression correlates with the 5-5-3-3 activity, because this channel generates less activity than the Kv1.3 wild type. Moreover, when normalized by their membrane co-localization, these half-moiety chimaeras exhibited roughly the same current density as the wild type channels (Fig. 13F). Our result would suggest that the internal C-terminal subunit recognition within the channel complex is important for their function.

4.1.3.3. S4-S5 linker and the SS6 region are not directly responsible for the rescue of the activity

Shaker, similar to other Kv channels, possess 6 transmembrane domains. Our results indicated that the C-terminal domain of Kv1.3 and Kv1.5 needs an interaction with some intracellular regions of the channel to function. Taking a closer look to our chimaeras, the cytoplasmic regions in the second moiety of the subunit are the C-terminus and the S4-S5 linker. Thus, we will assess whether the S4-S5 linker is the signal recognized by the C-terminus. Within the S4-S5 linkers there are some minor substitutions between the different Shaker channels. Therefore, by swapping the S4-S5 linker, the chimaera 5-5-3-3 mut-link was generated. Thus, this chimaera has the first moiety of Kv1.5, the second of Kv1.3, but the S4-S5 linker of Kv1.5; separating this way the linker from the C-terminus (Fig. 10G). However, studies performed with these mutants gave similar results to the previous 5-5-3-3 chimaera.

These mutants also exhibited the same shift in voltage-dependence that the 5-5-3-3 chimaera showed in comparison with the wild type channels. This outcome would suggest that the linker is not necessary rather the C-term for the function of the channel (Fig. 24B).

Because the chimaera 5-5-3-3 Mut-Link has no other recognised cytoplasmic domains available for the C-terminus to connect, this raises the possibility of the P-loop being somewhat implicated. Within the P-loop, there are two regions which are distinct between Kv1.3 and Kv1.5: The Turret region; and a short sequence between the Selectivity filter and the S6 domain, which we will call SS6 (Fig. 24A). Thus, the SS6 domain was mutated in both 5-5-3-3 and 3-3-5-5 chimaeras to generate the 5-5-3-3 Mut-SS6 (Fig. 10H) and 3-3-5-5 Mut-SS6 chimaeras (Fig. 10I).

Once again, these new chimaeras were transfected and analysed. Finally, the current density values of the channels were once again similar to the non-mutated chimaeras (Fig. 24B). This would also rule the interaction with the SS6 region out of the discussion as being necessary for the channel activity.

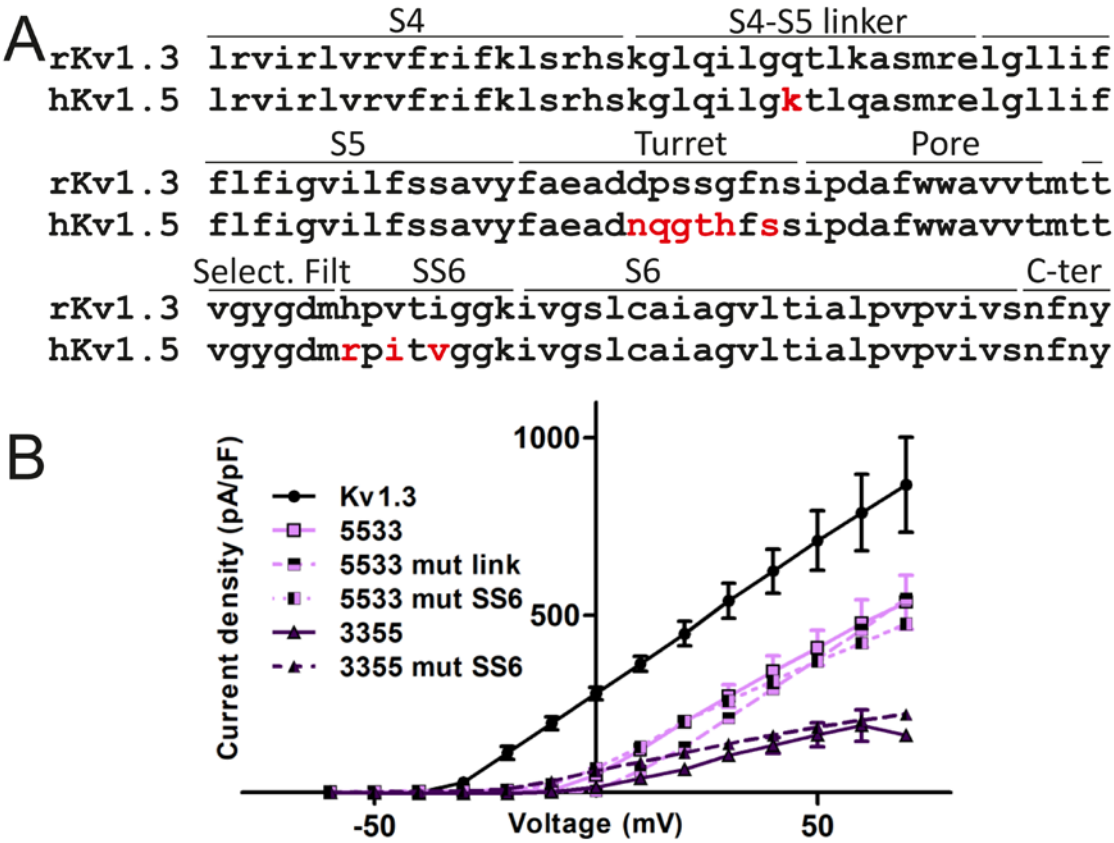

Fig. 14: *S4 to proximal C-term sequence analysis between Kv1.3 and Kv1.5. HEK 293 cells were transfected with either Kv1.3, 3-3-5-5, 3-3-5-5 mut SS6, 5-5-3-3, 5-5-3-3 mut link or 5-5-3-3 mut SS6. Transfected cells were held at -60 mV and 250 ms pulses were applied from -60 mv to +80 mV in increments of 10 mV.* ***A:*** *Protein sequence alignment of Kv1.3 and Kv1.5 in the region between the S4 and the C-terminus. Differences between both proteins are highlighted in red.* ***B:*** *I/V relationship of the currents elicited in transfected HEK cells. Values used are those at the peak current. The mutated chimaeras are in the same colour as the non-mutated ones for easier comparison. Values are mean ± standard error of 3-5 independent cells.*

Thus, two main hypotheses remain open which would need further debate.

(i) It could the that the turret region, the only non-assessed region of the Shaker channels, is somehow involved in this phenomenon with the C-terminus. However, this region is extracellular.

(ii) On the other hand, it could be that the C-terminus only needs an additional partner to interact, not being necessary a specific region. This last hypothesis would be consistent with the C-terminus being an intrinsically disordered. That is, the C-terminus would only need to interact with 1 other region and this interaction would help it not to become structurally aberrant and save the protein from the abnormal traffic and activity.

4.2. CHANNEL MODULATION BY REGULATORY SUBUNITS

4.2.1. Effects of KCNE4 on the heterotetramer

4.2.1.1. KCNE4 interacts with Kv1.3 regardless of the presence of Kv1.5

CY15 dendritic cells express Kv1.3, together with a significant amount of Kv1.5 and KCNE4. Thus, it is a useful native model to demonstrate whether the heterotetramer interacts with the KCNE β subunit. Kv1.3 was immunoprecipitated and both Kv1.5 and KCNE4 were detected (Fig. 15A). Therefore, Kv1.3 interacted with Kv1.5 and KCNE4 in dendritic cells. However, this data does not prove whether Kv1.3 interacted with both at the same time. Unfortunately, it was not possible to immunoprecipitate Kv1.5 or KCNE4 in this cell model.

To demonstrate the formation of the triple complex Kv1.3, Kv1.5 and Tandem 1.3-1.5 were co-expressed in HEK 293 cells, in different combinations, with KCNE4 and channels were immunoprecipitated. The different conditions were: Kv1.3; Kv1.5; Tandem 1.3-1.5 and Kv1.3 /Kv1.5 (1:1 ratio) (YFP-tagged). While Kv1.3 and Tandem 1.3-1.5 immunoprecipitated KCNE4, Kv1.5 did not (Fig. 15B). Only in the presence of Kv1.3, Kv1.5 pulled down a very low amount of KCNE4 (Fig. 15C). This result suggests that KCNE4 is able to interact with Kv1.3 even when forming heterotetramers with Kv1.5. However, the effectivity is reduced.

4.2.1.2. KCNE4 has a dual role regulating Kv1.3 activity depending on Kv1.5 association

KCNE4 interacts with Kv1.3 modulating its function. To check whether KCNE4 affected the function of the Tandem 1.3-1.5, electrophysiology experiments on HEK 293 cells were conducted. KCNE4 typically diminished Kv1.3 currents (Fig. 16A, 16B). On the contrary, KCNE4 did not exert any action on Kv1.5, consistent with their incapacity to interact (Fig. 16C, 16D). Tandem 1.3-1.5 did not exhibit neither of these behaviours. Surprisingly, KCNE4 triggered a two-fold increase in current density (Fig. 16E, 16F). This effect, not previously observed, could imply that KCNE4 acts dually depending on the presence of Kv1.5.

Moreover, KCNE4 shifted the Tandem 1.3-1.5 I/V graphics to more depolarizing voltages. This result was not seen in any homotetrameric channel (Fig. 16G, 16H, 16I).

The inactivation kinetics of Tandem 1.3-1.5 also got altered by KCNE4. After being activated for 5 seconds, the C-type inactivation got slightly reduced from 65% to 50%. This reduction, although non-significant, could suggest a tendency (p-value = 0.0781) of KCNE4 modifying the inactivation kinetics of the heterotetramer (Fig. 17A, 17B, 17C).

Contrarily, KCNE4 showed no effects on the cumulative inactivation of the Tandem 1.3-1.5 (Fig. 17D). After a train of 30 depolarizing pulses, the Tandem 1.3-1.5 showed no changes in the cumulative inactivation (Fig. 17E). The peak current of the train of 30 pulses were fitted with a one-phase decay exponential equation (Eq. 1) to assess the mathematical components of the inactivation. No mathematical parameters were significantly different between the two conditions (Fig. 17F). Therefore, KCNE4 did not affect the cumulative inactivation of the Tandem.

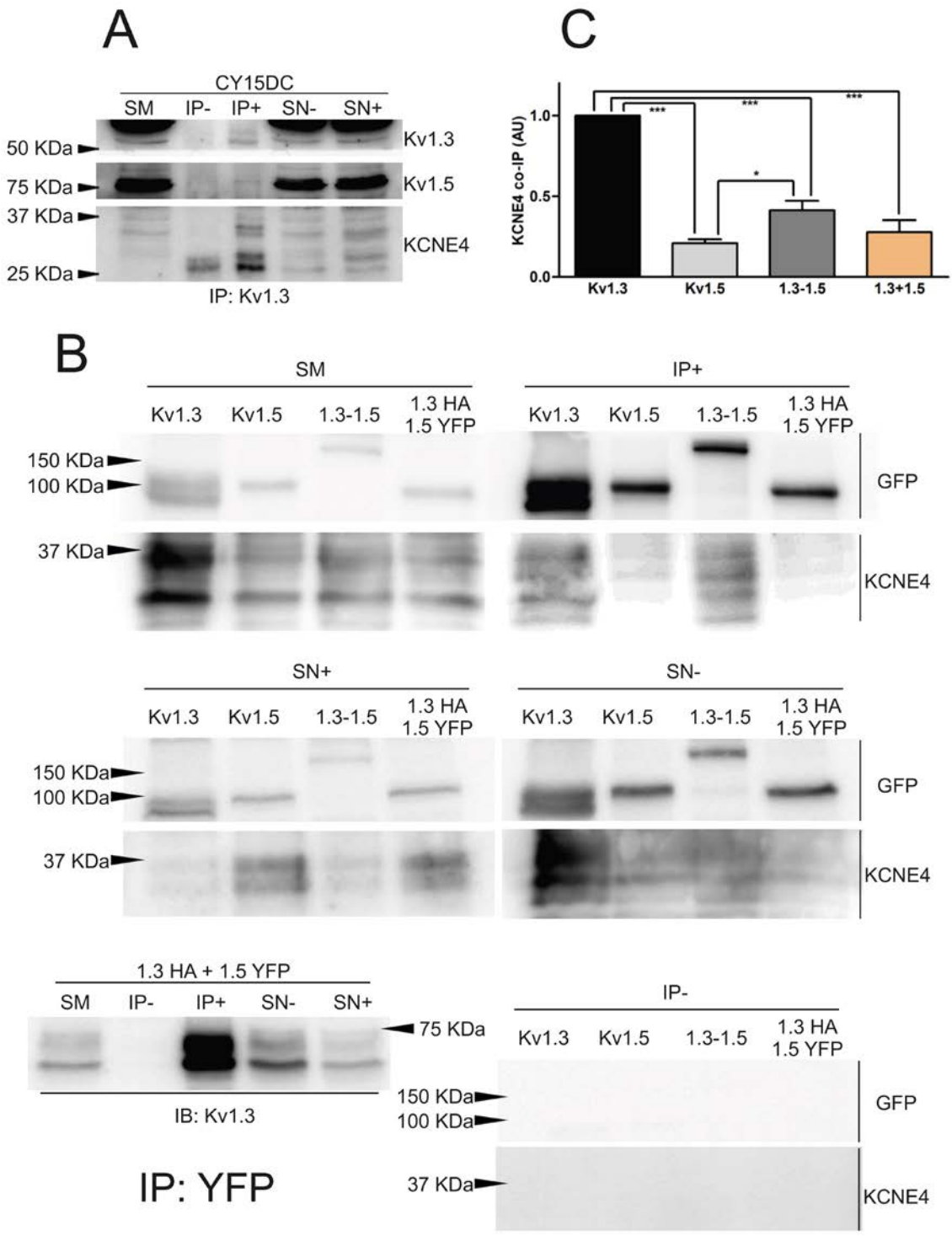

Fig. 15: *Interaction between KCNE4 and the complex formed by Kv1.3 and Kv1.5. CY15 dendritic and Jurkat T cells were lysated. Cell lysates were immunoprecipitated (IP) against Kv1.3 and samples were western blotted. Immunoblotting was performed against Kv1.3, Kv1.5, KCNE4 and KCNE1 (not shown) (**A**). HEK 293 cells were transfected with YFP-tagged Kv1.3, Kv1.5, Tandem 1.3-1.5 or Kv1.3+Kv1.5 in the presence or absence of KCNE4. HEK cells were lysated and processed for immunoprecipitation (IP) of the channel by YFP tag. In the Kv1.3+Kv1.5 condition Kv1.5-YFP was immunoprecipitated and Kv1.3 was tagged with HA. Samples were immunoblotted against GFP and KCNE4. Additionally, the Kv1.3+Kv1.5 condition was immunoblotted against Kv1.3 (**B**). SM: Starting Material; IP: Immuno-precipitated fraction; SN: Supernatants; IB: Immunoblot. [+]: presence of specific antibodies; [-]: absence of antibodies. **C:** KCNE4 co-immunoprecipitation of the different conditions relativized by the maximum (Kv1.3). Statistical analysis was performed by using the ANOVA test, followed by the Bonferroni test for pairwise comparison (n=3). Values are mean ± standard error of 3 independent experiments. *, p<0.05; ***, p<0.005 by One-way ANOVA test.*

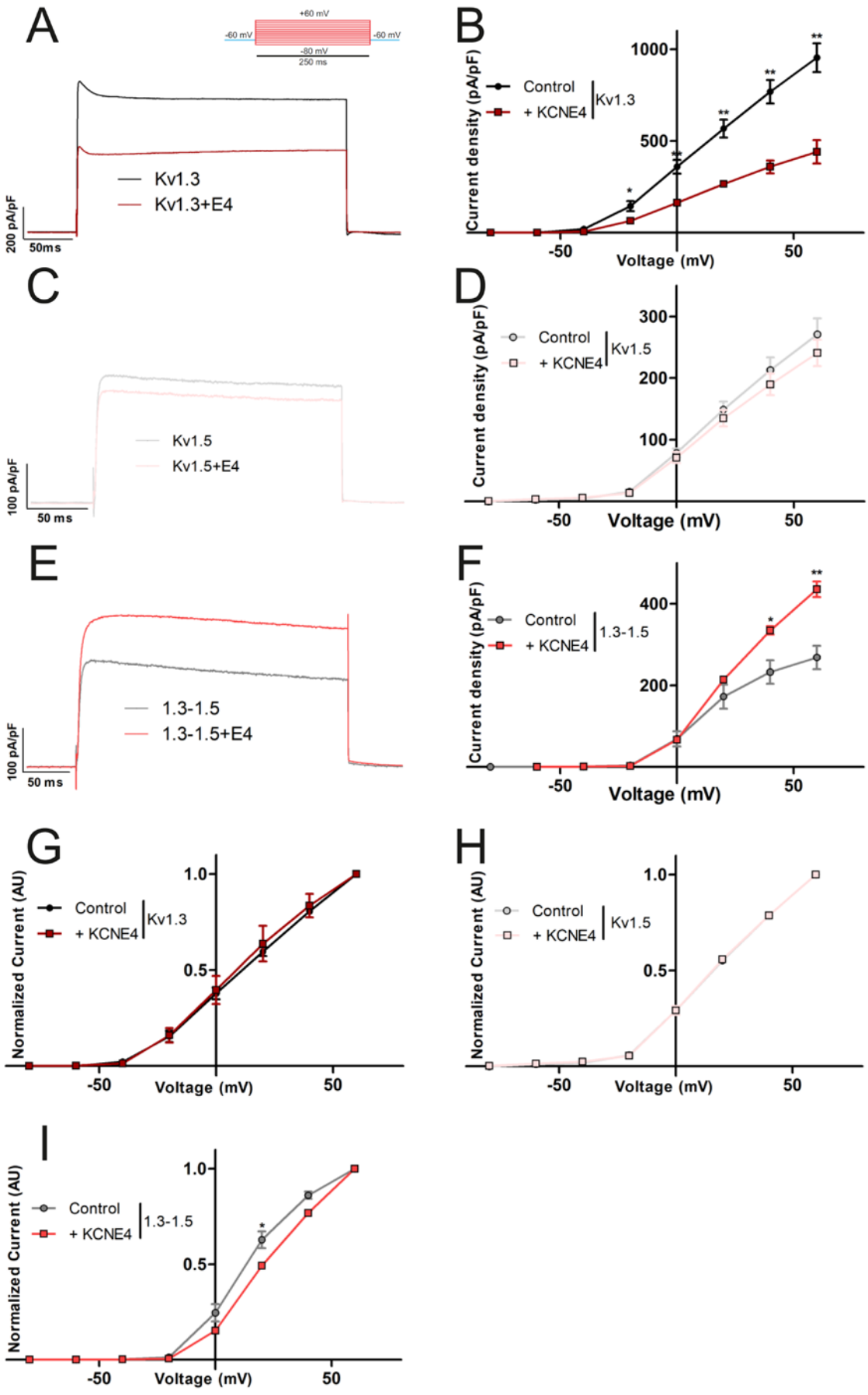
A
+60 mV
-60 mV
-60 mV
-80 mV
250 ms
Kv1.3
Kv1.3+E4
200 pA/pF
50ms
B
Current density (pA/pF)
Control
+ KCNE4
Kv1.3
Voltage (mV)
C
Kv1.5
Kv1.5+E4
100 pA/pF
50 ms
D
Current density (pA/pF)
Control
+ KCNE4
Kv1.5
Voltage (mV)
E
1.3-1.5
1.3-1.5+E4
100 pA/pF
50 ms
F
Current density (pA/pF)
Control
+ KCNE4
1.3-1.5
Voltage (mV)
G
Normalized Current (AU)
Control
+ KCNE4
Kv1.3
Voltage (mV)
H
Normalized Current (AU)
Control
+ KCNE4
Kv1.5
Voltage (mV)
I
Normalized Current (AU)
Control
+ KCNE4
1.3-1.5
Voltage (mV)

(←) Fig. 16: *Effect of KCNE4 on the activity of the different channels. HEK 293 cells were transfected with either Kv1.3, Kv1.5 or Tandem 1.3-1.5 in the presence or absence of KCNE4. Cells were held at -60 mV and 250 ms pulses were applied from -80 mV to +60 mV in increments of 10 mV. K^+ currents elicited in transfected cells by a +60 mV pulse in the absence or presence of KCNE4: Kv1.3 (**A**), Kv1.5 (**C**) and Tandem 1.3-1.5 (**E**). I/V relationship of the currents elicited in transfected HEK cells in the presence or absence of KCNE4: Kv1.3 (**B**), Kv1.5 (**D**) and Tandem 1.3-1.5 (**F**). I/V relationship representations were relativized at the maximum value for each condition: Kv1.3 (**G**), Kv1.5 (**H**) and Tandem 1.3-1.5 (**G**). Values are mean ± standard error of 3-8 independent cells. *, p<0.05; **, p<0.01 by Student's t test.*

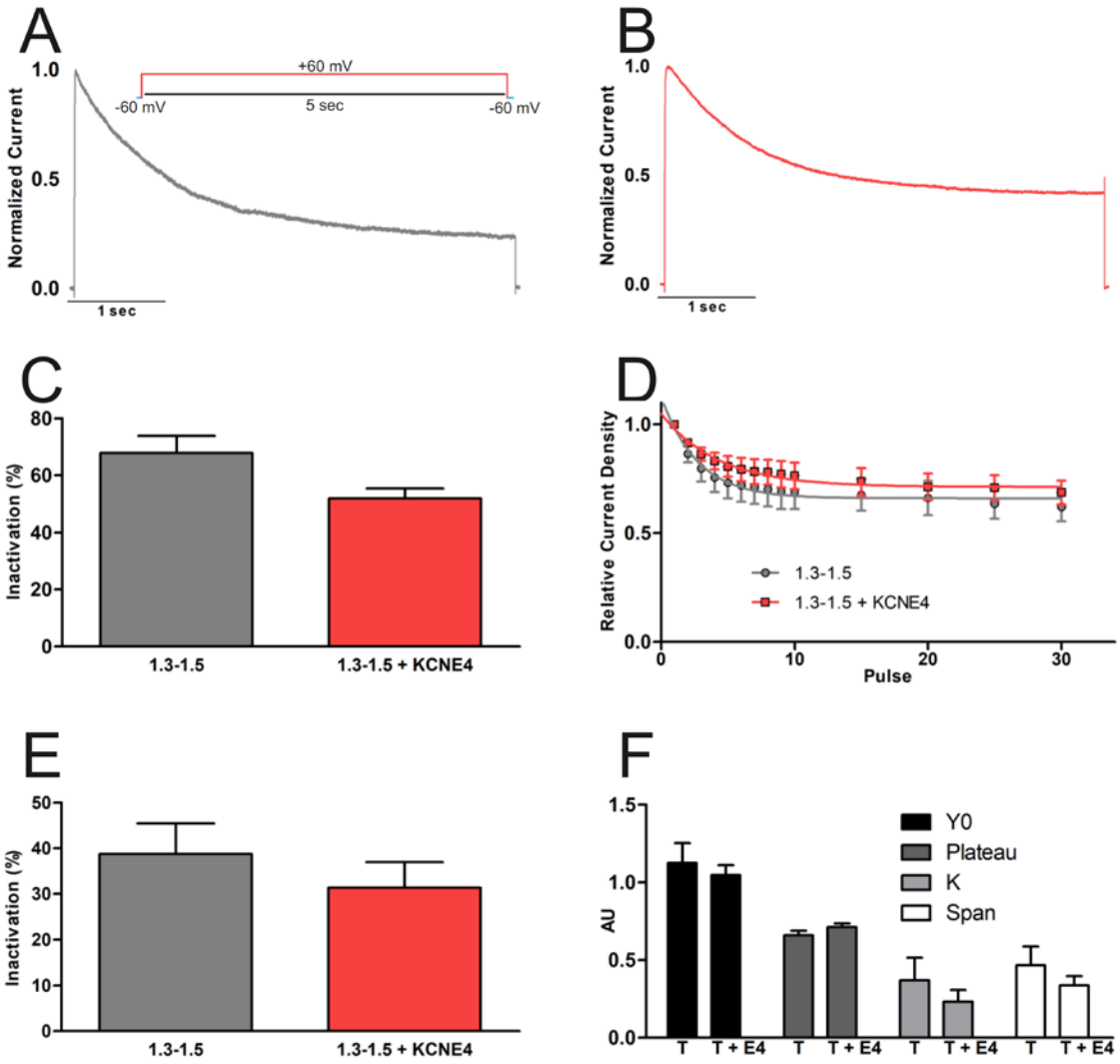

Fig. 17: *Effect of KCNE4 in the inactivations of Tandem 1.3-1.5. <u>C-type inactivation</u> is generated when channels are maintained in an open state because of a constant voltage. C-type inactivation leads to a gradual reduction of the current along the time that the channel is open. Cells were held at -60 mV and a 5 seconds pulse of +60 mV was applied. HEK 293 cells were transfected with Tandem 1.3-1.5 either in presence or absence of KCNE4. Currents elicited by this protocol were relativized to the maximum value: Tandem 1.3-1.5 alone (**A**) and with KCNE4 (**B**). **C:** Percentage of inactivation after the 5-second pulse. The inactivation was calculated by comparing the current after the 5-second pulse with the peak at the beginning of the pulse. **(D-F);** <u>Cumulative</u> inactivation is generated by a train of depolarizing pulses without enough interval to recover from their inactive state. Cumulative inactivation leads to a reduction of macroscopic currents after each pulse. Cells were held at -60 mV and a 30 pulses train of +60 mV was applied. Pulses were 250 ms long and had an interval of 250 ms in between. **D:** Peak currents were relativized by the peak current at the first pulse and were fitted to a one-phase decay equation [<u>1.3-1.5:</u> Y = (1.048 – 0.712) * exp (-0.2313 * X) + 0.7120; <u>1.3-1.5 + KCNE4:</u> Y = (1.126 – 0.6597) * exp (-0.3698 * X) + 0.6597]. **E:** Cumulative inactivation of the currents after 30 pulses. Inactivation was calculated by comparing the peak current of the last pulse with the one of the first pulse. The parameters of the cumulative inactivation were extracted from the one-phase decay equation (**F**) (T: Tandem 1.3-1.5; T + E4: Tandem 1.3-1.5 + KCNE4). Values are mean ± standard error of 4-6 independent cells. Statistics were assessed by Student's T test.*

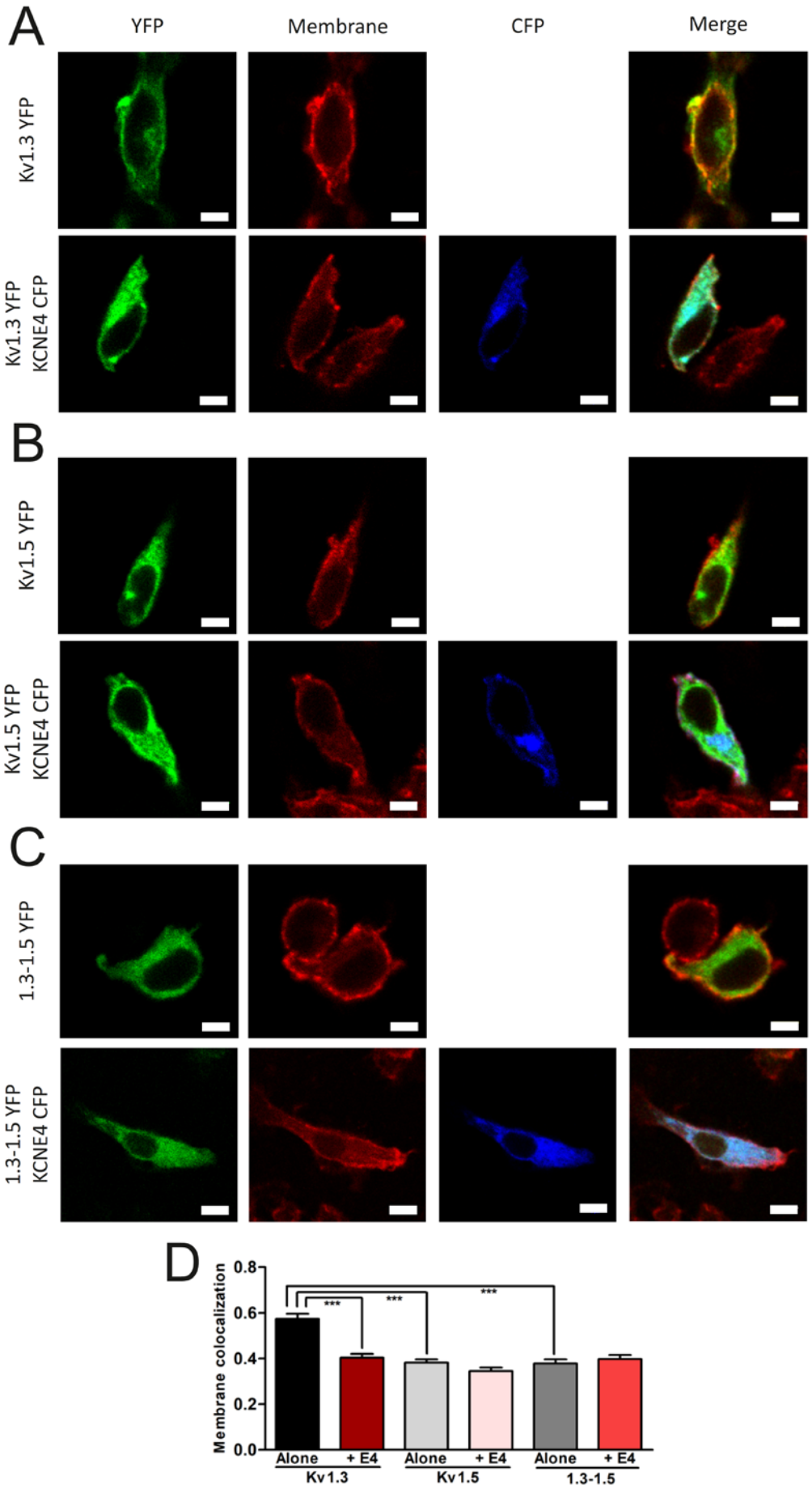
A
YFP
Membrane
CFP
Merge
Kv1.3 YFP
Kv1.3 YFP KCNE4 CFP
B
Kv1.5 YFP
Kv1.5 YFP KCNE4 CFP
C
1.3-1.5 YFP
1.3-1.5 YFP KCNE4 CFP
D
Membrane colocalization
0.0
0.2
0.4
0.6
0.8
***
***
***
Alone
+ E4
Alone
+ E4
Alone
+ E4
Kv1.3
Kv1.5
1.3-1.5

(←)Fig. 18: *Membrane colocalization of Tandem 1.3-1.5 when co-expressed with KCNE4. HEK 293 cells were transfected with different constructions: Kv1.3, Kv1.5, or Tandem 1.3-1.5; with or without KCNE4. Cells were stained with membrane marker WGA-Alexa555, fixated and mounted for microscopy observation. Preparations were observed in a confocal microscope and images were taken. Representative images of transfected cells with Kv1.3 (**A**), Kv1.5 (**B**) and Tandem 1.3-1.5 (**C**) are shown. Channel is painted in green, Membrane in red; and KCNE4 in blue. White bars represent 5 µm.* ***D:*** *Membrane colocalization of the different conditions calculated as a Manders coefficient. Values are mean ± standard error of 28-34 independent cells. ***, p<0.005 by One-way ANOVA test.*

Functional differences between the Tandem with or without KCNE4 could arise from two different possibilities. First, KCNE4 could affect somehow the Tandem 1.3-1.5 traffic, facilitating its membrane arrival. Second, KCNE4 could affect the structure of the heteromeric channel, resulting in the observed increase of activity. Even though the slight changes in activation and inactivation suggest a role of KCNE4 modifying the gating of the channel, the membrane expression must be assessed.

4.2.1.3. KCNE4 did not alter the traffic of the Tandem 1.3-1.5

Membrane targeting of channels was assessed by using confocal microscopy. HEK 293 cells were transfected with Kv1.3, Kv1.5 and Tandem 1.3-1.5 with and without KCNE4. In addition, the plasma membrane was stained with WGA-Alexa555 marker. Confocal images were taken, and the membrane co-localization was quantified (Fig. 18A, 18B, 18C).

KCNE4 retained Kv1.3 intracellularly in a similar way to the Tandem 1.3-1.5 alone. Consistent with previous studies, KCNE4 had no apparent effects on Kv1.5 membrane co-localization. Finally, Tandem 1.3-1.5 had a similar membrane co-localization regardless of KCNE4 expression (Fig. 18D). This means that the abovementioned increase in current density of the tandem was not apparently due to altering the membrane expression of the channel.

4.2.1.4. KCNE4 dual role is replicated in a native model

The abovementioned results were obtained by heterologous expression. For this reason, we further analysed a Kv1.3-Kv1.5 heterotetramer exposed to different concentrations of KCNE4 in a native model. CY15 dendritic cells notably express the three proteins of interest. We have previously generated a clone of CY15 which has the KCNE4 expression genetically-reduced by siRNA lentiviral particles. This cell line, named CY15 LvE4, was used as a low-KCNE4 model.

Expression of KCNE4, Kv1.3 and Kv1.5 were assessed in the CY15 cell lines by Western Blot (Fig. 19A). We confirmed that regardless KCNE4, Kv1.3 and Kv1.5 protein expression remained constant in CY15 LvE4.

K+ currents were measured by applying depolarizing pulses and it was possible to differentiate the wild type and the LvE4. CY15 WT exhibited around 13 pA/pF at +60 mV, whereas the LvE4 exhibited a 50% reduction (Fig. 19B, 19C, 19D). Thus, regarding current density, the reduction of KCNE4 expression leads to a decrement of the activity of the cell. This is consistent with electrophysiological assays performed in HEK 293 cells. All results suggest that KCNE4 is indeed acting dually depending on the presence of Kv1.5 in the complex. Whether this is a result of KCNE4 interacting with Kv1.5 by being attached to Kv1.3, or if it is caused by a triple interaction, remains to be discussed.

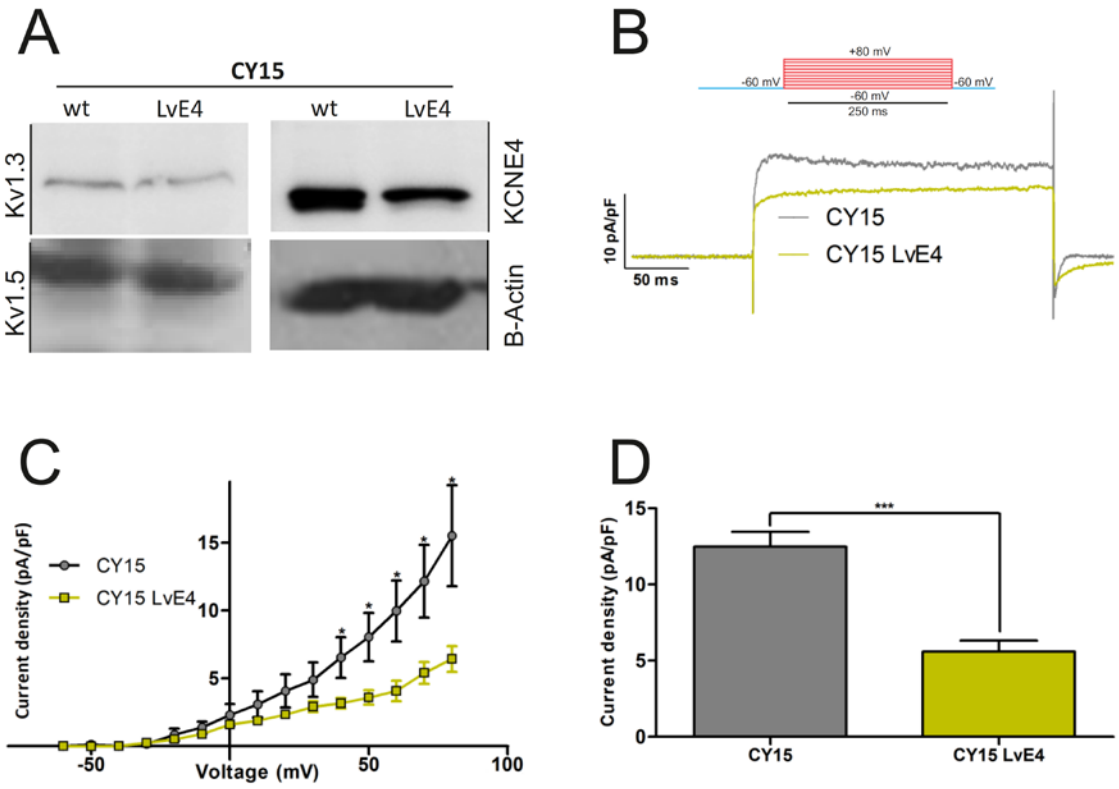

Fig. 19: *KCNE4 modulates voltage-dependent Kv currents in dendritic cells. CY15 LvE4 is a clone of the CY15 model with low protein expression of KCNE4 generated by genetic interference.* ***A:*** *Expression of Kv1.3, Kv1.5, KCNE4 and ß-Actin in CY15 and CY15 LvE4 cells. Cells were held at -60 mv and 250 ms pulses were applied from -60 mV to +80 mV in increments of 10 mV (****B****).* ***C:*** *I/V relationship of the currents elicited in CY15 and CY15 LvE4 cells. Values used were those at the peak current.* ***D:*** *Current density generated by CY15 and CY15 LvE4 at + 60 mV. Values are mean ± standard error of 3-4 independent cells. ***, p<0.005 by Student's t test.*

4.2.2. Interaction between Kv1.5 and KCNE1

4.2.2.1. KCNE1 interacts with Kv1.5

In leukocytes, Kv1.5 associates with Kv1.3. In addition, KCNE subunits differentially interact with Kv channels. Leukocytes not only express KCNE4 but also KCNE1. Because it was previously observed that KCNE1 could interact with Kv1.5, we wonder whether this interaction could affect the heteromeric complex physiology. Therefore, this interaction was definitely assessed in the present dissertation.

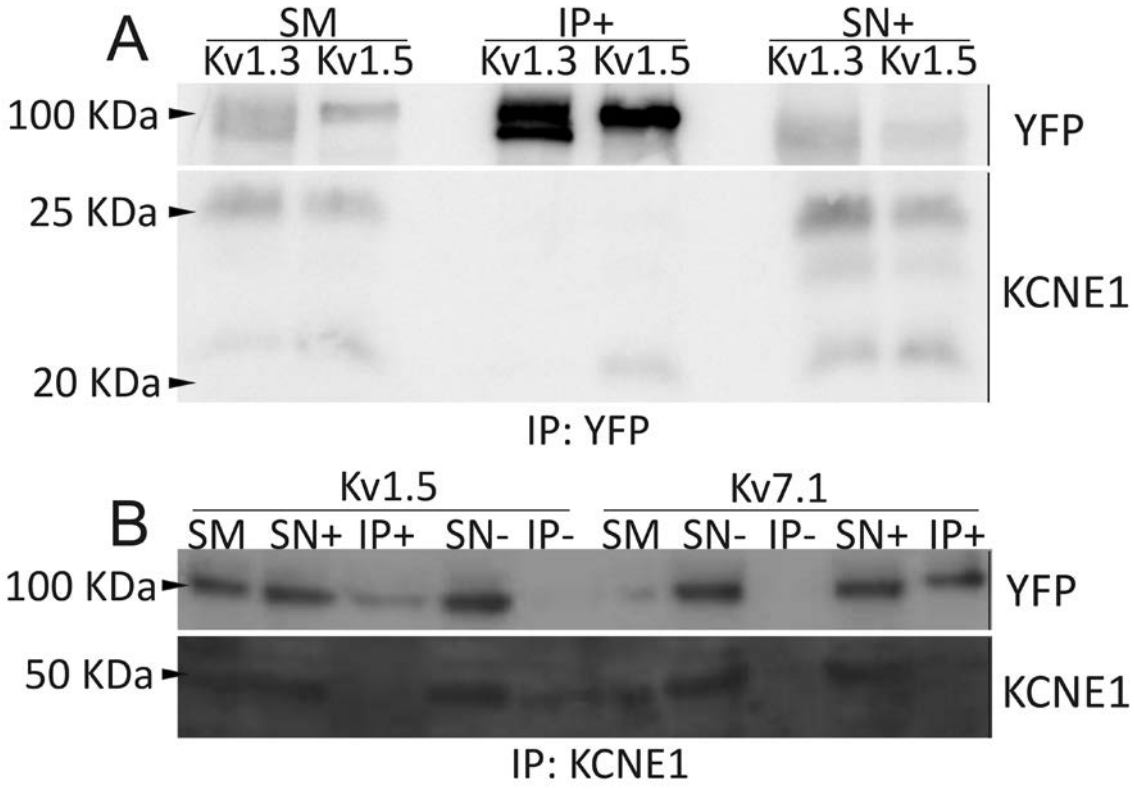

Fig.20: *Interaction between Kv1.5 and KCNE1. HEK 293 cells were transfected with Kv1.5, Kv1.3 (negative control) or Kv7.1 (positive control) with KCNE1 in two different experiments. (**A**) YFP-tagged Kv1.3 and Kv1.5 were immunoprecipitated (IP) in the presence of KCNE1. Samples were immunoblotted against either YFP or KCNE1. (**B**) KCNE1 was immunoprecipitated (IP) in the presence of YFP-tagged Kv7.1 or Kv1.5. Samples were immunoblotted against either YFP or KCNE1. SM: Starting Material; IP: Immuno-precipitate; SN: Supernatant; IB: Immunoblot. [+]: presence of antibodies; [-]: absence of antibodies. Representative experiments are shown.*

HEK 293 cells were co-transfected with Kv1.5, Kv1.3 (used as a negative control) or Kv7.1 (used as a positive control), as well as KCNE1. The interaction between subunits was assessed by co-immunoprecipitation. Kv1.5 and KCNE1 co-immunoprecipitated no matter the protein which was pulled down. KCNE1 also pulled-down Kv7.1, which has long been described to interact with KCNE1. On the contrary, Kv1.3 co-IP was negative (Fig. 16).

4.2.2.2. KCNE1 potentiates Kv1.5 activity and modifies its activation dynamics

Kv1.5 is physiologically relevant in both cardiomyocytes, antigen presenting cells and cancer progression. The activity of Kv1.5 channel was assessed both alone and in co-expression with KCNE1 or KCNE3 by Patch-clamp experiments. KCNE1 was able to potentiate the peak current of Kv1.5 two-fold. KCNE3, used as a negative control, showed no effects on Kv1.5 peak current (Fig. 21A, 21B).

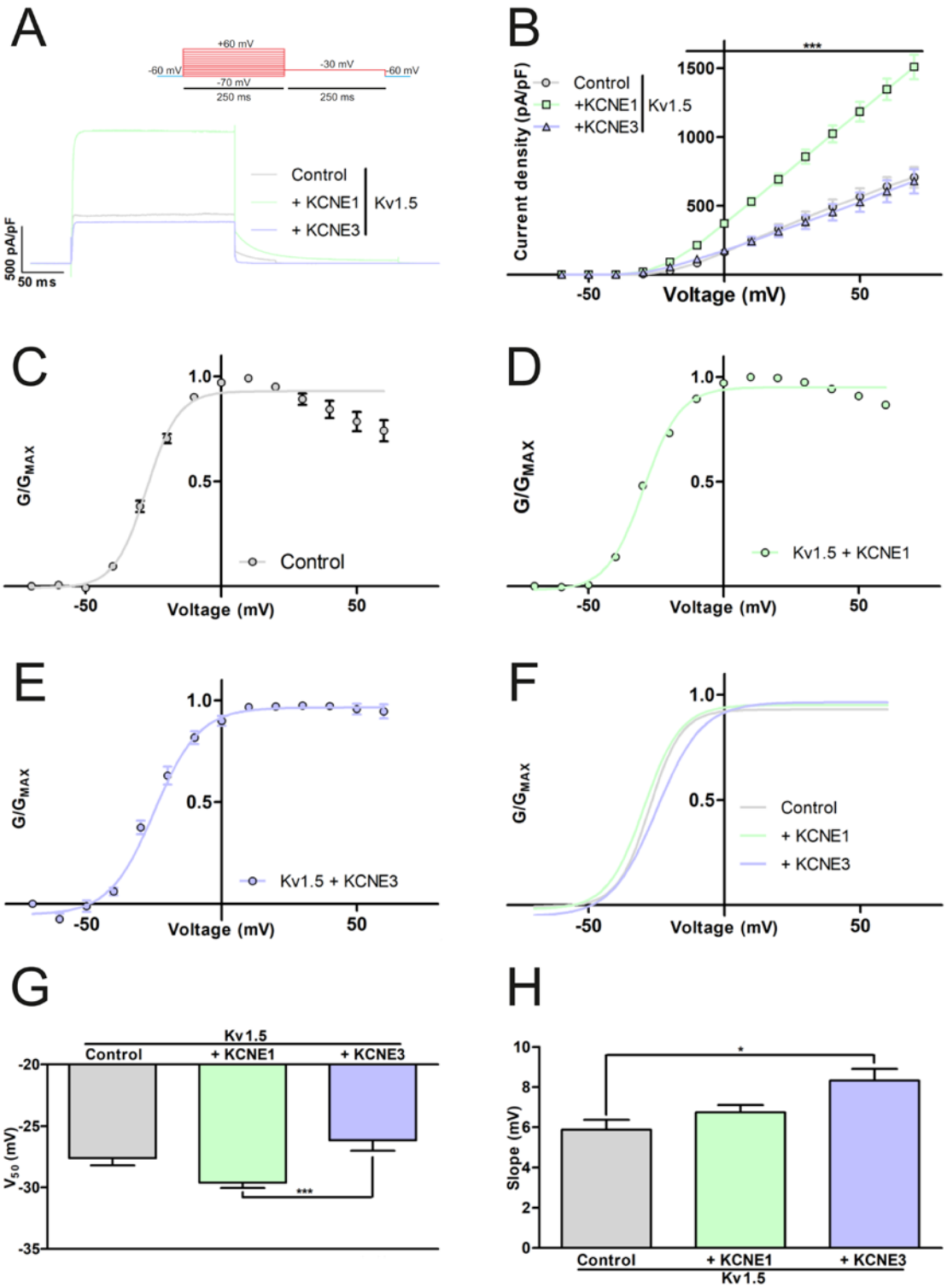

Fig. 21: *Effects of KCNE1 on the activity of Kv1.5. HEK 293 cells were transfected with Kv1.5, either alone or with KCNE1 or KCNE3. Cells were held at -60 mV and 250 ms pulses were applied from -60 mV to +80 mV in increments of 10 mV. Activation dynamics can be of easier study from a constant-voltage tail after an activation pulse (steady-state activation). Therefore, a mentioned 250 ms pulse is followed by a 250 ms pulse of near-activating voltage (-30 mV).* ***A:*** *Voltage-dependent K^+ Currents* ***B:*** *I/V relationship of the currents. Values are those at the peak current. Peak current of the tails was quantified and transformed into conductance [$G_N = I_N / (V_N – V_{REV})$]. Conductance was relativized to the maximum value and plotted against voltage to produce a G/G_{MAX} graphic. The G/G_{MAX} plot was fitted to a Boltzmann equation: Kv1.5 alone (**C**), with KCNE1 (**D**), and with KCNE3 (**E**). An additional representation of the three graphics together is also shown (**F**). The parameters of the steady-state activation were extracted from the Boltzmann equation: V_{50} (**G**) and Slope (**H**). Values are mean ± standard error of 12-20 independent cells. *, p<0.05; ***, p<0.005 by One-way ANOVA test.*

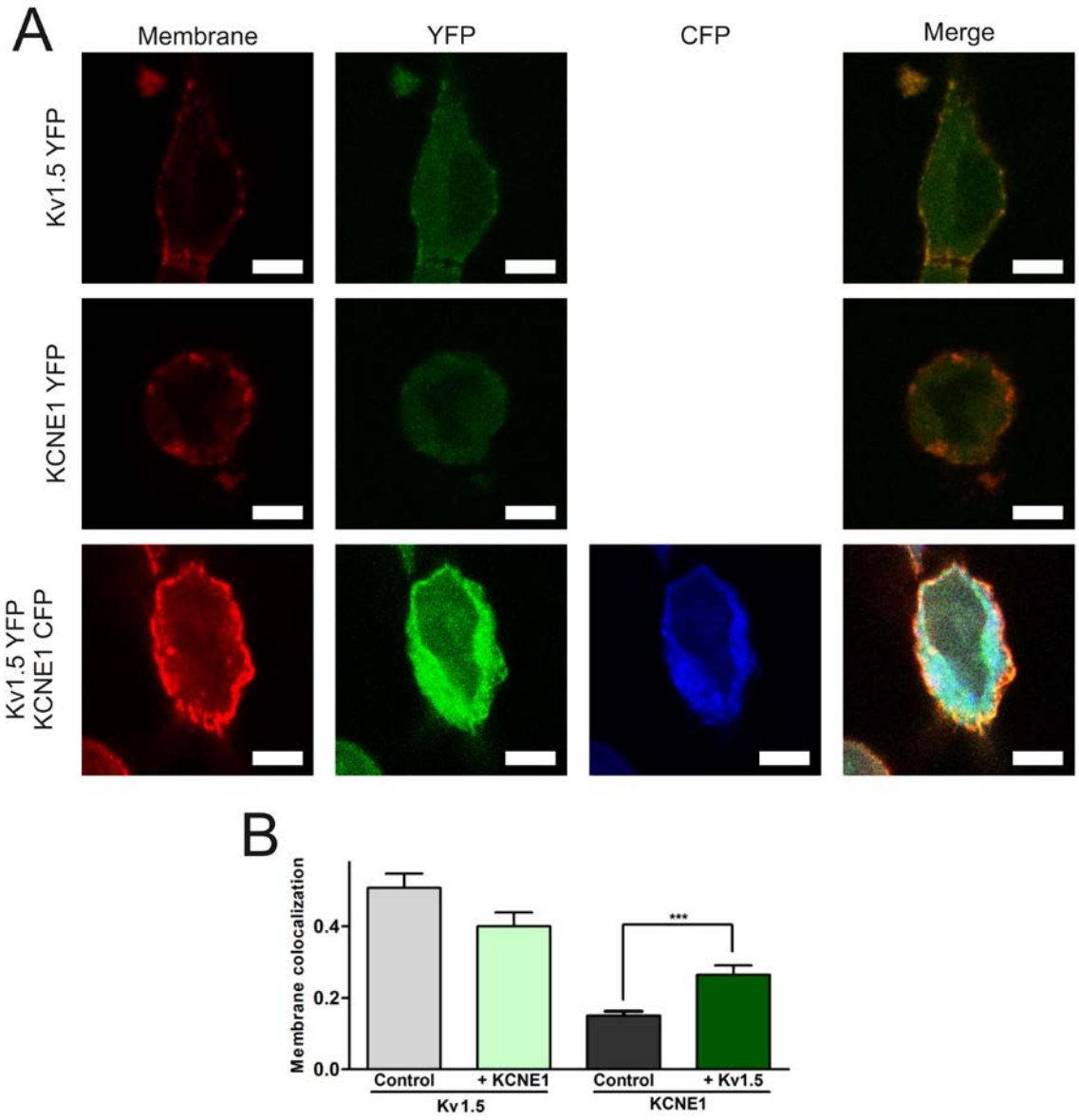

(←) Fig. 22: *Membrane colocalization of Kv1.5 in presence of KCNE1. HEK 293 cells were transfected with Kv1.5 with or without KCNE1. Cells were stained with the membrane marker WGA-Alexa555, fixated and mounted for microscopy observation. Preparations were observed in a confocal microscope and images were taken. (**A**) Representative images of transfected cells with Kv1.5, KCNE1 and both together. Kv1.5 and KCNE1 are painted in green when alone, and membrane in red. In the co-transfection panels, Kv1.5 is painted in green and KCNE1 in blue. White bars represent 5 µm.* ***B:*** *Membrane colocalization of the different conditions calculated by a Manders coefficient. Values are mean ± standard error of 22-25 independent cells. ***, p<0.005 by Student's t test.*

Cells expressing Kv1.5 alone in the presence or the absence of KCNE1 and KCNE3 were exposed to a train of pulses with tails of near-depolarizing voltage (-30 mV). By this way, the dynamics of channel opening is easier to study, as the voltage is constant. The conductance was obtained from the tail current by applying the following equation: $G_N = I_N / (V_N - V_{rev})$. V_{rev} is the reversal potential for K^+), which in this case is -79.67 mV. Thus, the G/G_{MAX} graphic was obtained (Fig. 21C, 21D, 21E) and fitted to a Boltzmann equation (Eq. 2) (Fig. 21F).

With the Boltzmann correlation we can obtain the V_{50} and Slope. The slope represents the activation dynamics (Fig. 21H). V_{50} represents the Voltage at which the channels get a 50% of activation. KCNE1 caused no apparent effect on the Slope of Kv1.5, whereas both KCNE1 and KCNE3 altered the V_{50} (Fig. 21G).

$$Eq.2 - Boltzmann\ eq: Y = Bot + \frac{(Top - Bot)}{(1 + \exp(\frac{V_{50} - X}{Slope}))}$$

Kv1.5 alone (Eq. 3) and with KCNE1 (Eq. 4) presenting differences in some dynamics parameters would seem logical taking into account the differences in peak current. Kv1.5 with KCNE3 (Eq. 5) being different to Kv1.5, though, arises plenty of questions. KCNE3 has not been described to interact with Kv1.5 and does not seem to alter its peak current. Therefore, further assessments should be performed to clarify the role of KCNE3.

$$Eq.3 - \ Kv1.5\ Boltzmann\ eq: Y = -0.007388 + \frac{(0.9297 + 0.007388)}{(1 + \exp(\frac{-27.62 - X}{5.880}))}$$

$$Eq.4 - Kv1.5 + KCNE1\ Boltzmann\ eq: Y = -0.01944 + \frac{(0.9515 + 0.01944)}{(1 + \exp(\frac{-2961 - X}{6.746}))}$$

$$Eq.5 - Kv1.5 + KCNE3\ Boltzmann\ eq: Y = -0.05528 + \frac{(0.9596 + 0.05528)}{(1 + \exp(\frac{-26.15 - X}{8.388}))}$$

4.2.2.3. KCNE1 alters Kv1.5 lipid raft targeting

Kv1.5 presents a notable intracellular retention. Thus, KCNE1 could potentiate Kv1.5 activity by facilitating the anterograde traffic. The KCNE1 interaction could mask Kv1.5 endogenous ER retention motives.

HEK 293 cells were transfected with either Kv1.5 in the presence or the absence of KCNE1 (1:1 ratio). Cells were treated with WGA-Alexa555 and images were taken in a confocal microscope to assess the membrane co-localisation.

KCNE1 exhibited less membrane targeting than Kv1.5 and their co-expression showed an intermediate phenotype. While KCNE1 did not improve the anterograde traffic of Kv1.5, the KCNE subunit slightly increased its membrane expression in the presence of Kv1.5 (Fig. 22).

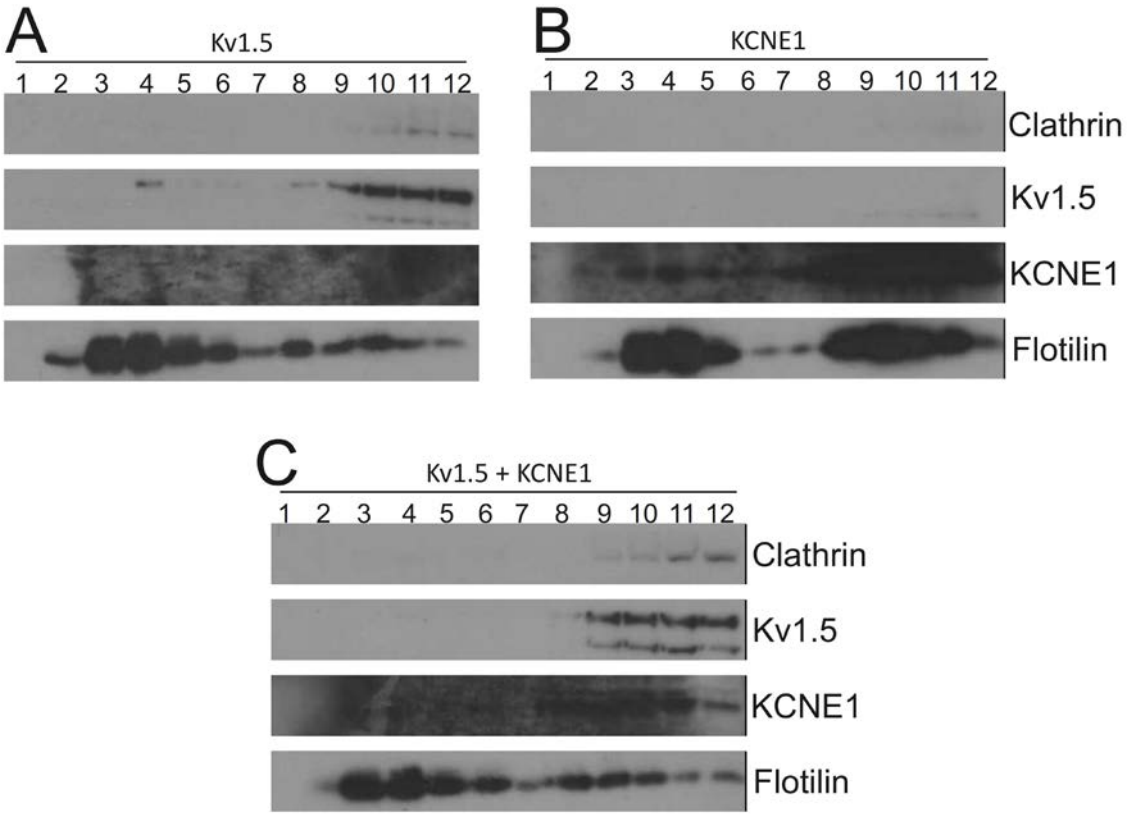

Fig. 23: *Kv1.5 and KCNE1 lipid raft microdomain targeting. HEK 293 cells were transfected with Kv1.5, KCNE1, or both together. Cells were lysated without detergents and protein lysates were separated by using a sucrose density gradient. Therefore, 12 fractions were extracted: fraction 1 represents the least dense, while fraction 12 is the heaviest. Lipid raft microdomains are special detergent-resistant regions in membranes with lower density than the rest of the membrane. Therefore, proteins located in lipid raft microdomains like Flotillin are found in high-bouyant fractions. Proteins not located in lipid raft microdomains like Clathrin appear in the low-bouyant fractions. Fractions were western blotted and immunoblotted against Kv1.5, KCNE1, Clathrin and Flotillin: Kv1.5 (**A**), KCNE1 (**B**) and both together (**C**). Representative results from 5 independent experiments.*

To sum up, results of membrane co-localization experiments support that changes of Kv1.5 activity cannot be explained by an increase of membrane targeting.

Regional membrane localization is an important factor on the channel activity. Therefore, some membrane lipid raft microdomain inclusion greatly alters function. Accordingly, lipid raft microdomain purification was performed in HEK 293 cells transfected with Kv1.5, KCNE1 or both proteins (Fig. 23). Flotillin was used as a floating fraction marker, whereas clathrin served as a non-floating fraction marker. Kv1.5 showed a partial lipid raft localization, as well as KCNE1. However, upon co-expression, Kv1.5 and KCNE1 shifted out from the lipid raft domains.

Kv1.5 is typically retained intracellularly and has half current density compared with Kv1.3. Like Kv1.3, whose interaction with KCNE4 modifies its electrophysiology; Kv1.5 is able to interact with KCNE1 and this interaction causes a significant increase in the activity of the channel. Our results demonstrated that this effect cannot be explained by an increase on membrane expression or lipid raft localization.

4.3. GENOMIC SEQUENCING OF MULTIPLE SCLEROSIS PATIENTS

The mutual relationships between subunits can greatly affect the function and behaviour of the channels. KCNE4 not only inhibits Kv1.3, but also rescues the Kv1.3 heterotetramer from Kv1.5 inhibition when expressed in a 1:1 stoichiometry. Similarly, KCNE1 potentiates Kv1.5 activity. The effect of KCNE1 on the Kv1.3/Kv1.5 heterotetramer is not assessed in the present work, however it remains as a possibility given the effects of KCNE4 on the complex.

Kv1.3, Kv1.5, KCNE1 and KCNE4 are present in leukocytes. However, KCNE1 was not detectable by Western blot in the present work. The cross-interaction between β and α subunits could end up in different events of competition, negative dominance or unpredictable changes in traffic or function. Thus, mutations or SNPs could trigger great influences in the characteristics of the channels.

4.3.1. Results of the sequencing

From the neurological tissue bank were obtained 6 samples from patients of Multiple Sclerosis. The genomic DNA was obtained and sequenced for Kv1.3, Kv1.5, KCNE1 and KCNE4. Only the coding region of KCNE1 was sequenced. Genes were amplificated by PCR, purified by agarose gel electrophoresis and finally sequenced by the Sanger method. Primers used are detailed in Annex F.

A total of 21 different polymorphisms were found in this work, 5 of which were located in the codificant region. Proportion of the polymorphisms in the Iberian (IBS) population was extracted from the 1000 Genomes database [http://www.internationalgenome.org/]. The polymorphisms and their proportion are as follow (Tables 1-4):

Table 1: KCNA3 Polymorphisms

rs#	Position	Alleles	Proportion sample	Proportion IBS population
rs1058184	2234	T / G	0'083 / 0'917	0'321 / 0'679
rs3215042	2615	-- / CC	0'917 / 0'083	0'679 / 0'321

Table 2: KCNA5 Polymorphisms

rs#	Position	Alleles	Proportion sample	Proportion IBS population
rs3741930	113	C / T	0'583 / 0'417	0'607 / 0'393
rs2359641	1428	T / C	0 / 1	0 / 1
rs1056468	2629	A / T	0'667 / 0'333	0'5 / 0'5

Table 3: KCNE4 Polymorphisms

rs#	Position	Alleles	Proportion sample	Proportion IBS population
rs13031825	201	G / A	0'917 / 0'083	0'964 / 0'036
rs3795886	1148	C / T	0'333 / 0'667	0'214 / 0'786
rs10201907	1331	T / C	0'167 / 0'833	0'071 / 0'929
rs12621643	1502	T / G	0'333 / 0'667	0'321 / 0'679
rs17221840	1538	G / A	0'917 / 0'083	1 / 0
rs10189762	1599	C / G	0'167 / 0'833	0'071 / 0'929
rs3795884	1882	T / C	0'167 / 0'833	0'071 / 0'929
rs753890072	2736	C / T	0'917 / 0'083	
rs10208429	3193	T / C	0'167 / 0'833	0'286 / 0'714
rs10172380	3256	A / G	0'167 / 0'833	0'286 / 0'714

Table 4: KCNE1 Polymorphisms				
rs#	**Position**	**Alleles**	**Proportion sample**	**Proportion IBS population**
rs1805127	162	A / G	0'417 / 0'583	0'357 / 0'643
rs2070357	564	A / G	0'5 / 0'5	0'429 / 0'571
rs2070356	896	C / T	0'417 / 0'583	0'429 / 0'571
rs41314803	1508	A / C	0'917 / 0'083	1 / 0
rs11909074	1659	A / G	0'5 / 0'5	0'429 / 0'571
rs74508995	1778	C / A	0'917 / 0'083	0'964 / 0'036
rs11373310	1987	- / G	0 / 1	----------
rs2211696	2447	T / C	0 / 1	0 / 1
rs13050198	2901	A / G	0'917 / 0'083	0'964 / 0'036
rs3453	2920	A / G	0'417	0'429 / 0'571

The relative position of each SNP can be observed in Annexes G and H.

Among the 5 polymorphisms located in the coding region of their respective genes, 4 were located in KCNE4 and 1 was located in KCNE1. Among these 5 polymorphisms, only 2 implicated a change in the amino acid sequence of the protein: rs12621643 in KCNE4 and rs1805127 in KCNE1.

4.3.2. KCNE4 D145E (rs12621643)

Rs12621643, named KCNE4 D145E from now on, is located in the position 1502 of hKCNE4 and implies a transversion between T and G. This transversion results in an amino acid change between Aspartate (D) and Glutamate (E), respectively, in position 145 of the short KCNE4 protein sequence. This change, which conserves the charge, is located further 3' respective to the transmembrane domain of the protein, in the cytoplasmic region.

This polymorphism, albeit being very conservative, is linked to childhood acute lymphoblastic leukemia and allergic rhinitis, both of which are tightly associated with immune activity. In addition, KCNE4 D145E increases the activity of Kv7.1. All these previous results would indicate a possible effect of this SNP on Kv1.3.

Therefore, KCNE4 was mutated to substitute the 145E (which was the form deposited in our research group) by 145D. Some functional properties of this association were analyzed. Thus, co-immunoprecipitation experiments were performed. The immunoprecipitation of Kv1.3 resulted in the detection of more 145D than 145E, thus suggesting a higher affinity for the first form (Fig. 24A and 24B).

On the other side, the 145D inhibit Kv1.3 rather potentiate. However, this surprising result remains preliminary. The peak current potentiation would need to be contrasted with the membrane co-localization and lipid raft presence of the channel, as both events affect the activity of Kv1.3 (Fig. 24C and 24D).

To further understand the effect of KCNE4 D145E in the function of the channel, a model of the molecular structure of Kv1.3 with KCNE4 was developed (Fig. 26A and 26B). In this model, the position 145 of KCNE4 is located far away from the transmembrane domain of the protein and not near the Kv1.3 channel. Thus, even by modifying the rotation of the carbon bonds of that residue, it was impossible to find any interaction between residues. Comparing 145D and 145E, the only apparent difference was that, unlike 145E, 145D was able to form an H-bond with its neighbor residue 146E (Fig. 26C and 26D). Despite this, this difference by itself does not explain the difference in interaction or activity of Kv1.3. Thus, this polymorphism should be further studied in the future.

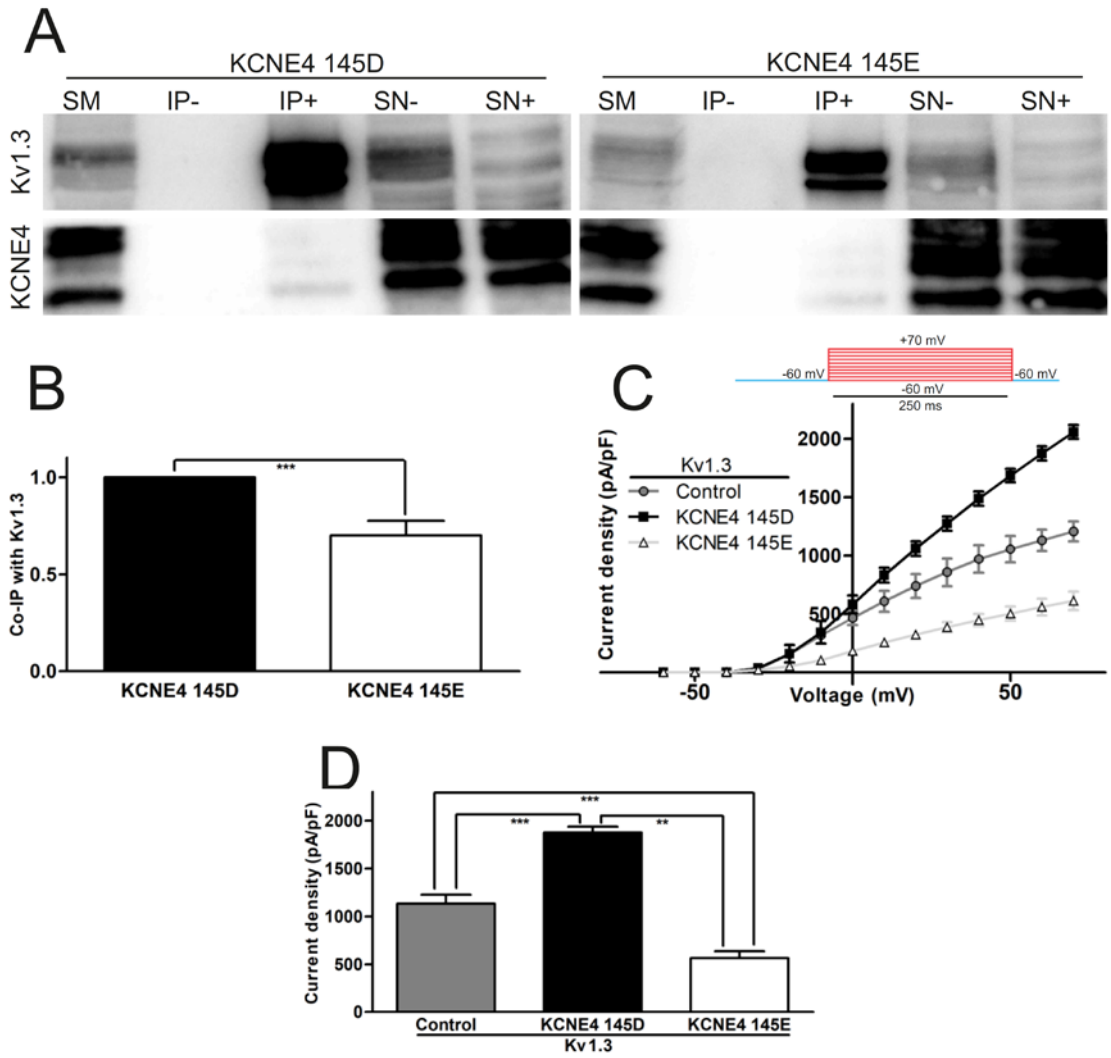

Fig. 24: *Effects of polymorphism D145E of KCNE4 in Kv1.3. KCNE4 145D was generated by site-directed mutagenesis of the KCNE4 145E. HEK 293 cells were transfected with Kv1.3 and either KCNE4 145D or 145E. Cells were lysated and immunoprecipitated against Kv1.3. Samples were western blotted and immunoblotted against Kv1.3 or KCNE4 (**A**). SM: Starting Material; IP: ImmunoPrecipitate; SN: Supernatant; IB: Immunoblot. [+]: presence of antibody; [-]: absence of antibody. KCNE4 co-immunoprecipitation with Kv1.3 was quantified in both conditions and relativized to the maximum value (KCNE4 145D) (**B**). In addition, HEK 293 cells were transfected with Kv1.3, with or without KCNE4 145D and KCNE4 145E. Cells were held at -60 mV and 250 ms pulses were applied from -60 mV to +70 mV in increments of 10 mV. **C:** I/V relationship of the K^+ currents elicited in transfected cells. **D:** Current density at +60 mV. Values are mean ± standard error of 2-3 cells. **, p<0.01; ***, p<0.005 by One-way ANOVA test.*

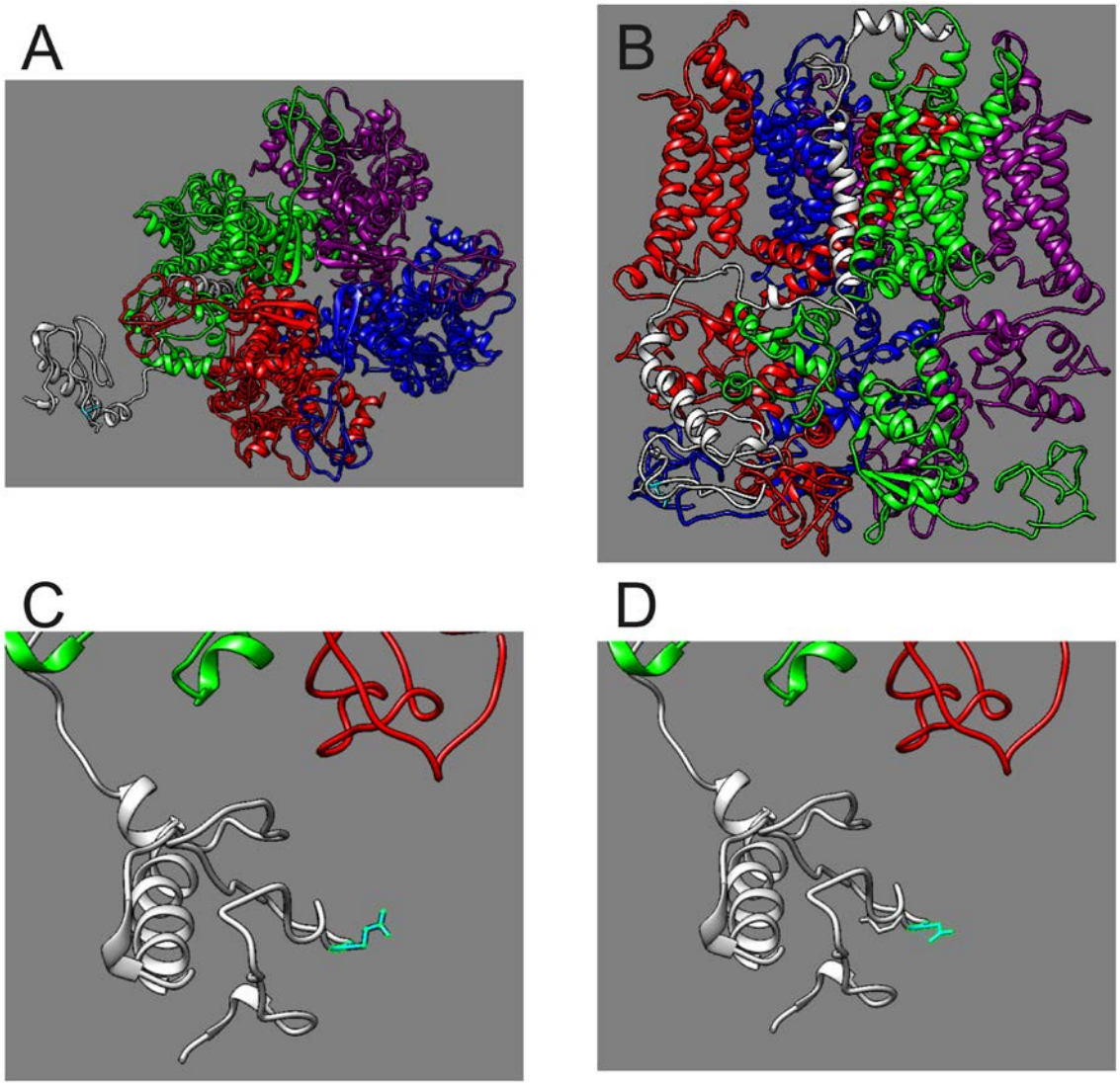

Fig. 26: *Molecular model of Kv1.3 and KCNE4. The Kv1.3 and KCNE4 interaction was modelled using high-resolution templates of remote or close homologs available from the Protein Data Bank.* ***A:*** *Overhead view.* ***B:*** *Side-view.* ***C:*** *Close-up of 145E (cyan).* ***D:*** *Close-up of 145D (cyan). Kv1.3 subunits are colored in red, blue, green and magenta. KCNE4 is colored in white. H-bonds are depicted as a light-blue line.*

4.3.3. KCNE1 S38G (rs1805127)

Rs1805127, named KCNE1 S38G from now on, is located in the position 162 of hKCNE1 and implies a transition between A and G. This transition results in a change between Serine (S) and Glycine (G) in the position 38. This change is located long before the transmembrane domain, thus it resides in the extracellular domain.

Previous KCNE1 structural analyses with NMR spectroscopy shows that this position 38 corresponds to a β-turn, a secondary structure that changes the orientation of the protein chain. Structurally, Glycine is much more flexible than Serine, which could result in an important effect of this amino acid change on the functionality of the protein (Fig. 26A). Regardless, by manipulating the tridimensional NMR model, no interactions could be found between the residue 38 (Gly nor Ser) and any other residue of the protein (Fig. 26B, 26C).

In addition, S38G has been genetically linked to atrial fibrillation in different populations and protection against some cases of deafness. Thus, if this polymorphism alters in some way the effects of KCNE1 on Kv7.1, it could also affect Kv1.5.

KCNE1 S38G was transfected into HEK 293 cells and the effects on Kv1.5 were evaluated. Our data demonstrates that the substitution of Serine by Glycine in the position 38 of KCNE1 showed no differences in current density on Kv1.5 (Fig. 27A and 27B). Additionally, the tails of the pulses were quantified in order to fit the Steady-state activation to a Boltzmann equation (Eq.2 and Fig. 27C). No differences could be appreciated between S38G (Eq. 6) and the WT form (Eq. 4) (Fig. 27D, 27E, 27F). Thus, KCNE1 S38G had no apparent effects on KCNE1 on Kv1.5, at least, from the electrophysiological point of view.

$$Eq.6 - Kv1.5 + KCNE1\ 38G\ Boltzmann\ eq: Y = 0.01913 + \frac{(0.9464 - 0.01931)}{(1 + \exp(\frac{-27.27 - X}{6.048}))}$$

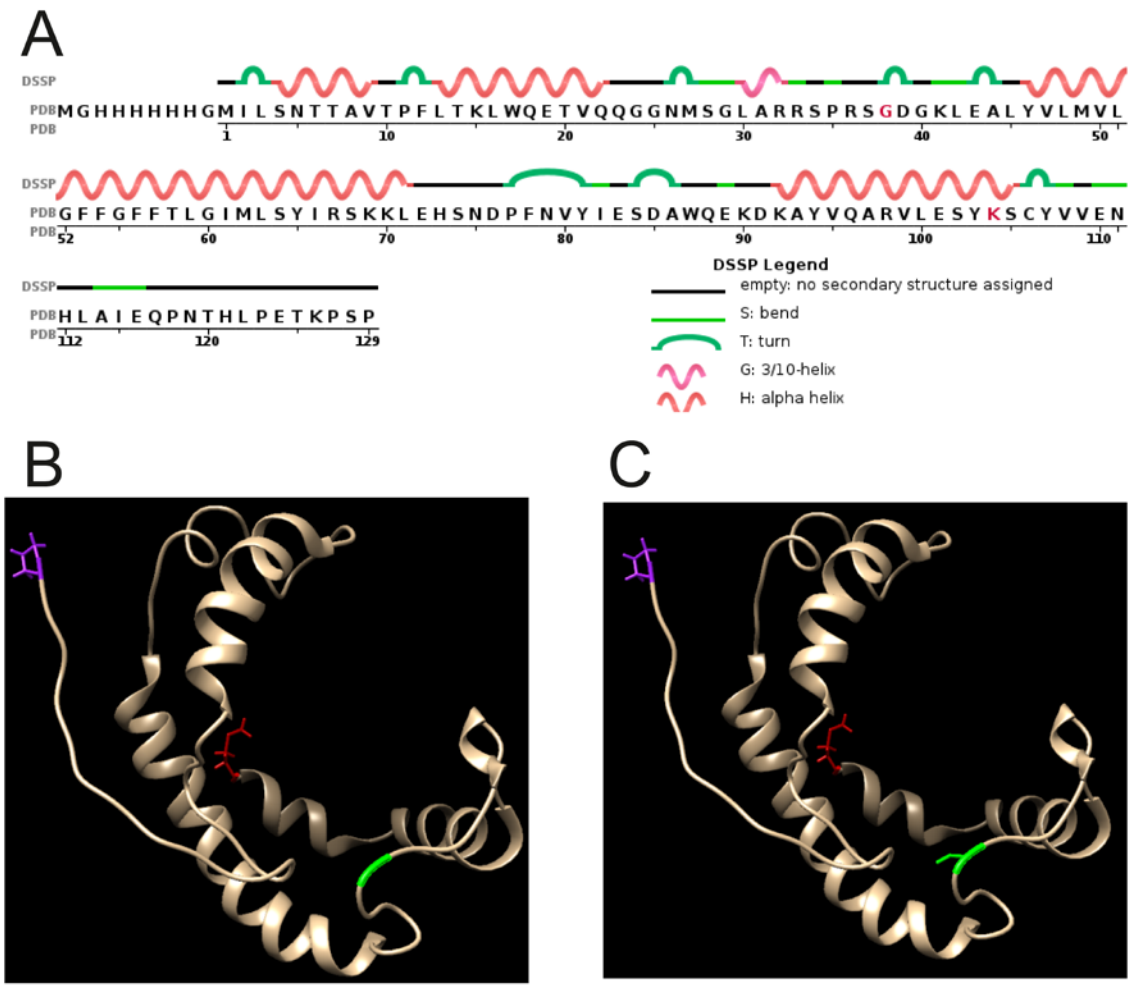

Fig. 26: *S38G polymorphism of KCNE1.* ***A:*** *Protein sequence of KCNE1 with simplified secondary structure (PDB 2K21). KCNE1 S38G is highlighted in red.* ***B:*** *NMR tridimensional structure of KCNE1 (PDB 2K21) with the 38G form.* ***C:*** *NMR tridimensional structure of KCNE1 (PDB 2K21) with the 38S form. N-terminal methionine is marked in red. C-terminal proline is marked in purple. S38G is marked in green. No possible H-bonds could be predicted.*

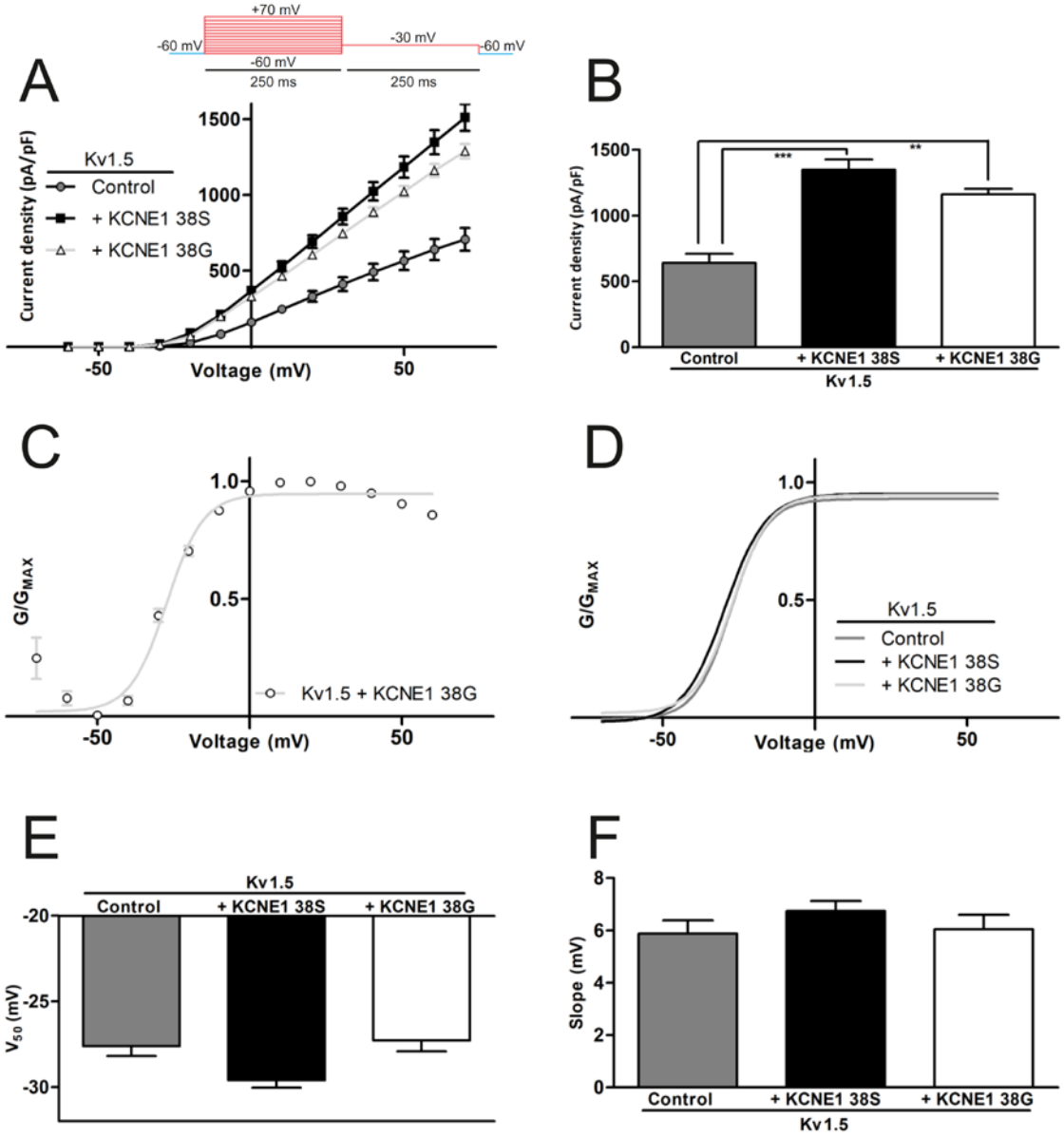

Fig.27: *Effects of KCNE1 S38G on Kv1.5 activity. HEK 293 cells were transfected with Kv1.5 with or without KCNE1 38S and KCNE1 38G. Cells were held at -60 mV and 250 ms pulses were applied from -60 mV to +80 mV in increments of 10 mV. Activation dynamics are calculated from a constant-voltage tail after an activation pulse (steady-state activation). Therefore, the 250 ms pulse is followed by a 250 ms pulse of near-activating voltage (-30 mV).* ***A:*** *K^+ currents generated by transfected cells.* ***B:*** *I/V relationship of the currents. Values are those at the peak current. Peak current of the tails was quantified and transformed into conductance [$G_N = I_N / (V_N - V_{REV})$]. Conductance was relativized by its maximum value and plotted against voltage to generate a G/G_{MAX} graphic. The G/G_{MAX} graphic was fitted to a Boltzmann equation: Kv1.5 + KCNE1 38G (**C**). Kv1.5 alone (Fig. 21C) and with KCNE1 38S (Fig. 21D) were shown previously. An additional representation of the three graphics together is also shown (**D**). The parameters of the steady-state activation were extracted from the Boltzmann equation: V_{50} (**E**) and Slope (**F**). Values are mean ± standard error of 12-20 independent cells. **, p<0.01; ***, p<0.005 by One-way ANOVA test.*

DISCUSSION

5. DISCUSSION

Shaker channels are an important piece in the immune regulation of mammals [193]. Kv1.3 has long been described to be implicated in the activation and proliferation processes of T and B lymphocytes and the macrophage lineage [67, 193-195].

Thus, it comes as no surprise that the channel could easily be detected in Jurkat (T lymphocytes) and CY15 (dendritic cells). Besides, channel Kv1.5 and regulatory subunit KCNE4 were also identified in said cell lines. Kv1.5 has been found to be expressed in cell types of monocyte precursor, such as microglia, macrophages and dendritic cells [109, 196, 197]. As Kv1.5 was co-expressed in Kv1.3-centric cells, their interaction was studied, which resulted in the description of the Kv1.3-Kv1.5 heterotetramer [74]. KCNE4 was described in 2003 to greatly inhibit Kv1.3, as well as Kv1.1 [168]; and later identified to be expressed in macrophages, a cell type whose precursor is also the monocytes [198-200].

Kv1.3 has been described to possess glycosylations on N228NS and N229ST, which are two residues present on the S1-S2 linker of rat Kv1.3 (or 278 and 279, respectively, for human) [201]. This two glycosylations, together with other post-translational modifications could explain the two different bands on the CY15 Kv1.3 (mouse). Human Kv1.3 is 50 amino acids longer, which supports the Jurkat Kv1.3 band being higher than the superior CY15 band. Dislike CY15, Jurkat Kv1.3 only showed a single band, suggesting that these glycosylations have a very high prevalence in human T lymphocytes.

Regarding the electrophysiological activity of the cells, results were consistent with previous studies. CY15 cells exhibited both less overall activity when normalized by the area of cell membrane (capacitance) and less C-type inactivation. The reduced activity could be caused by dendritic cells expressing both KCNE4 and Kv1.5: proteins which actively interact and partially inhibit Kv1.3 [198, 200]. As commented before, C-type inactivation is a characteristic property of Kv1.3 and is mostly minor in Kv1.5. Thus, it's normal for Kv1.3-Kv1.5 heterotetramers to show a reduced C-type inactivation [200].

Finally, margatoxin (MgTx) is a specific blocker for Kv1.3. The almost total inhibition of Jurkat cells by MgTx would suggest that the channel expression of T-cells is mostly composed of Kv1.3. On the other side, CY15 cells are only half-blocked, suggesting a higher expression of channels, at least opening in the voltages assessed [74]. This result is consistent with the expression of Kv1.5 in dendritic cells, as Kv1.3-Kv1.5 heteromeric channels have been described to compromise the pharmacological responses in macrophages [138].

Recent studies have suggested that MgTx is not as selective for Kv1.3 as it was considered before [202]. MgTx has a high affinity for Kv1.3 (Kd = 11.7 pM), but also for Kv1.2 in a slightly lower range (Kd = 6.4 pM). Kv1.1 is also inhibited by MgTx, albeit with a much lower affinity (Kd = 4.2 nM). Thus, from a pharmacological point of view, the possibility of Jurkat expressing Kv1.1 or Kv1.2 could not be ruled out. In fact, it has been recently described the expression of Kv1.1 channel in normal human $CD4^+$ helper T cells and its activation of a non-canonical

pathway of the NFκB [203]. As Kv1.1 and Kv1.3 are able to tetramerize, at least in the brain, the study of Kv1.1 in T-cells and its relationship with Kv1.3 would be recommended [204].

Finally, the blockage of channels in both Jurkat and CY15 caused a small and non-significant increase in cell capacitance. Cell capacitance is directly proportional to the area of the membrane (roughly 1 $\mu F/cm^2$) [205]. Kv1.3 is implicated in volume regulation; thus, even not being significant, this result would be expected [101].

Regarding the heterologous expression, both Kv1.3 and Kv1.5 showed a higher molecular weight compared with the native cells due to them being translated with a YFP tag (~25 KDa). Also, consistent with the profile of Kv1.3 in CY15 (mouse), our Kv1.3 construct (rat) also showed a shift in molecular weight due to the glycosylations.

As it would be expected, Tandem 1.3-1.5 showed a molecular weight very similar to the sum of the proteins that compose it: Kv1.3, Kv1.5 and YFP. Moreover, similar to Kv1.3, Tandem 1.3-1.5 shows a little shift in molecular weight, which could be due to Kv1.3 glycosylations.

Tandem 1.3-1.5 was detected using either of the three antibodies for its components. Notably, the tandem is easier to detect when using the Kv1.5 antibody than the Kv1.3 one. Antibodies for Shaker channels typically target the C-terminal domain, as it is the most divergent region for channels of this family: transmembrane domains are almost totally identical, and the N-terminus is dominated by the conserved tetramerization domain. Thus, it comes to no surprise that the antibody for Kv1.3 has less affinity for the tandem, as the C-terminus of Kv1.3 could be masked by the N-terminus of Kv1.5 in the Tandem construct. Finally, as the GFP antibody is able to detect all three proteins with an acceptable affinity, it was used as the primary antibody both for immunoblot and immunoprecipitation.

From a functional point of view, Kv1.3 exhibits a 3-fold higher peak current than Kv1.5. This result is consistent with Kv1.5 impaired membrane traffic due to its lack of the YMVIEE signal [47], as well as Kv1.5 having a lower conductance (8 pS) than Kv1.3 (13 pS) [206]. The heteromeric channel formed by Tandem 1.3-1.5 shows a peak current similar to Kv1.5. In previous studies, the shift in voltage dependence or the pharmacology of the heteromeric channel was assessed, but the activity was not meticulously compared [74]. The Kv1.5 fraction of the tandem retains it intracellularly to the levels of Kv1.5, greatly limiting the capacity of the channel to generate currents. Besides, other mechanisms like a decrease of the proportion of the channel which arrives to lipid raft microdomains [89], or the impairment of post-translational modifications [201] should be further assessed, as they are events with important effects on the channel function.

Regarding other electrophysiological properties, it seems apparent that Kv1.3 is activated at more electronegative values than Kv1.5 and Tandem 1.3-1.5. This result was already described in past studies [74], where the 1:1 ratio heterotetramer shows an intermediate phenotype between Kv1.3 and Kv1.5. In this case, however, the Tandem 1.3-1.5 functions very similarly to Kv1.5. This could be caused by the former experiments being performed in co-transfection models, which freely permits the formation of Kv1.3 and Kv1.5 homotetramers, even taking into account that the ratio of transfection on a cell basis is indeed 1:1.

Concerning C-type inactivation, Kv1.3 (80%) showed it in a much higher degree than Kv1.5 (30%), as indicated in past studies [3, 156]. If the effect was summatory, the C-type inactivation of both channels on a 1:1 ratio would result in a 55% of inactivation: far away from the 70% that the Tandem 1.3-1.5 shows. As such, the strong C-type inactivation of Kv1.3 is mostly transferred to the Tandem 1.3-1.5, even at a 1:1 ratio. Between Kv1.3 and Tandem 1.3-1.5, no differences were appreciated between the inactivation percentage after a pulse of 5 seconds, but the profile of said inactivation was slightly different. Kv1.3 rapidly inactivated during the first second to the maximum value, while Tandem 1.3-1.5 gradually inactivated for four seconds to arrive to its maximum value. This is consistent with Kv1.5 exhibiting a much slower C-type inactivation.

The cumulative inactivation is a similar case, as no differences can be observed between Kv1.3 and Tandem 1.3-1.5 after 30 pulses, while Kv1.5 has an almost absent one. Once again, the percentage of inactivation of Tandem 1.3-1.5 (38%) is nearer Kv1.3 (50%) than Kv1.5 (10%). Fitting the inactivation curves to the one phase decay equation corroborated this result, as both Kv1.3 and Tandem 1.3-1.5 shared the K and displayed similar half-life and Tau, pointing to them having similar inactivation dynamics. On the contrary, Kv1.5 displayed a much slower and less potent cumulative inactivation [151, 207].

In past studies, it was described how the association with Kv1.5 provoked Kv1.3 to be intracellularly retained, but the extent was not quantified [89]. In the present work, both by microscopy and biochemistry it is proven that Kv1.5 is able to impair Kv1.3 membrane expression significantly. There were no significant differences between the Tandem 1.3-1.5 and the co-expression of Kv1.3 and Kv1.5, suggesting that normal interaction or being artificially linked do not differ in the capacity of Kv1.5 to retain the complex. This result is also supported by the fact that Shaker channels tend to multimerize even before being inserted in the membrane [38, 39].

When immunoprecipitating Kv1.3 in CY15 cells, Kv1.5 and KCNE4 are also pulled down. This feat indicates that Kv1.3 is able to interact with both of them in dendritic cells. The formation of the Kv1.3-Kv1.5 heterotetramer had already been described in native models in the past [74, 207], but not in dendritic cells. By confirming this interaction in dendritic cells, the use of this cell line as a model to study the heterotetramer seems logical. While the interaction of KCNE4 had been assessed in heterologous models before [110, 198], this is the first time that it has been shown in native immune cells. Even though Kv1.3 is able to interact with both protein, this result does not support the formation of the tripartite hetero-oligomer. Also, it is impossible to differentiate if KCNE4 is interacting with Kv1.3 or Kv1.5, as some research groups disagree about whose protein does KCNE4 interact with [110, 168, 174].

When pulling-down the alpha subunits in heterologous expression, it seemed apparent that KCNE4 is indeed able to interact with Kv1.3, regardless of it being alone, interacting with Kv1.5, or in tandem. KCNE4 cannot interact with Kv1.5, at least in the current model, contrary to what was discussed in previous studies [174]. In that study, mouse KCNE4 was able to interact with human Kv1.5 and provoke a potentiation of peak current. In comparison, other two parallel studies with human and rat Kv1.5 were unable to detect interaction or functional effect from mouse KCNE4 [110, 198]. The only difference between these studies stems from

the former using CHO (Chinese Hamster Ovary) cells, while the latter ones used HEK 293 cells. Being different kind of immortalized cells, it could well be that Kv1.5 is unable to interact with KCNE4 by itself but depend on a third-party molecule to do it. This could explain why KCNE4 has an effect on one cell type and another in a different one.

This theory is corroborated when assessing the activity and traffic of the constructs with and without KCNE4. KCNE4 reducing Kv1.3 activity has long been described, both by affecting the channel gating and by impairing its membrane targeting [110, 168]. The lack of interaction between KCNE4 and Kv1.5 is also replicated, as no effect can be appreciated on function or traffic of the channel [110]. Nevertheless, the addition of KCNE4 to the Tandem 1.3-1.5 had notable effects, as the interaction did not inhibit its current like Kv1.3 but potentiate it. This is not caused by a modification of the channels presence in the membrane, but the presence in lipid raft microdomains should be assessed, as it could also explain the increase in activity. This results are similar to those reported when KCNE4 interacted with Kv1.5 [174]. The current results suggest that Kv1.3 could serve as a platform for Kv1.5 and KCNE4 to interact.

On a functional level, similar results were attained in CY15 cells when they had their KCNE4 expression knocked-down. Contrary to the effect on Kv1.3, less KCNE4 resulted in a higher peak current in dendritic cells. This corroborates the results from heterologous expression and also presents a paradigm change in the way ion channels are studied. KCNE4 can have different roles on Shaker channels depending on the heterotetramer composition: Kv1.3 alone is inhibited; Kv1.5 alone is unaffected; and Kv1.3 with Kv1.5 get potentiated. This opens up the possibility of different ratios having different degree of effects, or heterotetramers with different channels having totally non-predicted effects when affected by specific β subunits. This, in fact, expands the possibilities of the combinations (thus, of the phenotypes) by a huge margin.

On the other side, KCNE4 is retained on specific intracellular regions when co-transfected. Kv1.5 and KCNE4 do not interact in HEK 293 cells. When looking at the immunoprecipitation experiments carefully, it can be appreciated that KCNE4 expression is lower when co-expressed with Kv1.5. This could suggest that, as Kv1.5 is retained in the ER, saturating it; less KCNE4 can effectively be expressed and it's accumulated in the Golgi instead.

In parallel, Kv1.5 is able to interact with KCNE1. Such interaction had already been suggested in a published article from almost fifteen years ago [166], but the topic was not looked upon until recently. In that work, KCNE1 interaction with Kv1.5 was assessed, as Kv1.5, like Kv7.1 and KCNE1, is a cardiac channel. Unfortunately, this interaction was not discussed in that work albeit being the first description of such event.

In the present work, this interaction was assessed again compared with a positive (Kv7.1) and negative (Kv1.3) controls. Both experiments reported the positive immunoprecipitation with Kv1.5, while the controls also functioned as expected. This confirms the interaction between Kv1.5 and KCNE1, both of which are expressed in heart myocytes.

This interaction has notable effects on the Kv1.5 channel, as its peak current gets a 2-fold increase when co-transfected in HEK 293 cells. This effect is not replicated when co-expressed with KCNE3, a β-subunit which does not interact with Kv1.5.

When analysing the G/G_{MAX} graphics for Kv1.5, some interesting differences are found when the channel is co-expressed with KCNE1 and KCNE3. KCNE1 has already been established as interacting and modifying Kv1.5, but nothing seemed to indicate that KCNE3 is able to interact with Kv1.5, even less modify it. A recent article has described that *KCNE3 -/-* mice suffer from hyperaldosteronism-caused atrial fibrillation [208]. In that work, no proves of direct interaction were provided and is defended the theory that the atrial myocytes of KCNE3 -/- mice exhibited an augmented peak current from 4-aminopyridine sensitive Kv1.5. This increase, nevertheless, is postulated to be caused by a subcellular reorganization of the Kv1.5 channels, and not by KCNE3 changing Kv1.5 electrophysiology by direct interaction. Thus, no effects were to be expected from KCNE3 and this possible interaction should need to be further explored by immunoprecipitation and confocal microscopy.

Kv1.5 has a mostly intracellular phenotype with some membrane arrival. On the other side, KCNE1 is intracellularly retained even more than Kv1.5. When co-transfected, both proteins get dragged by the other one, so Kv1.5 is dragged more intracellularly, while KCNE1 shows a slightly better membrane presence. Unlike Kv1.3, though, these differences do not follow the dominant or dominant-negative relationship of KCNE4.

Moreover, KCNE1 interaction also seem to have an effect on the channel's traffic to lipid raft microdomains. Kv1.5 is able to arrive to lipid raft microdomains when transfected into HEK 293 cells. When co-transfected with KCNE1, though, this lipid raft targeting gets impaired; possibly by the previously described intracellular retention or by additional mechanisms. Kv1.5 relationship with lipid raft microdomains has been widely studied and debated, as they served as important platforms for ion channels in cardiomyocytes. Some studies in transfected mouse fibroblasts suggested that Kv1.5 preferentially localize to caveolae and lipid rafts [209, 210]. In more recent works it has been described that Cav-3 recruits Kv1.5 from non-lipid raft regions onto caveolae, thus modifying its gating [211, 212]. Among these studies, it was described the potentiation of Kv1.5 current in atrial myocytes when treated with MCD (Methil-cyclo-dextrin), a compound which binds and chelates cholesterol from the cell [213]. Without cholesterol, lipid raft microdomains disappear, thus Kv1.5 locates back to non-lipid raft microdomains. More studies must be conducted regarding the Kv1.5-KCNE1 interaction, but for the time being, the bibliography supports the peak current increase being caused by the delocalisation from lipid raft microdomains.

Regardless, neither of these results rule out the possibility of KCNE1 potentiating Kv1.5 activity by provoking a conformational change. The interaction between KCNE1 and Kv7.1 is still being deciphered, but some studies point towards KCNE1 packing the S4 domain of the channel or hindering its movement [214-216]. Other studies also point to KCNE1 interacting with the pore region of the channel [166, 217-219]. Kv1.5 shares very few residues with Kv7.1, as they have a 16% homology. Therefore, it is difficult to extrapolate this finding in Kv7.1 to Kv1.5. In fact, the S4 domains only share the arginine residues, characteristic of voltage-sensing domains. On the contrary, the pore domain is very conserved between all K^+ channels and could explain the convergent effect in both channels (Annex I). Regardless, too many residues in the rest of the channel are different for this causality relationship to be established. Also, being so conserved in all K^+ channels, this effect on the pore could also be

extrapolated to a plethora of different channels. In conclusion, more experiments should be conducted on this topic to detect the location of this interaction and its exact effects.

This interaction is relevant to Kv1.5 in heart physiology, but it can also be significant in other physiological systems. In fact, KCNE1 was firstly cloned in Jurkat T-cells simultaneously with Kv1.3 [91]. As already exposed, Kv1.5 is mostly expressed in antigen-presenting cells in the immune system, but its presence in T lymphocytes should not be underestimated. Thus, in T lymphocytes we can find Kv1.3, Kv1.5, KCNE4 and KCNE1. Although the typical dancing partners are Kv1.3-KCNE4 and Kv1.5-KCNE1, the interaction between KCNE4 and a Kv1.3-Kv1.5 heterotetramer has already demonstrated the physiological importance of the heteromultimeric complexes. KCNE1 could have a different effect on Kv1.3-Kv1.5 heteromers; or could have a different effect in conjunction with KCNE4; or they could even compete for the association to the channel. Thus, more experiments must be conducted to characterise these multimeric interactions.

The role of the C-terminal domain in Shaker channels have long been discussed, as it is one of the most divergent regions in the family [35, 220]. As the rest of the channel tends to be homologous between isoforms, most of the differences in regulation reside in this specific region. One of such regulation signals is the YMVIEE sequence in some of the Shaker channels, which enables the anterograde trafficking to the membrane [47]. This sequence is a *si ne qua non* condition for Kv1.3 and Kv1.4 to have acceptable membrane expression. Also, said sequence is implicated in the interaction of Kv1.3 with KCNE4, which consequently impairs Kv1.3 traffic [110].

In the current work a new role of the C-terminus is presented. When the C-terminal domain of Kv1.3 is swapped by the one of Kv1.5, and vice versa; it is unable to elicit normal currents. Resulting currents are abysmally low, while the shape of the pulse is aberrant. Also, this change in the C-terminus results in an abnormally low membrane trafficking of the channel, which could explain the dysfunctional currents.

Surprisingly, co-transfection of both chimaeras results in a total recovery of membrane presence to the levels of Kv1.5 and a partial recovery of function higher than the sum of the separated chimaeras. These results point us towards the C-terminal domains of each channel recognizing the rest of the channel and that step being mandatory for a correct trafficking and activity.

Previous works with Kv channels analyse the interaction of the C-terminal region of S6 with the S4-S5 linker [221, 222] which results in a key movement transfer for the gating of the channel. Regardless, no interactions have been described before between the C-terminal domain of Kv with the rest of the channel.

The S4-S5 chimaeras (3-3-5-5 and 5-5-3-3) further supported the C-terminus contacting with another region of the channel, specifically the S4-S5 linker or the pore domain. These chimaeras have normal membrane expression for Kv1.5 standards and show an activity comparable to thus of wild type channels once normalized by their membrane expression.

By looking closely to the channel topology, the only regions of the channel which are exposed to the intracellular media are the N- and C-terminal domains, the S2-S3 linker and the S4-S5 linker. When assessing the interaction between the C-terminal domain and the S4-

S5 linker in the 5-5-3-3 mut link chimaera it seemed apparent that this mutant resulted in no functional differences in comparison with the 5-5-3-3 chimaera.

Discarding the S4-S5 linker from the interaction, no additional domains are left in the intracellular face of the protein. The only additional region which differs from Kv1.3 and Kv1.5 is the P-loop. Two small sequences are different in Kv1.3 and Kv1.5: The Turret region and the SS6 region. By generating new mutants, though, the SS6 region is also discarded, as no differences can be appreciated from the original chimaeras.

Finally, the Turret region is the only one not yet assessed in the described experiments and it represents the main hypothesis of the C-terminal interactions. Nonetheless, the C-terminal domain of Shaker channels have been described to be intrinsically disordered regions [223, 224]. Intrinsically disordered proteins tend to be amorphous or glomerular when not interacting with any other protein. When interacting with a substrate or being modified, though, intrinsically disordered proteins adopt a defined structure which can hide or expose determinate residues or active regions [225-227]. By following this logic, it could be that the swapped C-terminal domain, not being able to interact with the other regions (N-terminus, S4-S5 linker, pore domain), simply remains in an intrinsically disordered form, which gets detected by the quality controls of the cell, thus retained or degraded. This hypothesis is consistent with the 1.3Ct1.5 and 1.5Ct1.3 chimaeras having less membrane expression and activity. It also would explain why the traffic and activity is recovered when there is a region available from the same channel as the inserted C-terminal.

Even though this last theory seems logical, more work must be done to arrive to a definite conclusion in that regard.

As already discussed, Kv1.3 is one of the main actors in immune activation. This channel has its dynamics altered by association with KCNE4 or Kv1.5. Kv1.5 is also able to be modified by KCNE1, another protein present in T lymphocytes. Being in close interaction to one another, a slight modification of one of them could affect the totality of the cell.

Thus, these genes were sequenced in patients of Multiple Sclerosis to check for polymorphisms. More than 20 polymorphisms were found and amongst them, some were highlighted for their importance.

- rs1058284 is located in the exon of gene *KCNA3*, 3' of the codifying region. Some differences can be appreciated between the frequencies in the samples (T:G, 0.083:0.917) and the ones from the 1000Genomes project of the IBS population (T:G, 0.321:0.679). On the other side, it has been described a higher susceptibility to autoimmune pancreatitis associated with allele T on Japanese population [228]. This autoimmune disease presents a similar origin to other autoimmune diseases like Multiple Sclerosis. Nevertheless, our results indicate a higher G proportion, not T. Thus, further assessments should be performed to conclude anything.
- rs3215042 is a polymorphism located in the most 3' region of *KCNA3* and consists in a GG indel. In this case, differences between the samples (--:GG, 0.917:0.083) and the IBS population (--:GG, 0.67:0.321) can be found. It is also noteworthy that this polymorphism is located a few nucleotides away from the polyadenylation region Hs.169948.1.3 (Annex H and J).

- Rs12621643 is a polymorphism located in the second exon of KCNE4 that results in an amino acid change between D and E in position 145, in the cytoplasmic face of the protein. While the D form of this polymorphism seems to have a higher interaction with Kv1.3, it also seems to modify the effect of KCNE4 on Kv1.3 from inhibition to potentiation. A study already established a similar effect of these two polymorphisms on Kv7.1 [229]. In that study, the 145D form potentiated Kv7.1; while the 145E form inhibited the channel. Even though Kv1.3 and Kv7.1 are both Kv channels, their homology is very low aside from the pore domain (15% total match in a protein alignment, Annex I). Moreover, KCNE4 interacts with Kv1.3 in a domain which is not even present in Kv7.1, thus the comparison between the two channels in regard to the effect of KCNE4 is difficult to assess. On the other side, a molecular dynamics model of the Kv1.3-KCNE4 interaction does not seem to locate the polymorphism in a position which could interact with the rest of KCNE4 or the Kv1.3 channel. As it is a mathematical model and the C-terminus of Kv1.3 is described to be intrinsically disordered [224], it could interact *in vivo*, but this is as far as the model can predict. Regarding other genetic association analyses, the T allele (D) have been linked to an increment of the likelihood of suffering childhood acute lymphoblastic leukaemia [230]. As Kv1.3 is implicated in the activation and proliferation of such cells, a higher current could facilitate the replication of cancer cells. On the other side, a genetic analysis from Russian residents of Western Siberia genetically associated a higher frequency of the G genotype (E) with a higher incidence of allergic rhinitis [231]. The results of this last study differ from the ones described in the present work, but as already defended during all the discussion, different types of cells could react differently depending on the proteins they express.
- rs1805127 is another polymorphism which results in amino acid change: in this case, between S and G in position 38 of KCNE1, located in the extracellular face. This amino acid position is located inside a β-turn and, although Glycine is more flexible than the Serine, this does not seem to affect the electrophysiological effect of KCNE1 on Kv1.5. KCNE1, with 38S as well as 38G, interacts with Kv1.5 and potentiates its current and shows no additional effects on activation dynamics. In previous works, the 38G form had been genetically linked to atrial fibrillation [232, 233] in different populations. This effect of the KCNE1 polymorphism could be due to its interaction with Kv1.5 or Kv7.1, though. Also, the effect of KCNE1 on the Kv1.3-Kv1.5 heterotetramer, which remains to be assessed, should not be underestimated.

CONCLUSIONS

6. CONCLUSIONS

1. The association of Kv1.3 and Kv1.5 define the electrophysiological properties of immune cells. Cells with high Kv1.3/Kv1.5 stoichiometry, such as T lymphocytes, show a phenotype similar to Kv1.3, while the low Kv1.3/Kv1.5 ratio of dendritic cells results in intermediate phenotypes.
2. The properties of Kv1.3-Kv1.5 heterotetramer merge specific features from the two subunits. While fixed to a 1:1 stoichiometry, the resulting channel shows similar activity and traffic to Kv1.5 homotetramer, but the channel inactivation characteristics emulate those of the Kv1.3 homotetramer.
3. C-terminal domain interaction is needed for a proper function of Kv channels. Swapped C-terminus greatly impairs traffic and function of Kv1.3 and Kv1.5. However, the restitution of the S5-S6 domain to the channel partially rescues the function.
4. Kv1.5 modifies the effect of KCNE4 on Kv1.3. While KCNE4 impairs Kv1.3 traffic and function, it potentiates the activity of the Kv1.3/Kv1.5 complex without modifying the traffic.
5. KCNE1 binds to Kv1.5. KCNE1 potentiates the activity of Kv1.5 without affecting the channel gating. Besides, the association of KCNE1 and Kv1.5 displaced both subunits out of lipid raft microdomains.
6. Sequencing of Kv1.3, Kv1.5, KCNE1 and KCNE4 in multiple sclerosis patients reported two notable SNPs: KCNE1 S38G, which exerted no apparent effects on Kv1.5; and KCNE4 D145E, which shows some promising effects on Kv1.3.

BIBLIOGRAPHY

7. BIBLIOGRAPHY

1. Hille, B., *Ion Channels of Excitable Membranes, 3rd Edition*2001: Sinauer Associates.
2. Gonen, T. and T. Walz, *The structure of aquaporins.* Q Rev Biophys, 2006. **39**(4): p. 361-96.
3. Gutman, G.A., et al., *International Union of Pharmacology. LIII. Nomenclature and molecular relationships of voltage-gated potassium channels.* Pharmacol Rev, 2005. **57**(4): p. 473-508.
4. Cahalan, M.D. and K.G. Chandy, *Ion channels in the immune system as targets for immunosuppression.* Curr Opin Biotechnol, 1997. **8**(6): p. 749-56.
5. Fu, J., et al., *Kv2.1 Clustering Contributes to Insulin Exocytosis and Rescues Human beta-Cell Dysfunction.* Diabetes, 2017. **66**(7): p. 1890-1900.
6. Li, Y., S.Y. Um, and T.V. McDonald, *Voltage-gated potassium channels: regulation by accessory subunits.* Neuroscientist, 2006. **12**(3): p. 199-210.
7. MacKinnon, R., *Determination of the subunit stoichiometry of a voltage-activated potassium channel.* Nature, 1991. **350**(6315): p. 232-5.
8. Catterall, W.A., *From ionic currents to molecular mechanisms: the structure and function of voltage-gated sodium channels.* Neuron, 2000. **26**(1): p. 13-25.
9. Catterall, W.A., *Structure and regulation of voltage-gated Ca2+ channels.* Annu Rev Cell Dev Biol, 2000. **16**: p. 521-55.
10. Tempel, B.L., et al., *Sequence of a probable potassium channel component encoded at Shaker locus of Drosophila.* Science, 1987. **237**(4816): p. 770-5.
11. Curran, M.E., G.M. Landes, and M.T. Keating, *Molecular cloning, characterization, and genomic localization of a human potassium channel gene.* Genomics, 1992. **12**(4): p. 729-37.
12. Folander, K., J. Douglass, and R. Swanson, *Confirmation of the assignment of the gene encoding Kv1.3, a voltage-gated potassium channel (KCNA3) to the proximal short arm of human chromosome 1.* Genomics, 1994. **23**(1): p. 295-6.
13. Yellen, G., *The voltage-gated potassium channels and their relatives.* Nature, 2002. **419**(6902): p. 35-42.
14. Naranjo, D., et al., *Pore size matters for potassium channel conductance.* J Gen Physiol, 2016. **148**(4): p. 277-91.
15. Heginbotham, L., et al., *Mutations in the K+ channel signature sequence.* Biophys J, 1994. **66**(4): p. 1061-7.
16. Guy, H.R. and P. Seetharamulu, *Molecular model of the action potential sodium channel.* Proc Natl Acad Sci U S A, 1986. **83**(2): p. 508-12.
17. Li, H.L., et al., *Two-dimensional crystallization and projection structure of KcsA potassium channel.* J Mol Biol, 1998. **282**(2): p. 211-6.
18. MacKinnon, R. and G. Yellen, *Mutations affecting TEA blockade and ion permeation in voltage-activated K+ channels.* Science, 1990. **250**(4978): p. 276-9.
19. Holmgren, M., P.L. Smith, and G. Yellen, *Trapping of organic blockers by closing of voltage-dependent K+ channels: evidence for a trap door mechanism of activation gating.* J Gen Physiol, 1997. **109**(5): p. 527-35.
20. Doyle, D.A., et al., *The structure of the potassium channel: molecular basis of K+ conduction and selectivity.* Science, 1998. **280**(5360): p. 69-77.
21. del Camino, D., et al., *Blocker protection in the pore of a voltage-gated K+ channel and its structural implications.* Nature, 2000. **403**(6767): p. 321-5.
22. del Camino, D. and G. Yellen, *Tight steric closure at the intracellular activation gate of a voltage-gated K(+) channel.* Neuron, 2001. **32**(4): p. 649-56.
23. Armstrong, C.M., *Sodium channels and gating currents.* Physiol Rev, 1981. **61**(3): p. 644-83.

24. Stuhmer, W., et al., *Structural parts involved in activation and inactivation of the sodium channel.* Nature, 1989. **339**(6226): p. 597-603.
25. Liman, E.R., et al., *Voltage-sensing residues in the S4 region of a mammalian K+ channel.* Nature, 1991. **353**(6346): p. 752-6.
26. Frances M. Ashcroft, F.M.A.P.T., Stephen J. Tucker, *Ion Channels and Disease*2000: Elsevier Science.
27. Ohlenschlager, O., et al., *Three-dimensional structure of the S4-S5 segment of the Shaker potassium channel.* Biophys J, 2002. **82**(6): p. 2995-3002.
28. Bezanilla, F., *How membrane proteins sense voltage.* Nat Rev Mol Cell Biol, 2008. **9**(4): p. 323-32.
29. Li, M., Y.N. Jan, and L.Y. Jan, *Specification of subunit assembly by the hydrophilic amino-terminal domain of the Shaker potassium channel.* Science, 1992. **257**(5074): p. 1225-30.
30. Shen, N.V., et al., *Deletion analysis of K+ channel assembly.* Neuron, 1993. **11**(1): p. 67-76.
31. Lee, T.E., L.H. Philipson, and D.J. Nelson, *N-type inactivation in the mammalian Shaker K+ channel Kv1.4.* J Membr Biol, 1996. **151**(3): p. 225-35.
32. Nichols, J., *From Neuron to Brain*. 8th ed2011: Sunderland.
33. Siegel, G.A., BW; Albers RW; Fisher, SK; Uhler MD, *Basic Neurochemistry: Molecular, Cellular and Medical Aspects*. 8th ed2012.
34. Aldrich, R.W., *Fifty years of inactivation.* Nature, 2001. **411**(6838): p. 643-4.
35. Hoshi, T., W.N. Zagotta, and R.W. Aldrich, *Two types of inactivation in Shaker K+ channels: effects of alterations in the carboxy-terminal region.* Neuron, 1991. **7**(4): p. 547-56.
36. Heinemann, S., et al., *The inactivation behaviour of voltage-gated K-channels may be determined by association of alpha- and beta-subunits.* J Physiol Paris, 1994. **88**(3): p. 173-80.
37. Palade, G., *Intracellular aspects of the process of protein synthesis.* Science, 1975. **189**(4206): p. 867.
38. Tu, L., et al., *Transmembrane biogenesis of Kv1.3.* Biochemistry, 2000. **39**(4): p. 824-36.
39. Schulteis, C.T., N. Nagaya, and D.M. Papazian, *Subunit folding and assembly steps are interspersed during Shaker potassium channel biogenesis.* J Biol Chem, 1998. **273**(40): p. 26210-7.
40. Papazian, D.M. and F. Bezanilla, *Voltage-dependent activation of ion channels.* Adv Neurol, 1999. **79**: p. 481-91.
41. Braakman, I. and N.J. Bulleid, *Protein folding and modification in the mammalian endoplasmic reticulum.* Annu Rev Biochem, 2011. **80**: p. 71-99.
42. Zerangue, N., et al., *A new ER trafficking signal regulates the subunit stoichiometry of plasma membrane K(ATP) channels.* Neuron, 1999. **22**(3): p. 537-48.
43. Ma, D., et al., *Role of ER export signals in controlling surface potassium channel numbers.* Science, 2001. **291**(5502): p. 316-9.
44. Kupershmidt, S., et al., *Defective human Ether-a-go-go-related gene trafficking linked to an endoplasmic reticulum retention signal in the C terminus.* J Biol Chem, 2002. **277**(30): p. 27442-8.
45. Li, D., K. Takimoto, and E.S. Levitan, *Surface expression of Kv1 channels is governed by a C-terminal motif.* J Biol Chem, 2000. **275**(16): p. 11597-602.
46. Steele, D.F., et al., *Localization and trafficking of cardiac voltage-gated potassium channels.* Biochem Soc Trans, 2007. **35**(Pt 5): p. 1069-73.
47. Martinez-Marmol, R., et al., *A non-canonical di-acidic signal at the C-terminus of Kv1.3 determines anterograde trafficking and surface expression.* J Cell Sci, 2013. **126**(Pt 24): p. 5681-91.
48. Zhu, J., et al., *Trafficking of Kv1.4 potassium channels: interdependence of a pore region determinant and a cytoplasmic C-terminal VXXSL determinant in regulating cell-surface trafficking.* Biochem J, 2003. **375**(Pt 3): p. 761-8.
49. Manganas, L.N., et al., *Identification of a trafficking determinant localized to the Kv1 potassium channel pore.* Proc Natl Acad Sci U S A, 2001. **98**(24): p. 14055-9.

50. Bowlby, M.R., et al., *Modulation of the Kv1.3 potassium channel by receptor tyrosine kinases.* J Gen Physiol, 1997. **110**(5): p. 601-10.
51. Fadool, D.A., et al., *Tyrosine phosphorylation modulates current amplitude and kinetics of a neuronal voltage-gated potassium channel.* J Neurophysiol, 1997. **78**(3): p. 1563-73.
52. Nitabach, M.N., et al., *Phosphorylation-dependent and phosphorylation-independent modes of modulation of shaker family voltage-gated potassium channels by SRC family protein tyrosine kinases.* J Neurosci, 2002. **22**(18): p. 7913-22.
53. Staub, O. and D. Rotin, *Regulation of ion transport by protein-protein interaction domains.* Curr Opin Nephrol Hypertens, 1997. **6**(5): p. 447-54.
54. Abriel, H., et al., *Regulation of the cardiac voltage-gated Na+ channel (H1) by the ubiquitin-protein ligase Nedd4.* FEBS Lett, 2000. **466**(2-3): p. 377-80.
55. Velez, P., et al., *Ubiquitin ligase Nedd4-2 modulates Kv1.3 current amplitude and ion channel protein targeting.* J Neurophysiol, 2016. **116**(2): p. 671-85.
56. Martinez-Marmol, R., et al., *Ubiquitination mediates Kv1.3 endocytosis as a mechanism for protein kinase C-dependent modulation.* Sci Rep, 2017. **7**: p. 42395.
57. Lock, L.F., et al., *Voltage-gated potassium channel genes are clustered in paralogous regions of the mouse genome.* Genomics, 1994. **20**(3): p. 354-62.
58. Hoegg, S. and A. Meyer, *Phylogenomic analyses of KCNA gene clusters in vertebrates: why do gene clusters stay intact?* BMC Evol Biol, 2007. **7**: p. 139.
59. Clark, E., H. Vacher, and J.S. Trimmer, *Kv1.1 takes a deTOR from the axon to the dendrite.* Neuron, 2006. **52**(3): p. 399-401.
60. Jensen, C.S., H.B. Rasmussen, and H. Misonou, *Neuronal trafficking of voltage-gated potassium channels.* Mol Cell Neurosci, 2011. **48**(4): p. 288-97.
61. Robbins, C.A. and B.L. Tempel, *Kv1.1 and Kv1.2: similar channels, different seizure models.* Epilepsia, 2012. **53 Suppl 1**: p. 134-41.
62. Fan, L., et al., *Impaired neuropathic pain and preserved acute pain in rats overexpressing voltage-gated potassium channel subunit Kv1.2 in primary afferent neurons.* Mol Pain, 2014. **10**: p. 8.
63. Wang, X.C., et al., *Alpha-Dendrotoxin-sensitive Kv1 channels contribute to conduction failure of polymodal nociceptive C-fibers from rat coccygeal nerve.* J Neurophysiol, 2016. **115**(2): p. 947-57.
64. Pena, S.D. and R.L. Coimbra, *Ataxia and myoclonic epilepsy due to a heterozygous new mutation in KCNA2: proposal for a new channelopathy.* Clin Genet, 2015. **87**(2): p. e1-3.
65. Tucker, K., et al., *Glucose sensitivity of mouse olfactory bulb neurons is conveyed by a voltage-gated potassium channel.* J Physiol, 2013. **591**(10): p. 2541-61.
66. Fischer, H.G., U. Bonifas, and G. Reichmann, *Phenotype and functions of brain dendritic cells emerging during chronic infection of mice with Toxoplasma gondii.* J Immunol, 2000. **164**(9): p. 4826-34.
67. Spencer, R.H., K.G. Chandy, and G.A. Gutman, *Immunological identification of the Shaker-related Kv1.3 potassium channel protein in T and B lymphocytes, and detection of related proteins in files and yeast.* Biochem Biophys Res Commun, 1993. **191**(1): p. 201-6.
68. Felipe, A., et al., *Targeting the voltage-dependent K(+) channels Kv1.3 and Kv1.5 as tumor biomarkers for cancer detection and prevention.* Curr Med Chem, 2012. **19**(5): p. 661-74.
69. Peng, Y., et al., *Blockade of Kv1.3 channels ameliorates radiation-induced brain injury.* Neuro Oncol, 2014. **16**(4): p. 528-39.
70. Trimmer, J.S. and K.J. Rhodes, *Localization of voltage-gated ion channels in mammalian brain.* Annu Rev Physiol, 2004. **66**: p. 477-519.
71. Tao, Y., et al., *Neuronal transmission stimulates the phosphorylation of Kv1.4 channel at Ser229 through protein kinase A1.* J Neurochem, 2005. **94**(6): p. 1512-22.
72. Fedida, D., et al., *Kv1.5 is an important component of repolarizing K+ current in canine atrial myocytes.* Circ Res, 2003. **93**(8): p. 744-51.
73. Gaborit, N., et al., *Regional and tissue specific transcript signatures of ion channel genes in the non-diseased human heart.* J Physiol, 2007. **582**(Pt 2): p. 675-93.

74. Vicente, R., et al., *Association of Kv1.5 and Kv1.3 contributes to the major voltage-dependent K+ channel in macrophages.* J Biol Chem, 2006. **281**(49): p. 37675-85.
75. Archer, S.L., et al., *Impairment of hypoxic pulmonary vasoconstriction in mice lacking the voltage-gated potassium channel Kv1.5.* FASEB J, 2001. **15**(10): p. 1801-3.
76. Dodson, P.D., M.C. Barker, and I.D. Forsythe, *Two heteromeric Kv1 potassium channels differentially regulate action potential firing.* J Neurosci, 2002. **22**(16): p. 6953-61.
77. Scott, V.E., et al., *Antibodies specific for distinct Kv subunits unveil a heterooligomeric basis for subtypes of alpha-dendrotoxin-sensitive K+ channels in bovine brain.* Biochemistry, 1994. **33**(7): p. 1617-23.
78. Li, G.R., et al., *Characterization of multiple ion channels in cultured human cardiac fibroblasts.* PLoS One, 2009. **4**(10): p. e7307.
79. Koh, S.D., et al., *Contribution of delayed rectifier potassium currents to the electrical activity of murine colonic smooth muscle.* J Physiol, 1999. **515 (Pt 2)**: p. 475-87.
80. Holtje, M., et al., *Differential distribution of voltage-gated potassium channels Kv 1.1-Kv1.6 in the rat retina during development.* J Neurosci Res, 2007. **85**(1): p. 19-33.
81. Glazebrook, P.A., et al., *Potassium channels Kv1.1, Kv1.2 and Kv1.6 influence excitability of rat visceral sensory neurons.* J Physiol, 2002. **541**(Pt 2): p. 467-82.
82. Finol-Urdaneta, R.K., N. Struver, and H. Terlau, *Molecular and Functional Differences between Heart mKv1.7 Channel Isoforms.* J Gen Physiol, 2006. **128**(1): p. 133-45.
83. Garcia-Villegas, R., et al., *Potassium channels lost during harvesting of epithelial cells are restored with a kinetics that depends on channel species.* Cell Physiol Biochem, 2007. **20**(5): p. 405-16.
84. Finol-Urdaneta, R.K., et al., *Block of Kv1.7 potassium currents increases glucose-stimulated insulin secretion.* EMBO Mol Med, 2012. **4**(5): p. 424-34.
85. Orias, M., et al., *Genomic localization of the human gene for KCNA10, a cGMP-activated K channel.* Genomics, 1997. **42**(1): p. 33-7.
86. Lee, S.I., et al., *A null mutation of mouse Kcna10 causes significant vestibular and mild hearing dysfunction.* Hear Res, 2013. **300**: p. 1-9.
87. Yao, X., et al., *Expression of KCNA10, a voltage-gated K channel, in glomerular endothelium and at the apical membrane of the renal proximal tubule.* J Am Soc Nephrol, 2002. **13**(12): p. 2831-9.
88. Carlisle, F.A., K.P. Steel, and M.A. Lewis, *Specific expression of Kcna10, Pxn and Odf2 in the organ of Corti.* Gene Expr Patterns, 2012. **12**(5-6): p. 172-9.
89. Vicente, R., et al., *Kv1.5 association modifies Kv1.3 traffic and membrane localization.* J Biol Chem, 2008. **283**(13): p. 8756-64.
90. Gazula, V.R., et al., *Localization of Kv1.3 channels in presynaptic terminals of brainstem auditory neurons.* J Comp Neurol, 2010. **518**(16): p. 3205-20.
91. Attali, B., et al., *Cloning, functional expression, and regulation of two K+ channels in human T lymphocytes.* J Biol Chem, 1992. **267**(12): p. 8650-7.
92. Swanson, R., et al., *Cloning and expression of cDNA and genomic clones encoding three delayed rectifier potassium channels in rat brain.* Neuron, 1990. **4**(6): p. 929-39.
93. Kues, W.A. and F. Wunder, *Heterogeneous Expression Patterns of Mammalian Potassium Channel Genes in Developing and Adult Rat Brain.* Eur J Neurosci, 1992. **4**(12): p. 1296-1308.
94. Fadool, D.A. and I.B. Levitan, *Modulation of olfactory bulb neuron potassium current by tyrosine phosphorylation.* J Neurosci, 1998. **18**(16): p. 6126-37.
95. Mourre, C., et al., *Distribution in rat brain of binding sites of kaliotoxin, a blocker of Kv1.1 and Kv1.3 alpha-subunits.* J Pharmacol Exp Ther, 1999. **291**(3): p. 943-52.
96. Panyi, G., et al., *Kv1.3 potassium channels are localized in the immunological synapse formed between cytotoxic and target cells.* Proc Natl Acad Sci U S A, 2004. **101**(5): p. 1285-90.
97. Wulff, H., et al., *K+ channel expression during B cell differentiation: implications for immunomodulation and autoimmunity.* J Immunol, 2004. **173**(2): p. 776-86.
98. Menteyne, A., et al., *Predominant functional expression of Kv1.3 by activated microglia of the hippocampus after Status epilepticus.* PLoS One, 2009. **4**(8): p. e6770.

99. Matzner, N., et al., *Ion channels modulating mouse dendritic cell functions.* J Immunol, 2008. **181**(10): p. 6803-9.
100. Beeton, C., et al., *Kv1.3 channels are a therapeutic target for T cell-mediated autoimmune diseases.* Proc Natl Acad Sci U S A, 2006. **103**(46): p. 17414-9.
101. Deutsch, C. and L.Q. Chen, *Heterologous expression of specific K+ channels in T lymphocytes: functional consequences for volume regulation.* Proc Natl Acad Sci U S A, 1993. **90**(21): p. 10036-40.
102. Defarias, F.P., S.P. Stevens, and R.J. Leonard, *Stable expression of human Kv1.3 potassium channels resets the resting membrane potential of cultured mammalian cells.* Receptors Channels, 1995. **3**(4): p. 273-81.
103. Serrano-Albarras, A., et al., *Kv1.3: a multifunctional channel with many pathological implications.* Expert Opin Ther Targets, 2018. **22**(2): p. 101-105.
104. Matko, J., *K+ channels and T-cell synapses: the molecular background for efficient immunomodulation is shaping up.* Trends Pharmacol Sci, 2003. **24**(8): p. 385-9.
105. Rus, H., et al., *The voltage-gated potassium channel Kv1.3 is highly expressed on inflammatory infiltrates in multiple sclerosis brain.* Proc Natl Acad Sci U S A, 2005. **102**(31): p. 11094-9.
106. Beeton, C. and K.G. Chandy, *Potassium channels, memory T cells, and multiple sclerosis.* Neuroscientist, 2005. **11**(6): p. 550-62.
107. Panyi, G. and C. Deutsch, *Assembly and suppression of endogenous Kv1.3 channels in human T cells.* J Gen Physiol, 1996. **107**(3): p. 409-20.
108. Koo, G.C., et al., *Blockade of the voltage-gated potassium channel Kv1.3 inhibits immune responses in vivo.* J Immunol, 1997. **158**(11): p. 5120-8.
109. Vicente, R., et al., *Differential voltage-dependent K+ channel responses during proliferation and activation in macrophages.* J Biol Chem, 2003. **278**(47): p. 46307-20.
110. Sole, L., et al., *The C-terminal domain of Kv1.3 regulates functional interactions with the KCNE4 subunit.* J Cell Sci, 2016. **129**(22): p. 4265-4277.
111. Schmitz, A., et al., *Design of PAP-1, a selective small molecule Kv1.3 blocker, for the suppression of effector memory T cells in autoimmune diseases.* Mol Pharmacol, 2005. **68**(5): p. 1254-70.
112. Vennekamp, J., et al., *Kv1.3-blocking 5-phenylalkoxypsoralens: a new class of immunomodulators.* Mol Pharmacol, 2004. **65**(6): p. 1364-74.
113. Comes, N., et al., *The voltage-dependent K(+) channels Kv1.3 and Kv1.5 in human cancer.* Front Physiol, 2013. **4**: p. 283.
114. Perez-Garcia, M.T., P. Cidad, and J.R. Lopez-Lopez, *The secret life of ion channels: Kv1.3 potassium channels and proliferation.* Am J Physiol Cell Physiol, 2018. **314**(1): p. C27-C42.
115. Szabo, I., et al., *A novel potassium channel in lymphocyte mitochondria.* J Biol Chem, 2005. **280**(13): p. 12790-8.
116. Szabo, I., et al., *Mitochondrial potassium channel Kv1.3 mediates Bax-induced apoptosis in lymphocytes.* Proc Natl Acad Sci U S A, 2008. **105**(39): p. 14861-6.
117. Djamgoz, M., *Biophysics of cancer: cellular excitability ("CELEX") hypotehsis of metastasis.* J Clin Exp Oncol, 2014.
118. Fadool, D.A., et al., *Kv1.3 channel gene-targeted deletion produces "Super-Smeller Mice" with altered glomeruli, interacting scaffolding proteins, and biophysics.* Neuron, 2004. **41**(3): p. 389-404.
119. Kubota, T., A.M. Correa, and F. Bezanilla, *Mechanism of functional interaction between potassium channel Kv1.3 and sodium channel NavBeta1 subunit.* Sci Rep, 2017. **7**: p. 45310.
120. Tucker, K., J.M. Overton, and D.A. Fadool, *Diet-induced obesity resistance of Kv1.3-/- mice is olfactory bulb dependent.* J Neuroendocrinol, 2012. **24**(8): p. 1087-95.
121. Das, P., et al., *Electrophysiological and behavioral phenotype of insulin receptor defective mice.* Physiol Behav, 2005. **86**(3): p. 287-96.
122. Kourrich, S., C. Mourre, and B. Soumireu-Mourat, *Kaliotoxin, a Kv1.1 and Kv1.3 channel blocker, improves associative learning in rats.* Behav Brain Res, 2001. **120**(1): p. 35-46.

123. Bell, G.A. and D.A. Fadool, *Awake, long-term intranasal insulin treatment does not affect object memory, odor discrimination, or reversal learning in mice.* Physiol Behav, 2017. **174**: p. 104-113.
124. Perez-Verdaguer, M., et al., *Caveolar targeting links Kv1.3 with the insulin-dependent adipocyte physiology.* Cell Mol Life Sci, 2018.
125. Lucero, M.T. and P.A. Pappone, *Voltage-gated potassium channels in brown fat cells.* J Gen Physiol, 1989. **93**(3): p. 451-72.
126. Xu, J., et al., *The voltage-gated potassium channel Kv1.3 regulates energy homeostasis and body weight.* Hum Mol Genet, 2003. **12**(5): p. 551-9.
127. Straub, S.V., et al., *Pharmacological inhibition of Kv1.3 fails to modulate insulin sensitivity in diabetic mice or human insulin-sensitive tissues.* Am J Physiol Endocrinol Metab, 2011. **301**(2): p. E380-90.
128. Xu, J., et al., *The voltage-gated potassium channel Kv1.3 regulates peripheral insulin sensitivity.* Proc Natl Acad Sci U S A, 2004. **101**(9): p. 3112-7.
129. Li, Y., et al., *Voltage-gated potassium channel Kv1.3 regulates GLUT4 trafficking to the plasma membrane via a Ca2+-dependent mechanism.* Am J Physiol Cell Physiol, 2006. **290**(2): p. C345-51.
130. Cahalan, M.D., et al., *A voltage-gated potassium channel in human T lymphocytes.* J Physiol, 1985. **358**: p. 197-237.
131. Grissmer, S., et al., *Expression and chromosomal localization of a lymphocyte K+ channel gene.* Proc Natl Acad Sci U S A, 1990. **87**(23): p. 9411-5.
132. Miao, S., et al., *Benzamide derivatives as blockers of Kv1.3 ion channel.* Bioorg Med Chem Lett, 2003. **13**(6): p. 1161-4.
133. Miller, C., et al., *Charybdotoxin, a protein inhibitor of single Ca2+-activated K+ channels from mammalian skeletal muscle.* Nature, 1985. **313**(6000): p. 316-8.
134. Peter, M., Jr., et al., *Effects of toxins Pi2 and Pi3 on human T lymphocyte Kv1.3 channels: the role of Glu7 and Lys24.* J Membr Biol, 2001. **179**(1): p. 13-25.
135. Pennington, M.W., et al., *Identification of three separate binding sites on SHK toxin, a potent inhibitor of voltage-dependent potassium channels in human T-lymphocytes and rat brain.* Biochem Biophys Res Commun, 1996. **219**(3): p. 696-701.
136. Coleman, S.K., et al., *Subunit composition of Kv1 channels in human CNS.* J Neurochem, 1999. **73**(2): p. 849-58.
137. Shamotienko, O.G., D.N. Parcej, and J.O. Dolly, *Subunit combinations defined for K+ channel Kv1 subtypes in synaptic membranes from bovine brain.* Biochemistry, 1997. **36**(27): p. 8195-201.
138. Villalonga, N., et al., *Kv1.3/Kv1.5 heteromeric channels compromise pharmacological responses in macrophages.* Biochem Biophys Res Commun, 2007. **352**(4): p. 913-8.
139. McGahon, M.K., et al., *Kv1.5 is a major component underlying the A-type potassium current in retinal arteriolar smooth muscle.* Am J Physiol Heart Circ Physiol, 2007. **292**(2): p. H1001-8.
140. Koutsouki, E., et al., *Modulation of human Kv1.5 channel kinetics by N-cadherin.* Biochem Biophys Res Commun, 2007. **363**(1): p. 18-23.
141. Wettwer, E. and H. Terlau, *Pharmacology of voltage-gated potassium channel Kv1.5--impact on cardiac excitability.* Curr Opin Pharmacol, 2014. **15**: p. 115-21.
142. Matus-Leibovitch, N., et al., *Chronic morphine administration enhances the expression of Kv1.5 and Kv1.6 voltage-gated K+ channels in rat spinal cord.* Brain Res Mol Brain Res, 1996. **40**(2): p. 261-70.
143. Bielanska, J., et al., *Voltage-dependent potassium channels Kv1.3 and Kv1.5 in human fetus.* Cell Physiol Biochem, 2010. **26**(2): p. 219-26.
144. Wang, Z., B. Fermini, and S. Nattel, *Sustained depolarization-induced outward current in human atrial myocytes. Evidence for a novel delayed rectifier K+ current similar to Kv1.5 cloned channel currents.* Circ Res, 1993. **73**(6): p. 1061-76.
145. Priest, B.T. and J.S. McDermott, *Cardiac ion channels.* Channels (Austin), 2015. **9**(6): p. 352-9.
146. Olson, T.M., et al., *Kv1.5 channelopathy due to KCNA5 loss-of-function mutation causes human atrial fibrillation.* Hum Mol Genet, 2006. **15**(14): p. 2185-91.
147. Vigdor-Alboim, S., et al., *Discoordinate regulation of different K channels in cultured rat skeletal muscle by nerve growth factor.* J Neurosci Res, 1999. **56**(3): p. 275-83.

148. Attali, B., et al., *Characterization of delayed rectifier Kv channels in oligodendrocytes and progenitor cells.* J Neurosci, 1997. **17**(21): p. 8234-45.
149. McFarlane, S. and N.S. Pollock, *A role for voltage-gated potassium channels in the outgrowth of retinal axons in the developing visual system.* J Neurosci, 2000. **20**(3): p. 1020-9.
150. Kotecha, S.A. and L.C. Schlichter, *A Kv1.5 to Kv1.3 switch in endogenous hippocampal microglia and a role in proliferation.* J Neurosci, 1999. **19**(24): p. 10680-93.
151. Villalonga, N., et al., *Immunomodulation of voltage-dependent K+ channels in macrophages: molecular and biophysical consequences.* J Gen Physiol, 2010. **135**(2): p. 135-47.
152. Villalonga, N., et al., *Cell cycle-dependent expression of Kv1.5 is involved in myoblast proliferation.* Biochim Biophys Acta, 2008. **1783**(5): p. 728-36.
153. Barfield, J.P., C.H. Yeung, and T.G. Cooper, *Characterization of potassium channels involved in volume regulation of human spermatozoa.* Mol Hum Reprod, 2005. **11**(12): p. 891-7.
154. Boycott, H.E., et al., *Shear stress triggers insertion of voltage-gated potassium channels from intracellular compartments in atrial myocytes.* Proc Natl Acad Sci U S A, 2013. **110**(41): p. E3955-64.
155. Chapalamadugu, K.C., et al., *High level of oxygen treatment causes cardiotoxicity with arrhythmias and redox modulation.* Toxicol Appl Pharmacol, 2015. **282**(1): p. 100-7.
156. Snyders, D.J., M.M. Tamkun, and P.B. Bennett, *A rapidly activating and slowly inactivating potassium channel cloned from human heart. Functional analysis after stable mammalian cell culture expression.* J Gen Physiol, 1993. **101**(4): p. 513-43.
157. Feng, J., et al., *Antisense oligodeoxynucleotides directed against Kv1.5 mRNA specifically inhibit ultrarapid delayed rectifier K+ current in cultured adult human atrial myocytes.* Circ Res, 1997. **80**(4): p. 572-9.
158. Po, S., et al., *Heteromultimeric assembly of human potassium channels. Molecular basis of a transient outward current?* Circ Res, 1993. **72**(6): p. 1326-36.
159. Ravens, U. and E. Wettwer, *Ultra-rapid delayed rectifier channels: molecular basis and therapeutic implications.* Cardiovasc Res, 2011. **89**(4): p. 776-85.
160. Chevillard, C., et al., *Localization of a potassium channel gene (KCNE1) to 21q22.1-q22.2 by in situ hybridization and somatic cell hybridization.* Genomics, 1993. **15**(1): p. 243-5.
161. Sanguinetti, M.C., et al., *Coassembly of K(V)LQT1 and minK (IsK) proteins to form cardiac I(Ks) potassium channel.* Nature, 1996. **384**(6604): p. 80-3.
162. Barhanin, J., et al., *K(V)LQT1 and lsK (minK) proteins associate to form the I(Ks) cardiac potassium current.* Nature, 1996. **384**(6604): p. 78-80.
163. Kurokawa, J., L. Chen, and R.S. Kass, *Requirement of subunit expression for cAMP-mediated regulation of a heart potassium channel.* Proc Natl Acad Sci U S A, 2003. **100**(4): p. 2122-7.
164. Marx, S.O., et al., *Requirement of a macromolecular signaling complex for beta adrenergic receptor modulation of the KCNQ1-KCNE1 potassium channel.* Science, 2002. **295**(5554): p. 496-9.
165. McDonald, T.V., et al., *A minK-HERG complex regulates the cardiac potassium current I(Kr).* Nature, 1997. **388**(6639): p. 289-92.
166. Melman, Y.F., et al., *KCNE1 binds to the KCNQ1 pore to regulate potassium channel activity.* Neuron, 2004. **42**(6): p. 927-37.
167. Grunnet, M., et al., *KCNE4 is an inhibitory subunit to the KCNQ1 channel.* J Physiol, 2002. **542**(Pt 1): p. 119-30.
168. Grunnet, M., et al., *KCNE4 is an inhibitory subunit to Kv1.1 and Kv1.3 potassium channels.* Biophys J, 2003. **85**(3): p. 1525-37.
169. Teng, S., et al., *Novel gene hKCNE4 slows the activation of the KCNQ1 channel.* Biochem Biophys Res Commun, 2003. **303**(3): p. 808-13.
170. McCallum, L.A., I.A. Greenwood, and R.M. Tribe, *Expression and function of K(v)7 channels in murine myometrium throughout oestrous cycle.* Pflugers Arch, 2009. **457**(5): p. 1111-20.
171. Grunnet, M., et al., *hKCNE4 inhibits the hKCNQ1 potassium current without affecting the activation kinetics.* Biochem Biophys Res Commun, 2005. **328**(4): p. 1146-53.

172. Levy, D.I., et al., *MiRP3 acts as an accessory subunit with the BK potassium channel.* Am J Physiol Renal Physiol, 2008. **295**(2): p. F380-7.
173. Levy, D.I., et al., *The membrane protein MiRP3 regulates Kv4.2 channels in a KChIP-dependent manner.* J Physiol, 2010. **588**(Pt 14): p. 2657-68.
174. Crump, S.M., et al., *Kcne4 deletion sex- and age-specifically impairs cardiac repolarization in mice.* FASEB J, 2016. **30**(1): p. 360-9.
175. van der Eb, A., *USA FDA CTR for biologics evaluation and research vaccines and related biological products advisory committe meeting.* US FDA, 2012.
176. Louis, N., C. Evelegh, and F.L. Graham, *Cloning and sequencing of the cellular-viral junctions from the human adenovirus type 5 transformed 293 cell line.* Virology, 1997. **233**(2): p. 423-9.
177. Shaw, G., et al., *Preferential transformation of human neuronal cells by human adenoviruses and the origin of HEK 293 cells.* FASEB J, 2002. **16**(8): p. 869-71.
178. Schneider, U., H.U. Schwenk, and G. Bornkamm, *Characterization of EBV-genome negative "null" and "T" cell lines derived from children with acute lymphoblastic leukemia and leukemic transformed non-Hodgkin lymphoma.* Int J Cancer, 1977. **19**(5): p. 621-6.
179. Kammertoens, T., et al., *CY15, a malignant histiocytic tumor that is phenotypically similar to immature dendritic cells.* Cancer Res, 2005. **65**(7): p. 2560-4.
180. Vallejo-Gracia, A., *Kv1.3 and Kv1.5 channels in leukocytes*, in *Departament de Bioquímica i Biologia Molecular (Biologia)*2016, Universitat de Barcelona.
181. Brown, D.A. and J.K. Rose, *Sorting of GPI-anchored proteins to glycolipid-enriched membrane subdomains during transport to the apical cell surface.* Cell, 1992. **68**(3): p. 533-44.
182. Schneider, C.A., W.S. Rasband, and K.W. Eliceiri, *NIH Image to ImageJ: 25 years of image analysis.* Nat Methods, 2012. **9**(7): p. 671-5.
183. Bolte, S. and F.P. Cordelieres, *A guided tour into subcellular colocalization analysis in light microscopy.* J Microsc, 2006. **224**(Pt 3): p. 213-32.
184. Thompson, J.D., D.G. Higgins, and T.J. Gibson, *CLUSTAL W: improving the sensitivity of progressive multiple sequence alignment through sequence weighting, position-specific gap penalties and weight matrix choice.* Nucleic Acids Res, 1994. **22**(22): p. 4673-80.
185. Schwede, T., et al., *SWISS-MODEL: An automated protein homology-modeling server.* Nucleic Acids Res, 2003. **31**(13): p. 3381-5.
186. Krieger, E., G. Koraimann, and G. Vriend, *Increasing the precision of comparative models with YASARA NOVA--a self-parameterizing force field.* Proteins, 2002. **47**(3): p. 393-402.
187. Guex, N. and M.C. Peitsch, *SWISS-MODEL and the Swiss-PdbViewer: an environment for comparative protein modeling.* Electrophoresis, 1997. **18**(15): p. 2714-23.
188. Duan, Y., et al., *A point-charge force field for molecular mechanics simulations of proteins based on condensed-phase quantum mechanical calculations.* J Comput Chem, 2003. **24**(16): p. 1999-2012.
189. Kolaskar, A.S. and S. Sawant, *Prediction of conformational states of amino acids using a Ramachandran plot.* Int J Pept Protein Res, 1996. **47**(1-2): p. 110-6.
190. Laskowski, R.A., et al., *AQUA and PROCHECK-NMR: programs for checking the quality of protein structures solved by NMR.* J Biomol NMR, 1996. **8**(4): p. 477-86.
191. Guerois, R., J.E. Nielsen, and L. Serrano, *Predicting changes in the stability of proteins and protein complexes: a study of more than 1000 mutations.* J Mol Biol, 2002. **320**(2): p. 369-87.
192. Schymkowitz, J., et al., *The FoldX web server: an online force field.* Nucleic Acids Res, 2005. **33**(Web Server issue): p. W382-8.
193. Decoursey, T.E., et al., *Mitogen induction of ion channels in murine T lymphocytes.* J Gen Physiol, 1987. **89**(3): p. 405-20.
194. DeCoursey, T.E., et al., *Voltage-gated K+ channels in human T lymphocytes: a role in mitogenesis?* Nature, 1984. **307**(5950): p. 465-8.
195. DeCoursey, T.E., et al., *Ion channel expression in PMA-differentiated human THP-1 macrophages.* J Membr Biol, 1996. **152**(2): p. 141-57.

196. Jou, I., et al., *Expression of Kv1.5 K+ channels in activated microglia in vivo.* Glia, 1998. **24**(4): p. 408-14.
197. Zsiros, E., et al., *Developmental switch of the expression of ion channels in human dendritic cells.* J Immunol, 2009. **183**(7): p. 4483-92.
198. Sole, L., et al., *KCNE4 suppresses Kv1.3 currents by modulating trafficking, surface expression and channel gating.* J Cell Sci, 2009. **122**(Pt 20): p. 3738-48.
199. van Furth, R., et al., *The mononuclear phagocyte system: a new classification of macrophages, monocytes, and their precursor cells.* Bull World Health Organ, 1972. **46**(6): p. 845-52.
200. Sole, L., et al., *KCNE gene expression is dependent on the proliferation and mode of activation of leukocytes.* Channels (Austin), 2013. **7**(2): p. 85-96.
201. Zhu, J., J. Yan, and W.B. Thornhill, *N-glycosylation promotes the cell surface expression of Kv1.3 potassium channels.* FEBS J, 2012. **279**(15): p. 2632-44.
202. Bartok, A., et al., *Margatoxin is a non-selective inhibitor of human Kv1.3 K+ channels.* Toxicon, 2014. **87**: p. 6-16.
203. Fellerhoff-Losch, B., et al., *Normal human CD4(+) helper T cells express Kv1.1 voltage-gated K(+) channels, and selective Kv1.1 block in T cells induces by itself robust TNFalpha production and secretion and activation of the NFkappaB non-canonical pathway.* J Neural Transm (Vienna), 2016. **123**(3): p. 137-57.
204. Koch, R.O., et al., *Complex subunit assembly of neuronal voltage-gated K+ channels. Basis for high-affinity toxin interactions and pharmacology.* J Biol Chem, 1997. **272**(44): p. 27577-81.
205. Barbour, B. *Electronics for electrophysiologists*. 2014.
206. Felipe, A., C. Soler, and N. Comes, *Kv1.5 in the immune system: the good, the bad, or the ugly?* Front Physiol, 2010. **1**: p. 152.
207. Shimizu, Y., T. Kubo, and Y. Furukawa, *Cumulative inactivation and the pore domain in the Kv1 channels.* Pflugers Arch, 2002. **443**(5-6): p. 720-30.
208. Lisewski, U., et al., *Increased aldosterone-dependent Kv1.5 recycling predisposes to pacing-induced atrial fibrillation in Kcne3-/- mice.* FASEB J, 2016. **30**(7): p. 2476-89.
209. Martens, J.R., et al., *Isoform-specific localization of voltage-gated K+ channels to distinct lipid raft populations. Targeting of Kv1.5 to caveolae.* J Biol Chem, 2001. **276**(11): p. 8409-14.
210. Shibata, E.F., et al., *Autonomic regulation of voltage-gated cardiac ion channels.* J Cardiovasc Electrophysiol, 2006. **17 Suppl 1**: p. S34-S42.
211. Folco, E.J., G.X. Liu, and G. Koren, *Caveolin-3 and SAP97 form a scaffolding protein complex that regulates the voltage-gated potassium channel Kv1.5.* Am J Physiol Heart Circ Physiol, 2004. **287**(2): p. H681-90.
212. McEwen, D.P., et al., *Caveolin regulates kv1.5 trafficking to cholesterol-rich membrane microdomains.* Mol Pharmacol, 2008. **73**(3): p. 678-85.
213. Abi-Char, J., et al., *Membrane cholesterol modulates Kv1.5 potassium channel distribution and function in rat cardiomyocytes.* J Physiol, 2007. **582**(Pt 3): p. 1205-17.
214. Shamgar, L., et al., *KCNE1 constrains the voltage sensor of Kv7.1 K+ channels.* PLoS One, 2008. **3**(4): p. e1943.
215. Nakajo, K. and Y. Kubo, *KCNE1 and KCNE3 stabilize and/or slow voltage sensing S4 segment of KCNQ1 channel.* J Gen Physiol, 2007. **130**(3): p. 269-81.
216. Ruscic, K.J., et al., *IKs channels open slowly because KCNE1 accessory subunits slow the movement of S4 voltage sensors in KCNQ1 pore-forming subunits.* Proc Natl Acad Sci U S A, 2013. **110**(7): p. E559-66.
217. Murray, C.I., et al., *Unnatural amino acid photo-crosslinking of the IKs channel complex demonstrates a KCNE1:KCNQ1 stoichiometry of up to 4:4.* Elife, 2016. **5**.
218. Wang, K.W., K.K. Tai, and S.A. Goldstein, *MinK residues line a potassium channel pore.* Neuron, 1996. **16**(3): p. 571-7.
219. Tapper, A.R. and A.L. George, Jr., *Location and orientation of minK within the I(Ks) potassium channel complex.* J Biol Chem, 2001. **276**(41): p. 38249-54.
220. Hajdu, P., et al., *The C-terminus SH3-binding domain of Kv1.3 is required for the actin-mediated immobilization of the channel via cortactin.* Mol Biol Cell, 2015. **26**(9): p. 1640-51.

221. Fernandez-Marino, A.I., et al., *Gating interaction maps reveal a noncanonical electromechanical coupling mode in the Shaker K(+) channel.* Nat Struct Mol Biol, 2018. **25**(4): p. 320-326.
222. Blunck, R. and Z. Batulan, *Mechanism of electromechanical coupling in voltage-gated potassium channels.* Front Pharmacol, 2012. **3**: p. 166.
223. Magidovich, E., S.J. Fleishman, and O. Yifrach, *Intrinsically disordered C-terminal segments of voltage-activated potassium channels: a possible fishing rod-like mechanism for channel binding to scaffold proteins.* Bioinformatics, 2006. **22**(13): p. 1546-50.
224. Magidovich, E., et al., *Intrinsic disorder in the C-terminal domain of the Shaker voltage-activated K+ channel modulates its interaction with scaffold proteins.* Proc Natl Acad Sci U S A, 2007. **104**(32): p. 13022-7.
225. Romero, P., et al., *Sequence complexity of disordered protein.* Proteins, 2001. **42**(1): p. 38-48.
226. Williams, R.M., et al., *The protein non-folding problem: amino acid determinants of intrinsic order and disorder.* Pac Symp Biocomput, 2001: p. 89-100.
227. Dunker, A.K., et al., *Intrinsically disordered protein.* J Mol Graph Model, 2001. **19**(1): p. 26-59.
228. Ota, M., et al., *Polymorphism in the KCNA3 gene is associated with susceptibility to autoimmune pancreatitis in the Japanese population.* Dis Markers, 2011. **31**(4): p. 223-9.
229. Ma, K.J., et al., *Modulation of KCNQ1 current by atrial fibrillation-associated KCNE4 (145E/D) gene polymorphism.* Chin Med J (Engl), 2007. **120**(2): p. 150-4.
230. Trevino, L.R., et al., *Germline genomic variants associated with childhood acute lymphoblastic leukemia.* Nat Genet, 2009. **41**(9): p. 1001-5.
231. Freidin, M.B., et al., *[Effect of additional disease (comorbidity) on association of allergic rhinitis with KCNE4 gene rs12621643 variant].* Genetika, 2013. **49**(4): p. 541-4.
232. Lai, L.P., et al., *Association of the human minK gene 38G allele with atrial fibrillation: evidence of possible genetic control on the pathogenesis of atrial fibrillation.* Am Heart J, 2002. **144**(3): p. 485-90.
233. Haijun, M., et al., *Association between KCNE1 (G38S) genetic polymorphism and non-valvular atrial fibrillation in an Uygur population.* Wien Klin Wochenschr, 2012. **124**(21-22): p. 737-41.
234. Abbott, G.W., *Novel exon 1 protein-coding regions N-terminally extend human KCNE3 and KCNE4.* FASEB J, 2016. **30**(8): p. 2959-69.

ANNEXES

8. ANNEXES

A. FLOWCHART OF GENELUTE™ PLASMID MINIPREP KIT

All spins at ;12,000 3 *g, except as noted.*

1 Harvest & lyse bacteria

- Pellet cells from 1–5 ml overnight culture *1 minute* (1 ml from TB or 2xYT; 1–5 ml from LB medium). Discard supernatant.
- Resuspend cells in 200 µl Resuspension Solution. Pipette up and down or vortex.
- Add 200 µl of Lysis Solution. Invert gently to mix. Do not vortex. Allow to clear for :5 minutes

* *Prior to first time use, be sure to add the RNase A to the Resuspension Solution.*

2 Prepare cleared lysate

- Add 350 µl of Neutralization Solution (S3). Invert 4–6 times to mix.
- *Pellet debris 10 minutes at max speed.*

3 Prepare binding column

- Add 500 µl Column Preparation Solution to binding column in a collection tube.
- *Spin at ≥12,000 x g, 1 minute.* Discard flow-through.

4 Bind plasmid DNA to column

- Transfer cleared lysate into binding column.
- *Spin 30",1 minute.* Discard flow-through.

5 Wash to remove contaminants

- *Optional (EndA⁺ strains only):* Add 500 µl Optional Wash Solution to column. *Spin 30", 1 minute.* Discard flow-through.
- Add 750 µl Wash Solution to column. *Spin 30", 1 minute.* Discard flow-through.
- *Spin 1 minute* to dry column.

* *Prior to first time use, be sure to add ethanol to the concentrated Wash Solution.*

6 Elute purified plasmid DNA

- Transfer column to new collection tube.
- Add 100 µl Elution Solution. *Spin 1 minute.*

* *If a more concentrated plasmid DNA prep is required, reduce the elution volume to a minimum of 50 µl.*

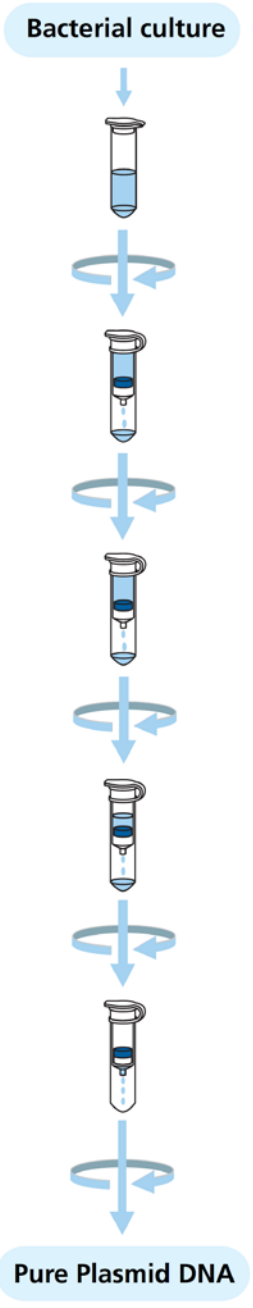

Annex A: *Flowchart of the protocol of GenElute™ Plasmid Miniprep kit for the purification of Plasmid DNA from bacteria.*

B. FLOWCHART OF PURELINK® GENOMIC DNA KIT

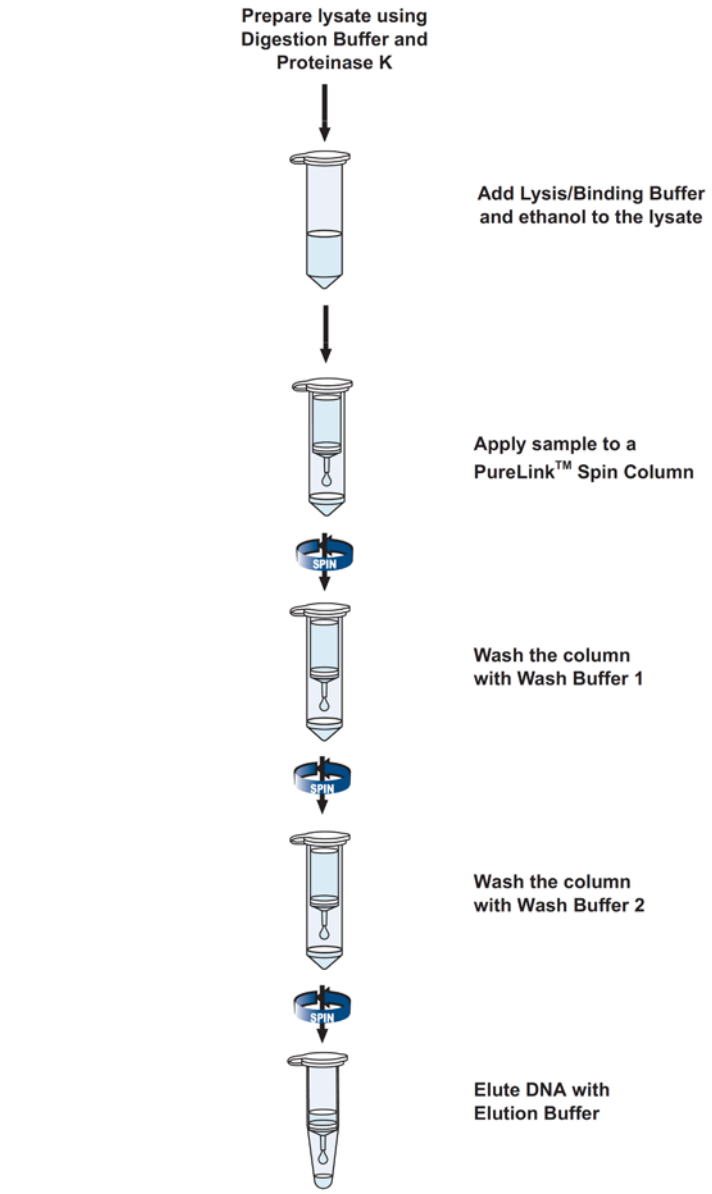

Annex B: *Flowchart of the protocol of PureLink® Genomic DNA kit for the purification of Genomic DNA from eukaryotic cells.*

C. FLOWCHART OF ATP™ GEL/PCR DNA FRAGMENT EXTRACTION KIT

Gel Extraction Protocol

Gel Dissociation

1. Excise the agarose gel slice containing interested DNA fragments and remove extra agarose to minimize the size of the gel slice.
   (It is better that using TAE buffer to make the gel than TBE buffer, because TBE buffer may probably affect the downstream experiment).
2. Transfer up to 300 mg of the gel slice into a microcentrifuge tube (provided by user).
3. Add 500 µl of DF Buffer to the sample and mix by vortexing.
4. Incubate at 60 ℃ for 10-15 minutes until the gel slice completely dissolves. During incubation, invert the tube every 2-3 min.
5. Cool down the dissolved sample mixture to room temperature.

DNA Binding

6. Place a DF Column in a 2 ml Collection Tube.
7. Apply 800 µl of the sample mixture from previous step into the DF Column.
8. Centrifuge at 10,000 xg (13,000 rpm) for 30 seconds.
9. Discard the flow-through and place the DF Column back in the Collection Tube.
10. If the sample mixture is more than 800 µl, repeat this DNA Binding Step.

Washing

11. Add 600 µl of Wash Buffer (ethanol added) into the DF Column.
12. Centrifuge at 10,000 xg (13,000 rpm) for 30 seconds.
13. Discard the flow-through and place the DF Column back in the Collection Tube.
    Note : For TAE gels, proceed to step 14. For TBE gels, repeat steps 11-13 of Washing procedure. Boric acid is difficult to be removed and can affect downstream application, therefore double wash is recommended.
14. Centrifuge again for 3 minutes at full speed (13,000 rpm) to dry the column matrix.

DNA Elution

15. Transfer dried column in a new microcentrifuge tube (provided by user).
16. Add 15-50 µl of Elution Buffer or water onto the center of the column matrix.
17. Stand for 2 minutes until Elution Buffer or water is absorbed by the matrix.
18. Centrifuge at full speed for 2 minutes to elute purified DNA.

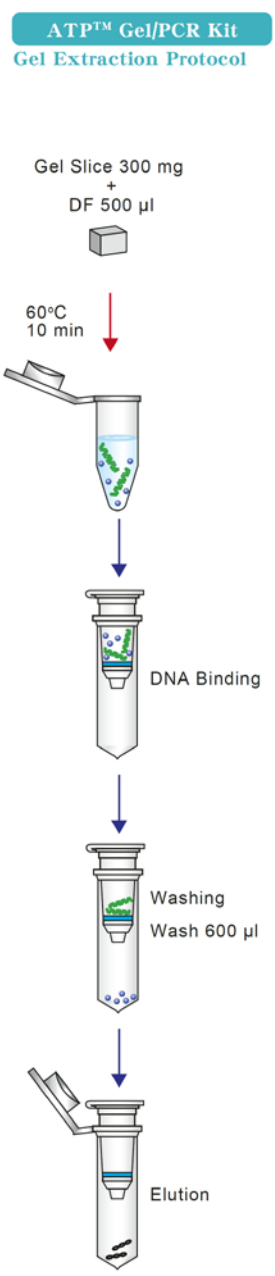

Annex C: *Flowchart of the protocol of ATP™ Gel/PCR DNA fragment extraction kit for the purification of agarose-embedded DNA.*

D. QUIKCHANGE LIGHTNING SITE-DIRECTED MUTAGENESIS KIT PROTOCOL

Mutant Strand Synthesis Reaction (Thermal Cycling)

Notes *Ensure that the plasmid DNA template is isolated from a* dam+ E. coli *strain. The majority of the commonly used* E. coli *strains are* dam+. ***Plasmid DNA isolated from* dam− *strains (e.g. JM110 and SCS110) is not suitable.***

To maximize temperature-cycling performance, ***we strongly recommend using thin-walled tubes****, which ensure ideal contact with the temperature cycler's heat blocks. The following protocols were optimized using thin-walled tubes.*

1. Synthesize two complimentary oligonucleotides containing the desired mutation, flanked by unmodified nucleotide sequence. Purify these oligonucleotide primers prior to use in the following steps (see *Mutagenic Primer Design*).

2. Prepare the control reaction as indicated below:

   5 µl of 10× reaction buffer
   5 µl (25 ng) of pWhitescript 4.5-kb control plasmid (5 ng/µl)
   1.25 µl (125 ng) of oligonucleotide control primer #1 [34-mer (100 ng/µl)]
   1.25 µl (125 ng) of oligonucleotide control primer #2 [34-mer (100 ng/µl)]
   1 µl of dNTP mix
   1.5 µl of QuikSolution reagent
   34 µl ddH_2O (to bring the final reaction volume to 50 µl)

   Then add:

   1 µl of QuikChange Lightning Enzyme

3. Prepare the sample reaction(s) as indicated below:

   Note *Set up a series of sample reactions using various amounts of dsDNA template ranging from 10 to 100 ng (e.g., 10, 25, 50, and 100 ng of dsDNA template) while keeping the primer concentration constant.*

   5 µl of 10× reaction buffer
   X µl (10–100 ng) of dsDNA template
   X µl (125 ng) of oligonucleotide primer #1
   X µl (125 ng) of oligonucleotide primer #2
   1 µl of dNTP mix
   1.5 µl of QuikSolution reagent
   ddH_2O to a final volume of 50 µl

   Then add:

   1 µl of QuikChange Lightning Enzyme

4. Cycle each reaction using the cycling parameters outlined in Table I. (For the control reaction, use a 2.5-minute extension time.)

TABLE I

Cycling Parameters for the QuikChange Lightning Site-Directed Mutagenesis Method

Segment	Cycles	Temperature	Time
1	1	95°C	2 minutes
2	18	95°C	20 seconds
		60°C	10 seconds
		68°C	30 seconds/kb of plasmid length*
3	1	68°C	5 minutes

* For example, a 5-kb plasmid requires 2.5 minutes per cycle at 68°C.

Dpn I Digestion of the Amplification Products

1. Add 2 µl of the provided *Dpn* I restriction enzyme directly to each amplification reaction.

Notes *Use only the* Dpn I *enzyme provided; do not substitute with an enzyme from another source.*

2. Gently and thoroughly mix each reaction mixture by pipetting the solution up and down several times. Briefly spin down the reaction mixtures and then immediately incubate at 37°C for 5 minutes to digest the parental (i.e., the nonmutated) supercoiled dsDNA.

Transformation of XL10-Gold Ultracompetent Cells

Notes *Please read the* Transformation Guidelines *before proceeding with the transformation protocol.*

XL10-Gold cells are resistant to tetracycline and chloramphenicol. If the mutagenized plasmid contains only the tet^R *or* cam^R *resistance marker, an alternative strain of competent cells must be used.*

1. Gently thaw the XL10-Gold ultracompetent cells on ice. For each control and sample reaction to be transformed, aliquot 45 µl of the ultracompetent cells to a *prechilled* 14-ml BD Falcon polypropylene round-bottom tube.

2. Add 2 µl of the β-ME mix provided with the kit to the 45 µl of cells. (Using an alternative source of β-ME may reduce transformation efficiency.)

3. Swirl the contents of the tube gently. Incubate the cells on ice for 2 minutes.

4. Transfer 2 µl of the *Dpn* I-treated DNA from each control and sample reaction to separate aliquots of the ultracompetent cells.

   As an optional control, verify the transformation efficiency of the XL10-Gold ultracompetent cells by adding 1 µl of 0.01 ng/µl pUC18 control plasmid (dilute the control provided 1:10 in high-quality water) to another 45-µl aliquot of cells.

5. Swirl the transformation reactions gently to mix and incubate the reactions on ice for 30 minutes.

   Note *The incubation time for this step may be reduced to 10 minutes without substantial losses in transformation efficiency.*

6. Preheat NZY$^+$ broth (see *Preparation of Media and Reagents*) in a 42°C water bath for use in step 9.

   Note *Transformation of XL10-Gold ultracompetent cells has been optimized using* ***NZY$^+$ broth****.*

7. Heat-pulse the tubes in a 42°C water bath for 30 seconds. The duration of the heat pulse is *critical* for obtaining the highest efficiencies. Do not exceed 42°C.

   Note *This heat pulse has been optimized for transformation in 14-ml BD Falcon polypropylene round-bottom tubes.*

8. Incubate the tubes on ice for 2 minutes.

9. Add 0.5 ml of preheated (42°C) NZY$^+$ broth to each tube, then incubate the tubes at 37°C for 1 hour with shaking at 225–250 rpm.

Annex D: *Protocol of the QuikChange Lightning Site-Directed Mutagenesis Kit.*

E. PIERCE™ CELL SURFACE PROTEIN ISOLATION KIT PROTOCOL

Procedure for Cell Surface Biotinylation

Note: Not every protein on the cell surface will be extracted with this kit. Steric hindrance, lack of primary amines, and/or minimal sequence with extra-cellular exposure may prevent or interfere with labeling.

A. Biotinylation

1. Prepare four T75 cm^2 flasks of 90-95% confluent cells.

   Note: If cells are grown in suspension, use 1×10^6 cells per milliliter of the biotin solution prepared in step 3. Do not exceed a total of 4×10^7 cells per labeling reaction.

2. Remove media and wash cells twice with 8mL of ice-cold PBS per flask. Quickly remove the PBS.

   Note: Do not allow PBS to remain in contact with cells for more than 5 seconds to prevent rounding and detachment of cells.

3. Dissolve the contents of one vial of Sulfo-NHS-SS-Biotin in 48mL of ice-cold PBS. Add 10mL of the biotin solution to each flask.

4. Place flasks on rocking platform or orbital shaker and gently agitate for 30 minutes at 4°C. This step ensures even coverage of the cells with the labeling solution.

5. Add 500µL of Quenching Solution to each flask to quench the reaction. Gently tip the flask back and forth to ensure even coverage of the solution.

6. Gently scrape cells into solution and transfer the contents of all four flasks to a single 50mL conical tube. Rinse all four flasks with a single 10mL volume of TBS and add rinse volume to transferred cells.

7. Centrifuge cells at 500 × *g* for 3 minutes and discard supernatant.

8. Add 5mL TBS to the cell pellet and gently pipette cells up and down twice with a serological pipette. Centrifuge at 500 × *g* for 3 minutes and discard supernatant.

B. Cell Lysis

1. Add protease inhibitors to 500µL of Lysis Buffer and add it to the cells. Transfer cells in the lysis solution to a 1.5mL microcentrifuge tube.

2. Pipette up and down to suspend the cells.

3. Using low power (e.g., 1.5) to prevent foaming, disrupt cells by sonicating on ice using five 1-second bursts.

4. Incubate cells 30 minutes on ice, vortexing every 5 minutes for 5 seconds. To improve solubilization efficiency, perform additional sonications during incubation.

5. Centrifuge cell lysate at 10,000 × *g* for 2 minutes at 4°C.

6. Transfer clarified supernatant to a new tube.

C. Isolation of Labeled Proteins

1. Insert a column into a collection tube.

2. Gently swirl the bottle of NeutrAvidin Agarose to obtain an even suspension. Add 500µL of the NeutrAvidin Agarose slurry to the column and cap the column.

3. Centrifuge 1 minute at 1000 × *g* and discard flow-through. Reuse the collection tube through Step C11.

4. Add 500µL of Wash Buffer to the gel, centrifuge for 1 minute at 1000 × *g* and discard flow-through. Repeat this step twice.

5. Apply bottom cap to column, add clarified cell lysate to the gel, and then apply top cap to column.

   Note: Make sure top and bottom caps are tightly in place.

6. Incubate for 60 minutes at room temperature with end-over-end mixing using a rotator. Alternatively, rock back and forth on a rocking platform.

7. Remove top cap and then bottom cap from column. Place column in the collection tube, and replace top.

   Note: Remove top cap before bottom cap to prevent lysate from leaking from the bottom of the column.

8. Centrifuge column for 1 minute at 1000 × *g* and discard flow-through.

9. Add protease inhibitors to 2.5mL of Wash Buffer.

10. Return column to the collection tube and add 500µL Wash Buffer. Cap the column and mix by inverting the column. Centrifuge for 1 minute at 1000 × *g*. Discard rinse and remove top cap. Repeat this step three times.

11. Replace bottom cap on column.

D. Protein Elution

1. Puncture the foil covering of one No-Weigh DTT Microtube with a pipette tip, and add 50µL of ultrapure water to yield 1M DTT.
2. Add 23.7µL of the DTT solution to 450µL SDS-PAGE Sample Buffer to make a final concentration of 50mM DTT.
3. Add 400µL of the Sample Buffer containing the DTT to the gel and cap the column. Incubate the reaction for 60 minutes at room temperature with end-over-end mixing on a rotator or rock back and forth on a rocking platform.

   Alternatively, place column in a new collection tube and heat in a heat block for 5 minutes at 95°C. Ensure that bottom cap is on tightly. Heating will cause recovery of some NeutrAvidin Protein monomer (15K) in the eluate. The monomer is not released when elution is performed at room temperature.
4. Remove the column's top cap first and then the bottom cap. Place column in a new collection tube and replace top cap.
5. Centrifuge column for 2 minutes at 1000 × *g*.
6. Add a trace amount of bromophenol blue to eluate and analyze by Western blot. Store sample at -20°C if not used immediately.

Annex E: *Protocol of the Pierce™ Cell Surface Protein Isolation kit. This protocol functions by binding biotin to extracellular tertiary amines, which later get captured by the Neutravidin beads. This way, transmembrane proteins get isolated from cytoplasmic ones.*

F. PRIMERS FOR GENE SEQUENCING OF SAMPLES OF MULTIPLE SCLEROSIS PATIENTS

A

KCNA3		
	Forward	Reverse
h 1.3 P1	TGGGCGGGAATCCTAAGGG	GAGCGGGTCGAAGTACCTC
h 1.3 P2	TTCGAGACGCAGCTGAAGAC	AGATGCGGAAGACCCTTACC
h 1.3 P3	AACGACAGGGCAATGGACAG	AAGGGCATAGGCAGACCAAG
h 1.3 P4	AAACGGGCAATTCCACTG	GGACATCTTGGGCATTTCC
h 1.3 P5	GGTTGCCTACCCTGTAGATATGTG	GTGCGGCTTATTCAAACAGTGG
h 1.3 P6	CCATGTTTCCTGGGAAACC	AGAGCTGTTGTGGGATCTG
h 1.3 PX	CCTTGAGGGCTGCAAGAAATG	

B

KCNA5		
	Forward	Reverse
h 1.5 P1	GGCTGAAGGTTGCATCTG	GCGGTCGAAGAAGTACTC
h 1.5 P2	CAGCGCGTCCACATCAACATC	ACGAGCAGCTCGAAGGTGAAC
h 1.5 P3	TTGGAGACCCTGCCTGAGTTC	TGATCCGTTTCCCGGTGGTAG
h 1.5 P4	ATGAGGCCCATCACTGTTG	CACATGGATGGAGGAGTTAC
h 1.5 P5	GGATGTATTTGTAGCCAGTCTC	ACTTGCCTCAACAAGGTAAC

C

KCNE1		
	Forward	Reverse
h E1 P1	AGGTGTGCCTGGGAAGTTTGAG	AGCAAGGCAGGGACAGATATGG
h E1 P2	GGCCATAGAACAACCCAACAC	AGGAGGATAGAGCCACAAGAG
h E1 P3	TGCCCTTACTGATACACC	CTGTGCTTCCTCTGAAAC
h E1 P4	AGGAAGGCCGAGGATGGATG	TAGCTGGGCTGCTACTGGTC
h E1 P5	AGTGGTTCTTTGGGTTAC	AGCGAAATCTCACTACTG

D

KCNE4		
	Forward	Reverse
h E4 P1	GACTGTAAATCCCGCACTTG	TGTAGCCTTGCTGACTTACC
h E4 P2	ACTGTCAGCCTTGGTAAGTC	CATGTAGCCCAGCATGATTC
h E4 P3	GTCAGCTGTTTGGCGAACCC	CTTCGCTGCTCTCGTTGAGG
h E4 P4	AATCCAAGAGGCGGGAGAAG	CAGCGTGTCCTAAGCATTCG
h E4 P5	GCTGCCACTTTGAAGAGACC	TGAGCAGCAGCAGAGCTAAC
h E4 P6	CATGCAGCATCACATGATGG	GGATCTGCGAAACTGTTGAC
h E4 P7	GGTTGGGAGGATGTCTTTAG	GGTGGGAGGATCATTTAAGG
h E4 P8	CCTGGCCTTAAATGATCC	CTGTGATGTCTTCGAAAC

Annex F: *Primers used for the sequencing of Multiple Sclerosis patients.* ***A:*** *KCNA3;* ***B:*** *KCNA5;* ***C:*** *KCNE1;* ***D:*** *KCNE4.*

G. GENES AND RELATIVE POSITION OF SNPS

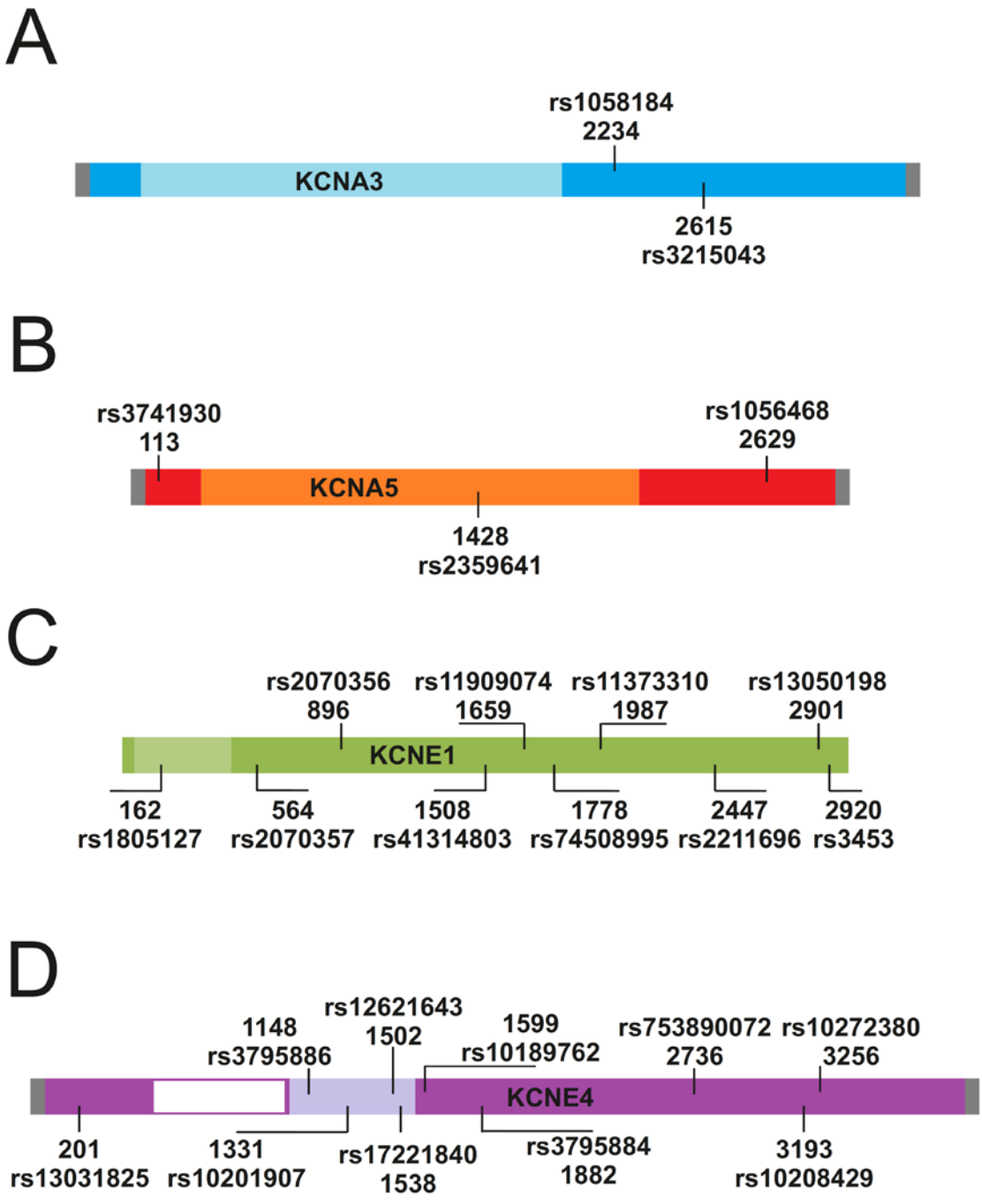

Annex G: *Schematic representation of the studied genes and the relative position of found SNPs. Size of gene bars and the location of SNPs are proportional to the real sequence.* ***A:*** *KCNA3;* ***B:*** *KCNA5;* ***C:*** *KCNE1;* ***D:*** *KCNE4. For all the genes, grey represents 5' or 3' UTR, white represents introns, and lighter colours represents the coding sequence.* ***A:*** *KCNA3 gene.* ***B:*** *KCNA5 gene.* ***C:*** *KCNE1 coding exon. As KCNE1 presents long intron sequences and alternative splicing, we decided just to sequence the coding exon.* ***D:*** *KCNE4 gene. The lighter coloured region only represents the short form of the KCNE4 protein [234].*

H. GENOTYPED SEQUENCES OF KCNA3, KCNA5, KCNE1 AND KCNE4

Genotyped sequences of human KCNA3, KCNA5, KCNE1 and KCNE4. Sequences were downloaded from ENSEMBL database (https://www.ensembl.org/index.html). Gene regions are coloured or highlighted depending on their nature.

Colour codes:

5′ upstream / 3′ downstream	Non-coding exon
Polymorphism	Coding exon
Amino acid-changing polymorphism	Intron
miRNA target	Poly-adenylation region

KCNA3

cccgagagcgggacgcgcgcccgcgcggtgggcgggaatcctaaggggacGCGGAGGCGGGCGCGCGC
CCCGCAGGGGAGGGGGCGGAGAGCGCGAGAAGGAGGGAGGAGGCGTCCCCGTGCGGGAGCCCGGCTGA
CCGCGCCAGACCCAGACAGAGCATCGCGGCTTTGGCTGCAACAGGCGGTGGGCTCGGCTCGGGGGCGG
AGGCGGCGAAAGGGCGGGGAGCGCGAGGAGGAGCGACCTGGCCTCACCGCTGCCGCCTCTTCCCCGCC
GCATGGACGAGCGCCTCAGCCTTCTGCGCTCGCCGCCGCCGCCCTCAGCCCGCCACCGCGCCCACCCT
CCTCAGCGCCCAGCGAGCAGCGGCGGTGCCCACACGCTGGTGAACCACGGCTACGCGGAGCCCGCCGC
AGGCCGCGAGCTGCCGCCCGACATGACCGTGGTGCCCGGGGACCACCTGCTGGAGCCGGAGGTGGCCG
ATGGTGGAGGGGCCCCGCCTCAAGGCGGCTGTGGCGGCGGCGGCTGCGACCGCTACGAGCCGCTGCCG
CCCTCACTGCCGGCCGCGGGCGAGCAGGACTGCTGCGGGGAGCGCGTGGTCATCAACATCTCCGGGCT
GCGCTTCGAGACGCAGCTGAAGACCCTTTGCCAGTTCCCCGAGACGCTGCTGGGCGACCCCAAGCGGC
GCATGAGGTACTTCGACCCGCTCCGCAACGAGTACTTCTTCGACCGCAACCGGCCCAGCTTCGACGCC
ATCCTCTACTACTATCAGTCCGGGGGCCGCATCCGCCGGCCGGTCAACGTGCCCATCGACATTTTCTC
CGAGGAGATCCGCTTCTACCAGCTGGGCGAGGAGGCCATGGAGAAGTTCCGCGAGGACGAGGGCTTCC
TGCGGGAGGAGGAGCGGCCCTTGCCCCGCCGCGACTTCCAGCGCCAGGTGTGGCTGCTCTTCGAGTAC
CCCGAGAGCTCCGGGCCGGCCCGGGGCATCGCCATCGTGTCCGTGCTGGTCATCCTCATCTCCATTGT
CATCTTCTGCCTGGAGACGCTGCCGGAGTTCCGCGACGAGAAGGACTACCCCGCCTCGACGTCGCAGG
ACTCATTCGAAGCAGCCGGCAACAGCACGTCGGGGTCCCGCGCAGGAGCCTCCAGCTTCTCCGATCCC
TTCTTCGTGGTGGAGACGCTGTGCATCATCTGGTTCTCCTTCGAACTGCTGGTGCGGTTCTTCGCTTG
TCCTAGCAAAGCCACCTTCTCGCGAAACATCATGAACCTGATCGACATTGTGGCCATCATTCCTTATT
TTATCACTCTGGGTACCGAGCTGGCCGAACGACAGGGCAATGGACAGCAGGCCATGTCTCTGGCCATC
CTGAGGGTCATCCGCCTGGTAAGGGTCTTCCGCATCTTCAAGCTGTCGCGCCACTCCAAGGGGCTGCA
GATCCTCGGGCAAACGCTGAAGGCGTCCATGCGGGAGCTGGGATTGCTCATCTTCTTCCTCTTTATTG
GGGTCATCCTTTTCTCCAGCGCGGTCTACTTTGCCGAGGCAGACGACCCCACTTCAGGTTTCAGCAGC
ATCCCGGATGCCTTCTGGTGGGCAGTGGTAACCATGACAACAGTGGGTTACGGCGATATGCACCCAGT
GACCATAGGGGGCAAGATTGTGGGATCTCTCTGTGCCATCGCCGGTGTCTTGACCATCGCATTGCCAG
TTCCCGTGATTGTTTCCAACTTCAATTACTTCTACCACCGGGAGACAGAAGGGGAAGAGCAATCCCAG
TACATGCACGTGGGAAGTTGCCAGCACCTCTCCTCTTCAGCCGAGGAGCTCCGAAAAGCAAGGAGTAA
CTCGACTCTGAGTAAGTCGGAGTATATGGTGATCGAAGAGGGGGGTATGAACCATAGCGCTTTCCCCC
AGACCCCTTTCAAAACGGGCAATTCCACTGCCACCTGCACCACGAACAATAATCCCAACTCTTGTGTC
AACATCAAAAAGATATTCACCGATGTTTAATATGTGATACAAGTGACATGCTGTGCTCAGTATTGTGT
GGAACGTGCCCCCTTGGTCTGCCTATGCCCTTGTTTTATACATTTCCAGACCATTCATCAAGGAAAGG
ACCTGAAGAAGTGGAAAGCACACTTCATTCTCCCTCTCCCTGCTGCTTCATACTGAAACAGGTGCCTG
TTTTGCAAGTGGGCTGCATTCTCTCAGCTCTCCTTTTCCCTCTTACCCTCTCTCTCTKAACATTGTAA
ACAACAGACTTACGTTAAACTTCATTTCTAGTACACGCCCTATTTAAAAAAGAGCAGTACATCCTGGG
AGGAAATGAAACTAAAGAACAGTTAGAGTAACTGTTTAACCTCAGAATTTTAAAGGCAGTTGTTTCTT
TCCTAAGCACATCAATTCGTAGTAAATGATGCTTCGGTTTGATGGACCTTTCAACGTTATTTATTGAA

ANNEXES

TATGTATTTCGGTTGCCTACCCTGTAGATATGTGGATGAAGAGTCTAACTAGAATAATGACTTGTAAA
CCCACCATGAGTTATTTGGTTTTTGACTTAAATTCCTATTTGAATCCCCTTTCCCGGAATTTTAAGTG
TCTCTACAACTTTGAATAAAGGGAAATGCCC[--/GG]AAGATGTCCTGATCTGACTAATTAGTTTAA
TTCTTTCGGGCTTGCTAAGCATTTCTAAAGCATTAGACTAACAGATTCCTGTGAAGTTCTGTGCATAT
GTCCCAGCCCCAACAACTATCAAAGTCTAGAAACAGATGTTTTCAGTGTTGCTGAGAGAAACAAAAAA
TTTCCTAATGCATCTGAGAGATAAGCTTCGGCAGTATCACAAGAAGATTAAAGTGGCAGACACCCCTT
CCAGCGGAAGTTACTAATTCGGACCTGACTGATGCAGTTTCCATAGCAACCCATGTTTCCTGGGAAAC
CCGAAAAAGGTTGTCATGGCATCTCTTGCTCTCTAGCCCCACCTCCCAGCCCCTGCCGTTTCCACAGT
AACCTTTCCAGATGGTTCCTACTTAAATGATTTCATAAGGAAAACCACTGTTTGAATAAGCCGCACAA
AAAATAAAGTTAAGTCTGAGACTCTAAGGAGGTGAAATGAATCCCAAATGCATTTTTTAACTATGAAA
ATCATTATGTCATTCCATAATGACTGAATCAAGGAGGAAAATATGGTGTTTGGAATGTTAGATATTAA
CCACAATAAGGCATGATCTGGATTAAATGCCATTTATTAGGCAATAATTTTTAAAGATGCTTCTCTAC
AGTTTTCTTTCTCCAAGAACTTTCAAGCCAACAAATGAAATTTAAAAGCAAATGTAAAAGTGTTCTGT
ACATAAGCAAATGAGAGATTCGATCAGTGTGCCTGAAACCTTACTACAAGGGACCTTCAGGCTTTCTC
TTTaaaaaaaaaaatacagatcccacaacagctctgtcatcatcacagcactt

KCNA5

cggcgcagccagagaggggcggctgaaggttgcatctgctggaaggaggcTTTTCGGCTGCTTGGTAA
CGGGCTGCCAGAAGAGAGAGAGGCAGAGAGCAGGGCAGCGGCTTYTTGACGTCAGGGCCAAGCGAGGG
GATCGCGCCAGCAACCCCAGCTCTCCCCAGAGAGGGGCCGGCCGACCGCTGGAGCGGAGCCTGACGCC
AGGCGCCCGCGGAGCGTGAGTAGGGGGCGCGGGAGCCGGTCAGCTGGGGCGCAGCATGCCCTCTGCTC
CCGCGCCATGGAGATCGCCCTGGTGCCCCTGGAGAACGGCGGTGCCATGACCGTCAGAGGAGGCGATG
AGGCCCGGGCAGGCTGCGGCCAGGCCACAGGGGGAGAGCTCCAGTGTCCCCCGACGGCTGGGCTCAGC
GATGGGCCCAAGGAGCCGGCGCCAAAGGGGCGCGGCGCGCAGAGAGACGCGGACTCGGGAGTGCGGCC
CTTGCCTCCGCTGCCGGACCCGGGAGTGCGGCCCTTGCCTCCGCTGCCAGAGGAGCTGCCACGGCCTC
GACGGCCGCCTCCCGAGGACGAGGAGGAAGAAGGCGATCCCGGCCTGGGCACGGTGGAGGACCAGGCT
CTGGGCACGGCGTCCCTGCACCACCAGCGCGTCCACATCAACATCTCCGGGCTGCGCTTTGAGACGCA
GCTGGGCACCCTGGCGCAGTTCCCCAACACACTCCTGGGGGACCCCGCCAAGCGCCTGCGCTACTTCG
ACCCCCTGAGGAACGAGTACTTCTTCGACCGCAACCGGCCCAGCTTCGACGGTATCCTCTACTACTAC
CAGTCCGGGGGCCGCCTGCGGAGGCCGGTCAACGTCTCCCTGGACGTGTTCGCGGACGAGATACGCTT
CTACCAGCTGGGGGACGAGGCCATGGAGCGCTTCCGCGAGGATGAGGGCTTCATTAAAGAAGAGGAGA
AGCCCCTGCCCCGCAACGAGTTCCAGCGCCAGGTGTGGCTTATCTTCGAGTATCCGGAGAGCTCTGGG
TCCGCGCGGGCCATCGCCATCGTCTCGGTCTTGGTTATCCTCATCTCCATCATCACCTTCTGCTTGGA
GACCCTGCCTGAGTTCAGGGATGAACGTGAGCTGCTCCGCCACCCTCCGGCGCCCCACCAGCCTCCCG
CGCCCGCCCCTGGGGCCAACGGCAGCGGGGTCATGGCCCCGCCCTCTGGCCCTACGGTGGCACCGCTC
CTGCCCAGGACCCTGGCCGACCCCTTCTTCATCGTGGAGACCACGTGCGTCATCTGGTTCACCTTCGA
GCTGCTCGTGCGCTTCTTCGCCTGCCCCAGCAAGGCAGGGTTCTCCCGGAACATCATGAACATCATCG
ATGTGGTGGCCATCTTCCCCTACTTCATCACCCTGGGCACCGAACTGGCAGAGCAGCAGCCAGGGGGY
GGAGGAGGCGGCCAGAATGGGCAGCAGGCCATGTCCCTGGCCATCCTCCGAGTCATCCGCCTGGTCCG
GGTGTTCCGCATCTTCAAGCTCTCCCGCCACTCCAAGGGGCTGCAGATCCTGGGCAAGACCTTGCAGG
CCTCCATGAGGGAGCTGGGGCTGCTCATCTTCTTCCTCTTCATCGGGGTCATCCTCTTCTCCAGTGCC
GTCTACTTCGCAGAGGCTGACAACCAGGGAACCCATTTCTCTAGCATCCCTGACGCCTTCTGGTGGGC
AGTGGTCACCATGACCACTGTGGGCTACGGGGACATGAGGCCCATCACTGTTGGGGGCAAGATCGTGG
GCTCGCTGTGTGCCATCGCCGGGGTCCTCACCATTGCCCTGCCTGTGCCCGTCATCGTCTCCAACTTC
AACTACTTCTACCACCGGGAAACGGATCACGAGGAGCCGGCAGTCCTTAAGGAAGAGCAGGGCACTCA
GAGCCAGGGGCCGGGGCTGGACAGAGGAGTCCAGCGGAAGGTCAGCGGGAGCAGGGGATCCTTCTGCA
AGGCTGGGGGGACCCTGGAGAATGCAGACAGTGCCCGAAGGGGCAGCTGCCCCCTAGAGAAGTGTAAC
GTCAAGGCCAAGAGCAACGTGGACTTGCGGAGGTCCCTTTATGCCCTCTGCCTGGACACCAGCCGGGA
AACAGATTTGTGAAAGGAGATTCAGGCAGACTGGTGGCAGTGGAGTAGGGAATGGGAGGCTTGCTGAA
CATGGATATCTACATTATACCGCAGAGTATTTGAAGTCACACTGTAACCTCAGTCTACCCCTCTCCTT
TCACTCCTTTCCTCCCTCCCTCGATCCCCCCATTTTCTCTATTCTTTCCATGACACCCAAGGGTCGCC
TATTTTTAAAAAGTACCACATTGCATGACGCAGGAGCTGTGGAAATGGTGAGCGCTGTGAGATGGATG
TATTTGTAGCCAGTCTCCTATACCCAGCAGAGGGATAACCCAAACAAAAATGACTCTAAATAGCCCAG
ATCCCAAGAGATTATGTAACTCCTCCATCCATGTGTTCCAAATTTGCTTTACATATGATTGTATTTGT
GTATAGGGGAAAATATTATTTTTATGCCTGGTAAGTGGCTTTTTGTACTGTAGTTCAGATAGAGATAT

TTTGGGTATATTTTCAAGATACATGTTGTATTTATGGAAGAAAGWGTTGTCCTGATGTTTTTCTGTGT
TACTTATATTAGAGTCAGAGATCTTGGTATGGGCTGTTCTGTTTCCTGTGTCTCCAAGCCTCTGTCTT
TTCTGGGATGTGGTATTGGTGCTTTGTGTCTAGGGCAGAGTATGTTCTTGAAGAAAGGCAAATCTGAC
TTTTTCTGTGCGCCTTAAACAATTCTTGTAACTTTCTTCAAAAAGCATTTTAATGATATTGGAGGAAT
ACTTCTGATAATTTATTGTCTTTATTTTTATCCCAGGAAATAAAAGGTTACCTTGTTGAggcaagtgt
tagtttttctgcagctgatacattttctgaaatttttaaaa

KCNE1

AGGTGTGCCTGGGAAGTTTGAGCTGCAGCAGTGGAACCTTAATGCCCAGGATGATCCTGTCTAACACC
ACAGCGGTGACGCCCTTTCTGACCAAGCTGTGGCAGGAGACAGTTCAGCAGGGTGGCAACATGTCGGG
CCTGGCCCGCAGGTCCCCCCGCAGCRGTGACGGCAAGCTGGAGGCCCTCTACGTCCTCATGGTACTGG
GATTCTTCGGCTTCTTCACCCTGGGCATCATGCTGAGCTACATCCGCTCCAAGAAGCTGGAGCACTCG
AACGACCCATTCAACGTCTACATCGAGTCCGATGCCTGGCAAGAGAAGGACAAGGCCTATGTCCAGGC
CCGGGTCCTGGAGAGCTACAGGTCGTGCTATGTCGTTGAAAACCATCTGGCCATAGAACAACCCAACA
CACACCTTCCTGAGACGAAGCCTTCCCCATGAACCCCACCACTGGCTAAAACTGGACACATCCTGCCT
GGCAACCTGATTTTCTAATCACATTCCTCTCATACTCTTTATTGTGATGGATACCACTGGATTTCTTT
TTGGCTGTTGTAAGGGGTGRGGGGTGGATTAATGACACTGTTTCACTGTTTCTCTAAAATCACGTTCT
TTTGTGATAGACTGTCAGTGGTTCCCCCATATCTGTCCCTGCCTTGCTAAATTTAGCAGAATCCCTGA
GGACATGGCCTCTGAGAATAGCAGCTGCATTTCCCAGACTCCCTTGCAGCTAGCAAGGTTGTGTGACT
AAGCCCTGGCCAGTAGGCATGGAAGTGAAGACTGTAATGTCCAAGTAATCCTTGGAAAGAAAAGAACG
TGCCCTTAACTAACTTTGTCCTGCTTCCCAGTGGCTGGATGTGGAGGAGGTGGAGAGCAGTTATGAGA
CTGGGAAAGAAYGGGGCACTCAAAGAGCCACACACATCTGGGCCTGGGCGACGTGGATCCTCCTTACC
ACCCACCAGGCCAGATTTACAGGAGAGAGAAATCCACTCCACTCTTCCTTAAGCCACTGTTATTCTGA
TCTCTGTTAAGGTCGCAGAATCAATGCCCTTACTGATACACCTACCTTATAGGACTGAACCTAAAGGC
ATGACATTTCCATACTTGTCACAAGCACACACTGATTCTGCCCTTGTCACTTCTGTGCTCACTCTTGT
GGCTCTATCCTCCTCCTGCCCTTCCGCCTTCCACTCCTCCCTTGCACCCATCCTGCACACATCTCCCT
GAAAACACACAGGCACATACACTCATATACATAGACACACATACACACCTCAATCTAGAAAGAACTTG
CTTTGTACAGGGCTGAGATGGAGGAGAAAAAAATGCCCCCTTCAGAATGCATACCAAGGGGAAGGTGC
TCGGTCACTGTGGGAGCAGGGAAAGGTGCCCCCACTCCCCGAGAGCCAGGGGAAGGAGTGGCTCTGGG
CAGAGAGGGACACATAGCACTGGGGTGGCAGGTCCTTTTGAGGTGATGGGCCGGTTTTGTGAGATGAA
TTGTATCCCCCMAAAAGACAGGTACCTTCAATGTGACCTAATTGGGAAATAGAGTCTTTGCAGATGAT
CTAGTTGAGATGAGGTCATTGGGGTGGGCCCTCACCCAATATGACTGGAGTCCTTATCGGAAGAGGGA
AATTCAGACACAGATGCATAGGGAGGRCACCATGCCGTGACAGAGGCAGAGGGTGCAGTGACACAGCC
ACAAACCAAGGAAGGCCGAGGATGGATGCGCATCCCCATCCCAAGAAGTCGGGAAGAAGCCAGGAAGG
CTCCTCTCCYACAGGTTTCAGAGGAAGCACAGCCCTGCTTGAATTCAAACTTTTGGCCTCCAGAACTG
TGAGTCAGTACCTGTTGTTGAAGCCACCCAGCTTAGGATACTCTGGCAGCCTACTGCCATACAGTATT
GGGATACTATAGTGAGCCCATGCAGCACCTCTCACCCACCCAGAGATGGAGCTGCTCTGCCTTCCAGC
GGGGCACCCGGAGG[-/G]CTGCCCCAGCAGATAGAGAGGGCCTCCGTTCTGCCACCT
GCCTTGAAAGGGTCTCCAGCTGCCATATGTAGCATTGGAGTCCTCTGCAATGCGACATCCTGAAAGCT
CAGCTGCCTGGGCATTCCTGAAGAGTATGGAATATTTAAATGAAACATATTTTTTTAAAACCTGCGCA
TAAGATAAAAGCAGCCCGTGTGCATCTTGGGCCATCCTCAAATGGACAGACTTGGTCTTGTGAGGTTC
CAGTCCTTGTTTCACATAATAAACACTGGCATGGCTCAGCCCCTGAGTTACCACAGTCCTTGAGATGA
GTGGTTCTTTGGGTTACAAAGTCCTCTGAAAGTCTAGTGAGAGCTGTGATCTTTGCCCCACCCGAATA
ATGCATATGGACACCACACCTTGCCTGCCGTGTCCAGGATTCATGACCAGTAGCAGCCCAGCTATGCC
TGCCACGTCTCAYGGCCCCTGTGTAAGCCAGACCCTTCTTAGGCAGTTGCATATTCCCAGACTGAGGC
AGGGCAGGTTTGCAGAGAGAGACCCAGAGTGCACGTGACCCGCAGTGTGATCCCTGGCACGCACTGAC
TTTGATATTCCAGGCACACGGACTGGCTATTTATCACCACTTCTTTTTCCCCACTAAGATTCCTGTGC
CTTTTAAGGCAGAGGGAGATCCCTATGGCGTTAGTCTTCCCAGGCCTTAAAGGGCCCTTGTCTTCACT
CACAAACCTCTTATCTCTTCTTCTCCTTCCTCTACATTTTAAAGGGGGAGAGGGAAAAGTAACCGGGA
GACAAATTGAGCCACATATTTTCAGACACTTGTTACCATATTTTAAAATCTGGCTTCACATACACAGA
GTCTTTGCTATGCACCATGTACTGTTCTAAGCTTCTTAAAAATAGAATCTCAATTATTRTTTTGCAGG
CAATACTCTRTGCATTCATTAGCTAGGACAACAATGCATTTGCAGTAGTGAGATTTCGCTAAAAAATT
AAAGCCATTTACTATGA

KCNE4

agttccttgactgtaaatcccgcacttgcttccaactgtctttcatccagATTATGGGATTCAGCTGC
CTCTGAAAACCTGTAGCCCAATAATGGTTATTCCCCAGGAGCCGCGCGAAGCATGAGCTAATTTTCAG

ANNEXES

TGAGCGCGGACTTTGGGGTAACGGTTCCAGCACAGCACATCCCTTTCTCCTCTTTTCACTCATCRTCA
CCGCTACCTGAAAACCCTGGCCGGGTGCTGGGGCTTGAGGAGCAGTTCCCACTTCCCAGTCTTTTTCA
CTTTTCACAGCTGCAAAGTTCAGGGAGTTGAACTGCAGTGCTTTCAGTTCACTGCTCACTCTGCCACG
ATCAATCTCTGTTGTAAATTTTCCTCCCAGAGCACGTGACGATGCACTTCTTGACTATATATCCCAAC
TGCAGCAGCGGAGTTGTCAGAGCGCAGAGCCGGACAGAGCAGAAGAACCCTCTTGGACTGGACGATTT
GGGAATTCAAAACTTGGGACAAACTGTCAGCCTTGgtaagtcagcaaggctacactttgctttcagaa
acatttgaaagagggacatttttgccaattaatagatgaatttttttcctttatttttcttcctgcttt
tctttgttctaaggaaacattgttttgaatttaaaatagtttggttttggaaacacaatgtaaacttt
gtttctgctcagttaaaatacgtttcccagttttaaagatactatttactgtatgctcctgtcttaca
ttgatttttttttaatcaaagtaatactgctcactacaaacaggacaaatgtgtacactaaaaaaaaa
aaaaaaaagtccttcttacttttcccagtgaaccttcccgggcttctctcccgtgcactccaagccct
catagctcactcttgtcagctgtttggcgaaccctcttatgctatttctttcatgcacttttaagctt
ttttggtattgcagttccacaaacctcgtgctcccccacctccctgtgcccaggacctgggggagagt
tctaacctgcggctttttccccagCCCCTGCTGTGGAGGCAGCCTCAATGCTGAAAATGGAGCCTCTG
AACAGCACGCACCCCGGCACCGCCGCCTCCAGCAGCCCCCTGGAGTCCCGTGCGGCCGGYGGCGGCAG
CGGCAATGGCAACGAGTACTTCTACATTCTGGTTGTCATGTCCTTCTACGGCATTTTCTTGATCGGAA
TCATGCTGGGCTACATGAAATCCAAGAGGCGGGAGAAGAAGTCCAGCCTCCTGCTGCTGTACAAAGAC
GAGGAGCGGCTCTGGGGGGAGGCCATGAAGCCGCTGCCBGTGGTGTCGGGCCTGAGGTCGGTGCAGGT
GCCCCTGATGCTGAACATGCTGCAGGAGAGCGTGGCGCCCGCGCTGTCCTGCACCCTCTGTTCCATGG
AAGGGGACAGCGTGAGCTCCGAGTCCTCCTCCCCGGACGTGCACCTCACCATTCAGGAGGAGGGGGCA
GACGAKGAGCTGGAGGAGACCTCGGAGACGCCCCTCAACGARAGCAGCGAAGGGTCCTCGGAGAACAT
CCATCAGAATTCCTAGCACCCCCGGGACCCCTGCSGGTGGCTCCATCAGCCAGCAACCTTAGAGAGAG
GAAAGACAGTTTTCAAGTGTCTGGTTTCACTTTCACAGTGCGGCTGCCACTTTGAAGAGACCCTTGGT
AAACCCCTGATTCGGGGTGGGGTGGGGGACTAGGCTCAGCCGGAACCAGCACCTCCAAGGAGTCCGGG
AGGTGCCTGTGGTTTGCACCCACCACTGAAAAAGCCGCGGAGATGCGCAGCGCGTACACTGACTTTGG
GGCCTGGGTGTTGGGGTTCTGATCAGAATTTGGCGGGATGATATGYTTGCCATTTTCTCACTGGATGC
CCTGGGTAGCTCCTGCAGGGTCTGCCTGTTCCCAGGGCTGCCGAATGCTTAGGACACGCTGAGAGACT
AGTTGTGATTTGCTATTTTGCCTAGAGCTTTGTCCTTCTAGATCTGATTGGCTGTAAGTATCTCTACT
GTGTACCTGTGGCATTCCTTCACAGTGGGTTACAAGCTTCTTTTGGATTAGAGGGGGATTTTTGATGG
GAGAAAGCTGGAGATCTGAACCCAGCCCATTTGCACACTATAAGAAAAAAAAAGTAACTTTTAAACCTG
TTAACATTGGCCGGGGTTATAAGAGATGATCTTCTATTTTGACCTTTTGTCTAACTTATGACCTTGAA
CTCTGACCTGTGACCATGCAGCATCACATGATGGCATGACGTTCTTTGGATCAGAAGAGCTTCCCCAG
AATCTAACCTGCACTCCCGATGGTGGTTCAGGAGACTCTTCCTGATCTTTCTAGAAGGGGTAAAGTGG
GGTTGAACAAGGCCAAGCCGTTAGCTCTGCTGCTGCTCAGTTTCCCAGCCTAGTTTTCTGAGCTGGGA
GAGGACATAATGTGGTATTTCGTCACGTAGCTGAGACCTAGAAGGGCATACTCAGGCGGAGATTGCAC
AAAGCTGGGCTCCAAGTTCTGTGCTTCCTGATCCCGAGCCCTGACACTCATTTGCTGTGTGGTCCCGG
GCATGTCATCAAGAAGCTCGCTGTCTGCATGAGGCTCCCGACGATCTCCATCCCCAGGGGGTTGGGAG
GATGTCTTTAGATTTTAGGACTCTGTGATAAATATTCCACAGCCTGGTGTGAGGAAGCTTGGACCAAA
TGCTTCCCCTTTGGCYGGTTAGTCTGAACAAGGATCTGCTGATTTAAAGGAGCAGTTGGAGATTCAGA
ACACATATAACTGGGGAATTCAGGGCAAGCTACCAACCCAGCCCTGCTGTAGTTTTCCCAGGACTGAA
GGAAAGAGGCAGACACCACATTCTCCTCTGCAAAGTTCTCTGGAGAATGTGTGATGTTAACACTCCCA
GCTAAGGGAAAGCAAAGTCTAAAGGAAAACACACAGGAATGCTTCCAATGTCTCCAAGTATTCCTGTG
GTCAACAGTTTCGCAGATCCGTTAGGCCCTTAAAGACAAGGAGGAAGTAAAAGGTCAAATTTAAATCT
ATTTAAAAAAACTTTTAAAAAAATTATTTATTTATTATTATTTTTTATTTTTAAGACAGAATCTCGCT
CTGTTGCCCAGGCTGGAGTGCAGTGGTGCAATCTTGGCTCACTGCAACCTCCACCTCCTGGGTTYCAG
CGATTCTCCTGCCTCAGCCTCCTGAGTAGCTGGGATTACAGGCGCCTGCCACCACGCCCRGCTAATTT
TTTGATTTTTAGTAGAGATGGGGTTTCGCCATTTTGGCCAGGCTGGTCTCAAACTCCTGGCCTTAAAT
GATCCTCCCACCTCGGCCTCCCAAAGTGCTGGGATTACAGGCATGAGCCACTGCACCCGGCCACTTTT
TTTTTTTTTAAAGAAAAATGCTCTGCATGGATTGGAGACACAGCAATAACTACTGTTGCCATGGAAGG
GTTAACAGTGTAGGAGCTGGTTTATCAGTCCGCTTTGACATACAGCTAAAGGAAATTTATGTTTGGGG
GAAAAAGGCCCTCTGTTCACTTTAAAATTCAGTGTGGACTTATGCCAAAGGGGGCTGTTTAAGTTGAA
AGAAGCCAAGTTAAGTTTGGCCTCTTGCCTGGAATCACTTGAATTCTGAAATTTCACTGCGACGGACA
TGTGCCTTGTCACATTTTCCATTGCTTAATCCTGAAGTTTGGTGCAAGTCTCTCTGCACCTATTAAAA
AGTGATGTATATACTTCCTTCTTATTCTGTTGAGTTGTATAGAATTGTCTTTTGTATTTAACACTTTG
TAATTTTCACAATATTTTTTAATTTAAATAAATAAACACATTTTTTCCCTCCTGGGAAGTCATGAAtt
ctttgtttgatttttcaatataattgttagtttcgaagacatcacaga

I. ALIGNMENT OF KV1.3 / KV1.5 / KV7.1

```
Alignment:   Global Protein alignment against reference molecule
Parameters:  Scoring matrix:  BLOSUM 62

   Reference molecule:  rKv1.3, Region 1 to 525
   Number of sequences to align:  3
   Total length of aligned sequences with gaps:  884 aas
   Settings:  Similarity significance value cutoff:  >= 60%


Summary of Percent Matches:
   Ref:  rKv1.3              1 to    525   (   525 aa)     --
     2:  hKv1.5              1 to    613   (   613 aa)     57%
     3:  hKv7.1              1 to    676   (   676 aa)     15%


rKv1.3            1 -------------mtvvpgdhlle---------p--eaagg--------ggg--------
hKv1.5            1 meialvplenggamtvrggdeara---------gcgqatggelqcpptagls--------
hKv7.1            1 -------------maaasspprаerkrwgwgrlp--garrg--------saglakkcpfs

rKv1.3           21 -dppqggcvsgggcdr-----yeplppalpaag---------------------------
hKv1.5           44 -dgpkepapkgrgaqrdadsgvrplpp-lpdpgvrplpplpeelprprrpppedeeeegd
hKv7.1           38 lelaeggpagga---l-----yapiapgapgpa---------------------------

rKv1.3           48 ------eqdccg------ervvinisglrfetqlktlcqfpetllgdpkrrmryfdplrn
hKv1.5          102 pglgtvedqalgtaslhhqrvhinisglrfetqlgtlaqfpntllgdpakrlryfdplrn
hKv7.1           63 ------------------------------------ppaspaapaa-----ppvas

rKv1.3           96 eyffdrnrpsfdailyyyqsggrirrpvnvpidifseeirfyqlgeeamekfredegflr
hKv1.5          162 eyffdrnrpsfdgilyyyqsggrlrrpvnvsldvfadeirfyqlgdeamerfredegfik
hKv7.1           78 d-lgprppvsldprvsiyst----rrpvlarthv---qgrvy--------------nfl-

rKv1.3          156 eeerplprrdfqrqvwllfeypessgpargiaivsvlvilisivifcletlpefrdekd-
hKv1.5          222 eeekplprnefqrqvwlifeypessgsaraiaivsvlvilisiitfcletlpefrderel
hKv7.1          115 --erptg--------wkcfvy----------hfavflivlvclifsvlstieqy-----

rKv1.3          215 --ypaspsqdvfeaannstsgassgas----------sfsdpffvvetlciiwfsfellv
hKv1.5          282 lrhppaphqppapapgangsgvmappsgptvapllprtladpffivettcviwftfellv
hKv7.1          149 --------------------------aa----------latgtlfwmeivlvvffgteyvv

rKv1.3          263 rffa--cpskat-------fsrnimnlidivaiipyfitlgtelaerqg-------ngqq
hKv1.5          342 rffa--cpskag-------fsrnimniidvvaifpyfitlgtelaeqqpgggggggngqq
hKv7.1          174 rlwsagcrskyvglwgrlrfarkpisiidlivvvasmvvlcv------g-------skgq

rKv1.3          307 amslailrvirlvrvfrifklsrhskglqilgqtlkasmrelglliffflfigvilfssav
hKv1.5          393 amslailrvirlvrvfrifklsrhskglqilgktlqasmrelglliffflfigvilfssav
hKv7.1          221 vfatsairgirflqilrmlhvdrqggtwrllgsvvfihrqelittlyigflglifssyfv

rKv1.3          367 yfaeaddpssg----fnsipdafwwavvtmttvgygdmhpvtiggkivgslcaiagvlti
hKv1.5          453 yfaeadnqgth----fssipdafwwavvtmttvgygdmrpitvggkivgslcaiagvlti
hKv7.1          281 ylaekdavnesgrvefgsyadalwwgvvtvttigygdkvpqtwvgktiascfsvfaisff

rKv1.3          423 alpvpvivsnf---------nyfyhre-----------------------------------
hKv1.5          509 alpvpvivsnf---------nyfyhre-----------------------------------
hKv7.1          341 alpagilgsgfalkvqqkqrqkhfnrqipaaasliqtawrcyaaenpdsstwkiyirkap

rKv1.3          441 --------------------------------tegeeqaqymhvgscq--------hlsss
hKv1.5          527 --------------------------------tdheepavlkee---q--------gtqsq
hKv7.1          401 rshtllspspkpkksvvvkkkkfkldkdngvtpgekmltvphi-tcdppeerrldhfsvd

rKv1.3          462 aee--lrka------------rsns---------------------------------tlsk
hKv1.5          545 gpg--ldrg------------vqrk---------------------------------vsg
hKv7.1          460 gydssvrksptllevsmphfmrtnsfaedldlegetlltpithisqlrehhratikvirr

rKv1.3          477 seymv----------------ieeggmnh---------------------safp----q
hKv1.5          559 srgsf----------------ckaggtle---------------------nadsarrgs
hKv7.1          520 mqyfvakkkfqqarkpydvrdvieqysqghlnlmvrikelqrrldqsigkpslfi----s
```

```
495 tpfkt---gnstatcttnnnpns---cvnikk---iftdv--------------------
581 cplek---cnvkaksnvdlrrslyalcldtsr---e-tdl--------------------
576 vsekskdrgsntigarlnrvedk---vtqldqrlalitdmlhqllslhggstpgsggppr

    ---------------------------------------------
    ---------------------------------------------
633 eggahitqpcgsggsvdpelflpsntlptyeqltvprrgpdegs
```

Annex I: *Protein alignment between Kv1.3, Kv1.5 and Kv7.1 performed with the Sci Ed Central Clone Manager Suite 7 software. The scoring matrix used was BLOSUM 62. Mismatches are highlighted in orange.*

J. GENE REGULATORY REGIONS IN KCNA3, KCNA5, KCNE1 AND KCNE4

KCNA3

Table A1: Regulatory regions of *KCNA3*				
Code	Type	Position	Length	Score
Hs.169948.1.3	Poly-A (observed)	2618 - 2631	13 nt	----------
NM_002232.polyA-1	Poly-A (predicted)	3046 - 3095	49 nt	690
NM_002232.polyA-2	Poly-A (predicted)	3200 - 3250	50 nt	814
miR-217	miRNA (predicted)	2880 - 2887	7 nt	35

KCNA5

Table A2: Regulatory regions of *KCNA5*				
Code	Type	Position	Length	Score
Hs.150208.1.1	Poly-A (observed)	2915 – 2920	5 nt	----------
NM_00234.polyA-1	poly-A (predicted)	2873 – 2923	50 nt	852
miR-1/206	miRNA (predicted)	2329 – 2337	8 nt	88
miR-101	miRNA (predicted)	2560 - 2568	8 nt	94

KCNE1

Table A3: Regulatory regions of *KCNE1*				
Code	Type	Position	Length	Score
Hs.121495.1.1	Poly-A (observed)	2995	1 nt	----------
Hs.121495.1.2	Poly-A (observed)	2914	1 nt	----------
Hs.121395.1.3	Poly-A (observed)	630	1 nt	----------
miR-193	miRNA (predicted)	755 - 763	8 nt	93

KCNE4

Table A4: Regulatory regions of *KCNE4*				
Code	Type	Position	Length	Score
miR-26AB/1297	miRNA (predicted)	3640 – 3647	7 nt	69
miR-542/542-3p	miRNA (predicted)	3679 – 3686	7 nt	41
miR-300	miRNA (predicted)	3774 - 3781	7 nt	63

Annex J: *Regulatory regions of studied genes. Genes KCNA3, KCNA5, KCNE1 and KCNE4 were browsed in the USCS Genome Browser (https://genome.ucsc.edu/), TargetScan (www.targetscan.org), and PolyA_DB databases (http://exon.umdnj.edu/polya_db/) for the study of poly-adenylation sites and miRNA binding sites. Both observed and predicted sites are reported. Score represents the likeness of the predicted region being real: 100 is the maximum for miRNA binding regions, while 1000 is the maximum for poly-adenylation sites.*